

**Bearing Failure Detection in Farm Machinery Using Low-Cost Acoustic Techniques**

by

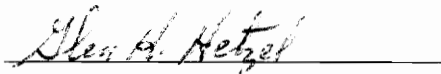
Stacy K. Worley

Thesis submitted to the Faculty of the  
Virginia Polytechnic Institute and State University  
in partial fulfillment of the requirements for the degree of  
Master of Science  
in  
Agricultural Engineering

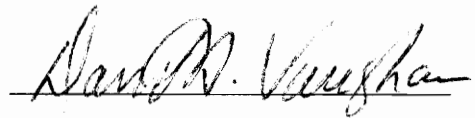
Approved:



Steven J. Thomson, Chairman



Glen H. Hetzel



David H. Vaughan

August 11, 1994

C.2

LD  
5655  
V855  
1994  
W675  
C.2

# **Bearing Failure Detection in Farm Machinery Using Low-Cost Acoustic Techniques**

by

Stacy K. Worley

Steven J. Thomson, Chairman

Agricultural Engineering

(ABSTRACT)

Unexpected bearing failures in agricultural equipment can result in considerable inconvenience, potential hazard, and monetary loss. Continuous bearing condition monitoring using vibration and audio spectrum analysis can detect imminent bearing failures before dangerous situations develop. Current application of bearing condition monitoring using vibration signature analysis has focused on fixed industrial applications involving high cost equipment and high shaft speeds. The feasible application of current technology on mobile agricultural equipment requires a lower-cost method of signal sensing and processing. Lower shaft speeds and the use of neural-net based pattern recognition techniques can allow the use of lower-cost transducers necessary for practical adoption on mobile equipment.

A test apparatus was developed and constructed to test the feasibility of using a electret microphone as a sensor for monitoring bearing condition through vibration signature analysis. Laboratory experiments designed to evaluate the sensors with test bearings at both an advanced and an early stage of wear were developed. A field-worn

bearing that had been removed from a unit of farm machinery was obtained and examined. Twelve new bearings identical in type to the field worn bearing were also examined, altered to simulate an early stage of wear, and re-examined. Identical experiments were conducted on both the field-worn and altered bearings. The signal acquired from a field-worn bearing was compared with the signal acquired from a new bearing using a two-sample, paired t-test for means at an alpha level of 0.05 and a graphical defect frequency analysis. The signals acquired from the altered bearings were compared with the signals acquired from the new bearings using the same statistical and graphical test performed on the field-worn bearings.

The goal of the analysis was to evaluate the performance of the microphone by attempting to identify significant frequency patterns that could be used to determine the condition of the test bearing while in operation. Duplicate experiments conducted using the accelerometer provided a comparison of sensor performance. The microphone performed well for bearings at an advanced stage of wear. The sensitivity of the accelerometer resulted in better performance when used with bearings at an early stage of wear.

## **Acknowledgments**

I would like to thank Dr. Steven J. Thomson for his endless patience and willingness to provide guidance and motivation as my advisor, committee chairman, and friend; and for generally making the pursuit of my Master's degree a thoroughly enjoyable chapter in my professional development. I would like to thank Dr. Glen H. Hetzel for his assistance and support in general and specifically in the development of the test apparatus. To Dr. David H. Vaughan, much gratitude is due for his support as my advisor during my undergraduate program, and his continued interest and participation in my professional development as a member of my Master's committee. I am indebted to Steve Spradlin for his patient assistance and considerable knowledge in the design and fabrication of the test apparatus. My appreciation goes to Keith Wright and the shop staff in the Industrial Engineering Department for their assistance in altering the bearings to simulate wear. Many thanks go to Dr. Raymond H. Myers for his invaluable expertise in statistics. Many

thanks to Patrick Phillips and Chris Wyckoff for the advice, assistance, and constructive criticism they gave so freely throughout the duration of my research. I would like to thank my wife, Maria, for all the lunches, errands, and for enduring the long hours, and late nights. Finally, I would like to thank God, to whom I owe everything.

## Table of Contents

Acknowledgments .....	iv
Table of Contents .....	vi
List of Tables.....	viii
List of Figures .....	x
Introduction.....	1
Objectives.....	4
Literature Review .....	5
Methods and Procedures.....	10
4.1 Test Jig.....	10
4.2 Data Acquisition and Processing .....	19

4.3 Experimental Procedure.....	22
Results and Discussion.....	29
5.1 Comparison of New and Field-Worn Bearing.....	29
5.2 Comparison of New and Artificially Worn Bearings.....	37
Conclusions and Recommendations.....	59
References.....	63
Appendix.....	65
A. Graphical Presentation of Data: Comparison of New and Field-Worn Bearing.....	66
B. Graphical Presentation of Data: Comparison of New and Artificially Worn Bearings.....	71
Vita.....	120

## List of Tables

Table 1.	Test Bearing Characteristic Defect Frequencies.....	26
Table 2.	Statistical Results: Comparison of New and Field-Worn Bearings.....	34
Table 3.	Statistical Results: Comparison of New and Artificially Worn Bearings, Bearings 1-3.....	38
Table 4.	Statistical Results: Comparison of New and Artificially Worn Bearings, Bearings 4-6.....	39
Table 5.	Statistical Results: Comparison of New and Artificially Worn Bearings, Bearing 7-9.....	40
Table 6.	Statistical Results: Comparison of New and Artificially Worn Bearings, Bearings 10-12.....	41
Table 7.	Statistical Results: Test Cases with No Significant Difference Between New and Altered Bearings.....	42

Table 8.	Statistical Results: Test Cases with Significant Differences Between New and Altered Bearings .....	43
Table 9.	Statistical Results: Test Cases with Significant Differences Between New and Altered Bearings and Significant PCC's.....	44
Table 10.	Statistical Results and Graphical Results: Test Cases where Positive Graphical Analysis Confirms Positive Statistical Analysis .....	54
Table 11.	Statistical Results and Graphical Results: Test Cases where Negative Graphical Analysis Contradicts Positive Statistical Analysis.....	55
Table 12.	Statistical Results and Graphical Results: Test Cases where Positive Graphical Analysis Contradicts Negative Statistical Analysis .....	56

## List of Figures

Figure 1.	Test Jig Bearing Housing and Clamping Tabs .....	12
Figure 2.	Test Jig Shaft Collars and Support Bearings.....	13
Figure 3.	Test Jig Loading Mechanism.....	14
Figure 4.	Test Jig Load Control Blocks and Loading Bolt.....	16
Figure 5.	Test Jig Sensor Mounting .....	17
Figure 6.	Test Jig Main Frame and Sub-Frames Assembly.....	18
Figure 7.	Block Diagram of Data Acquisition System .....	20
Figure 8.	Test Bearing: Timken LM11949 Cone and LM11910 Cup Set and CR Services 10034 Grease Seal.....	23
Figure 9.	FFT for New and Field-Worn Bearings: Microphone, Load C.....	30
Figure 10.	FFT for New and Field-Worn Bearings: Accelerometer, Load D.....	31
Figure 11.	Difference in New and Field-Worn FFT's: Microphone, Load C .....	32
Figure 12.	Difference in New and Field-Worn FFT's: Accelerometer, Load D .....	33

Figure 13.	Difference in New and Altered FFT's: Accelerometer, Load C, Bearing 1 .....	46
Figure 14.	Difference in New and Altered FFT's: Microphone, Load C, Bearing 3 .....	47
Figure 15.	Difference in New and Altered FFT's: Accelerometer, Load D, Bearing 4 .....	48
Figure 16.	Difference in New and Altered FFT's: Microphone, Load D, Bearing 5 .....	49
Figure 17.	Difference in New and Altered FFT's: Accelerometer, Load C, Bearing 8 .....	50
Figure 18.	Difference in New and Altered FFT's: Microphone, Load D, Bearing 7 .....	51
Figure 19.	Difference in New and Altered FFT's: Accelerometer, Load C, Bearing 11 .....	52
Figure 20.	Difference in New and Altered FFT's: Microphone, Load D, Bearing 12 .....	53

## **Chapter I**

### **Introduction**

Many modern machines have roller element bearings as their most carefully manufactured component. Despite their careful manufacture, a majority of bearings (as much as 80 to 90% in some applications) do not reach their design life. Proper installation, lubrication, and loading are key assumptions in the estimation of design life. Due to the high incidence of premature failure, design life is not a reliable means of scheduling bearing replacement (Berry, 1991). Various methods of bearing condition monitoring have been used, but each has disadvantages. Examining lubricating fluids for particles caused by wear is difficult to perform continuously, especially in most agricultural applications. Temperature measurements can also be used to indicate bearing condition, but often require an advanced stage of bearing wear to produce significant changes in temperature. A more ideal methodology would monitor a bearing during operation allowing use of evaluated bearing condition rather than maintenance schedules

to indicate bearing replacement. Such a system could maximize the utilization of the machine components and minimize unexpected failures.

Unexpected bearing failures occurring in agricultural machinery can result in significant financial losses. A critical failure in a combine during harvest, for example, could cause delays that would result in reduced crop yield, crop quality, or both. A system designed to warn the operator of impending bearing failure would allow scheduling of repairs and the minimization of down-time (especially in obtaining replacement parts and possibly obtaining a replacement combine while repairs are completed).

Systems that monitor bearing vibration spectra are currently being used in industrial applications. Frequencies specific to the location (inner race, outer race, roller element, or roller cage) of a bearing defect are produced as a bearing wears. As bearing wear progresses, the magnitude of the vibration spectra at the defect frequencies increases. Further bearing deterioration often results in spikes appearing in the vibration spectra at multiples of the defect frequencies and the development of sidebands at any or all of the following: rotational frequency, defect frequencies, and multiples of the rotational and defect frequencies. Berry (1991) provides an excellent and detailed description of vibration spectrum analysis of bearings.

Berry (1991), Harker and Sandy (1989), Li and Wu (1989), Braun and Datner (1979), Dyer and Stewart (1978), and Ehrich (1972) present systems with various means of signal analysis, but all systems use expensive transducers (high precision accelerometers and time-of-flight sensors) to detect the vibration spectra. The cost of the high-precision,

high-speed sensors is justified by the higher down-time cost, equipment cost, and shaft speeds (typically 1200 to 3600 rpm) common to industrial applications.

Down-time costs in agriculture, while significant to the agricultural producer, do not justify the high cost of systems currently used in industry. The identification of a lower-cost sensor is key to the feasible application of vibration spectra analysis as a means of bearing condition monitoring for agricultural applications. Typical agricultural applications involve shaft speeds (500 to 1000 rpm) and bearing geometries that result in lower defect frequencies than those prevalent in industrial applications.

## **Chapter II**

### **Objective**

The purpose of this study was to determine the applicability of electret microphones as transducers for bearing condition monitoring on mobile agricultural equipment. A suitable transducer should be cost-effective and provide a warning of imminent bearing failure sufficient to facilitate component replacement while reducing the timeliness cost of equipment failure. Laboratory experiments were conducted using bearings that had been replaced in field equipment and bearings that had been altered to simulate early stages of wear.

## **Chapter III**

### **Literature Review**

Agricultural producers are all too familiar with the cost of equipment failures. The most tangible costs are those associated with the repairs required to correct an equipment failure. However, less tangible and often more significant timeliness costs are frequently incurred as well. An obvious example of these timeliness costs is the reduction in crop yield, crop quality, or both that is commonly associated with delayed harvest. Similar costs may be incurred if planting operations are delayed. The key factor in minimizing down-time and therefore timeliness costs is the prediction of component failures. Prediction of failures by condition monitoring can reduce down-time by allowing time to schedule repairs and obtain replacement components or procure replacement equipment. Bearing condition monitoring allows greater utilization of machine components than using maintenance schedules to schedule maintenance.

Maintenance scheduling is a form of failure prediction based on a design life.

Design life can be estimated by the following equation (Berry, 1991):

$$L_{10}Life = \left( \frac{16,700}{rpm} \right) \left( \frac{Rating_B}{Load_E} \right)^3 \quad [1]$$

where:

- $L_{10}Life$  = number of hours that 90% of a group of bearings should attain or exceed prior to onset of fatigue failure
- rpm = shaft speed in revolutions per minute
- Rating<sub>B</sub> = basic dynamic load rating for a given bearing (N or lb)
- Load<sub>E</sub> = equivalent radial load impressed upon a bearing, including radial and axial loads (N or lb)

By examining equation [1], one can see that the design life for a given bearing is inversely proportional to shaft speed and to the bearing load to the third power. Shaft speed can be estimated with reasonable accuracy. Even if the shaft speed varies widely, using the maximum speed in the design process would result in a system that should meet or exceed the estimated design life. Bearing load, specifically dynamic load, is much more difficult to estimate accurately. Considering only easily estimated loads (i.e., static loads and belt tensions) in the design process may result in a gross under design, as dynamic loads can easily be one-third of the total load (Berry, 1991). Excluding one-third of the total load would result in a design life estimation more than three times the "true" design life. The difficulties in estimating the design life, coupled with improper lubrication, external contamination, improper installation, exposure to vibration while not rotating, and the passage of electric current through bearings result in failures for a majority of bearings

(as much as 80 to 90% in some applications) prior to reaching their design life (Harker and Sandy, 1989).

Due to the high incidence of premature failure, design life is not a reliable means of scheduling bearing replacement (Berry, 1991). Various methods of bearing condition monitoring have been used, but each has disadvantages. Examining lubricating fluids for particles caused by wear is difficult to perform continuously, especially in most agricultural applications. Temperature measurements can also be used to indicate bearing condition, but often require an advanced stage of bearing wear to produce significant changes in temperature. A more ideal methodology would monitor a bearing during operation allowing use of evaluated bearing condition rather than maintenance schedules to indicate bearing replacement.

Systems that monitor bearing vibration spectra are currently being used to monitor bearing condition in industrial applications. Wear of a properly designed, installed, and lubricated bearing is caused by the cyclic loading of the bearing components as they pass through the loaded zone (region in which loads are transmitted from the shaft to the bearing housing). The cyclic loads cause localized fatigue failures resulting in the dislodging of small flakes of metal, or spalls, from the surfaces of the roller elements and races. Vibrations are induced as these defects pass through the loaded zone, increasing the dynamic load and propagating the wear process. The frequencies of the induced vibrations are specific to the location (inner race, outer race, roller element, or roller cage) of the defect. Equations have been developed to estimate these defect frequencies based

on bearing geometry and shaft speed (Berry, 1991; Liu and Mengel, 1991; Li and Wu, 1989; Braun and Datner, 1979):

Defect Location

$$\text{Inner Race} \quad \text{BPFI} = \frac{N_b}{2} \left[ 1 + \left( \frac{B_d}{P_d} \cos \theta \right) \right] \times rpm \quad [2]$$

$$\text{Outer Race} \quad \text{BPFO} = \frac{N_b}{2} \left[ 1 - \left( \frac{B_d}{P_d} \cos \theta \right) \right] \times rpm \quad [3]$$

$$\text{Ball (or Roller)} \quad \text{BSF} = \frac{P_d}{2B_d} \left[ 1 - \left( \frac{B_d}{P_d} \cos \theta \right)^2 \right] \times rpm \quad [4]$$

$$\text{Cage} \quad \text{FTF} = \frac{1}{2} \left[ 1 - \left( \frac{B_d}{P_d} \cos \theta \right) \right] \times rpm \quad [5]$$

where:

BPFI = ball pass frequency, inner

BPFO = ball pass frequency, outer

BSF = ball spin frequency

FTF = fundamental train frequency

$B_d$  = ball or roller diameter (in or mm)

$N_b$  = number of balls or rollers

$P_d$  = bearing pitch diameter (in or mm)

$\theta$  = contact angle (degrees)

These equations assume that the outer race is stationary and the inner race rotates.

If the inner race is stationary and the outer race rotates, the minus sign in the parenthesis term of equation [5] must be changed to a plus sign. The relationships also assume that there is no relative slip within the bearing and as a result, the predicted values are approximate. These equations are widely used and the necessary geometric measurements or defect frequency (in Hz per RPM) may be obtained from the bearing manufacturer.

As bearing wear progresses, the magnitude of the vibration spectra at the defect frequencies increases. Further bearing deterioration often results in spikes appearing at multiples of the defect frequencies and the development of sidebands at any or all of the

following: rotational frequency, defect frequencies, and multiples of the rotational and defect frequencies. Defect frequencies can also appear as sums, differences, or averages of primary defect frequencies. High frequency vibrations are also present and have been used to indicate bearing condition. However, accurate bearing condition monitoring cannot be based solely on high frequency analysis as high frequencies are often overemphasized (especially when acceleration is being measured) and often result in premature indications of bearing deterioration. Berry (1991) provides an excellent and detailed description of vibration spectrum analysis of bearings.

Berry (1991), Harker and Sandy (1989), Li and Wu (1989), Braun and Datner (1979), Dyer and Stewart (1978), and Ehrich (1972) present systems with various means of signal analysis, but all systems use expensive transducers (high precision accelerometers and time-of-flight sensors) to detect the vibration spectra. The cost of the high-precision, high-speed sensors is justified by the higher downtime cost, equipment cost, and shaft speeds (typically 1200 to 3600 rpm) common to industrial applications.

## **Chapter IV**

### **Methods and Procedures**

#### **4.1 Test Jig**

Collection of data required the development of a test jig that could:

- Provide a stable housing for the test bearing.
- Provide proper lubrication of the test bearing.
- Provide a means of applying a radial load to the test bearing and resisting radial and thrust loads applied to the shaft by the bearing.
- Provide a means of controlling the load applied to the bearing.
- Provide mounting point for the sensors.
- Provide power to the shaft to turn the test bearing at approximately 540 rpm.

A steel housing designed to house the test bearing is shown in Figure 1. The bearing housing was secured in the test jig by four clamping tabs bolted to the center section. The left side of the cavity was sized to provide a press fit on the outer race and one grease seal. The right side of the cavity was sized to provide a clearance fit of the other grease seal, which was held in place by set screws, to facilitate easy removal. Four equally spaced notches were cut in the shoulder behind the outer race to allow easy removal of the outer race and left grease seal. The cup (outer race) of the test bearing was driven into the left side of the cavity. The cone (inner race), roller element, and cage assembly was lubricated and placed in the cup. One grease seal was driven into the left cavity over the cone assembly and the other was placed in the right side of the cavity and secured with set screws. Two collars were designed to secure the test bearing along the axis of the shaft, build the shaft diameter up to the inner bore diameter of the test bearing, and build the shaft diameter to the inner bore diameter of the grease seals (Figure 2). One collar transmitted both radial and thrust loads to the shaft and was secured by a screw drilled and tapped through the shaft and three set screws with locking nuts. The other collar transmitted no loads and was secured to the shaft by six set screws with locking nuts. The shaft was supported at each end by pillow block bearings (Browning 6X233C/VPS 110) which transmitted both radial and thrust loads to the base of the test jig. A guillotine type device was designed to apply radial loads to the test bearing (Figure 3). The T-shaped center section had tongues on each side that moved in grooves in the supports on each side. Two bolts were used to apply radial loads. The magnitude of the

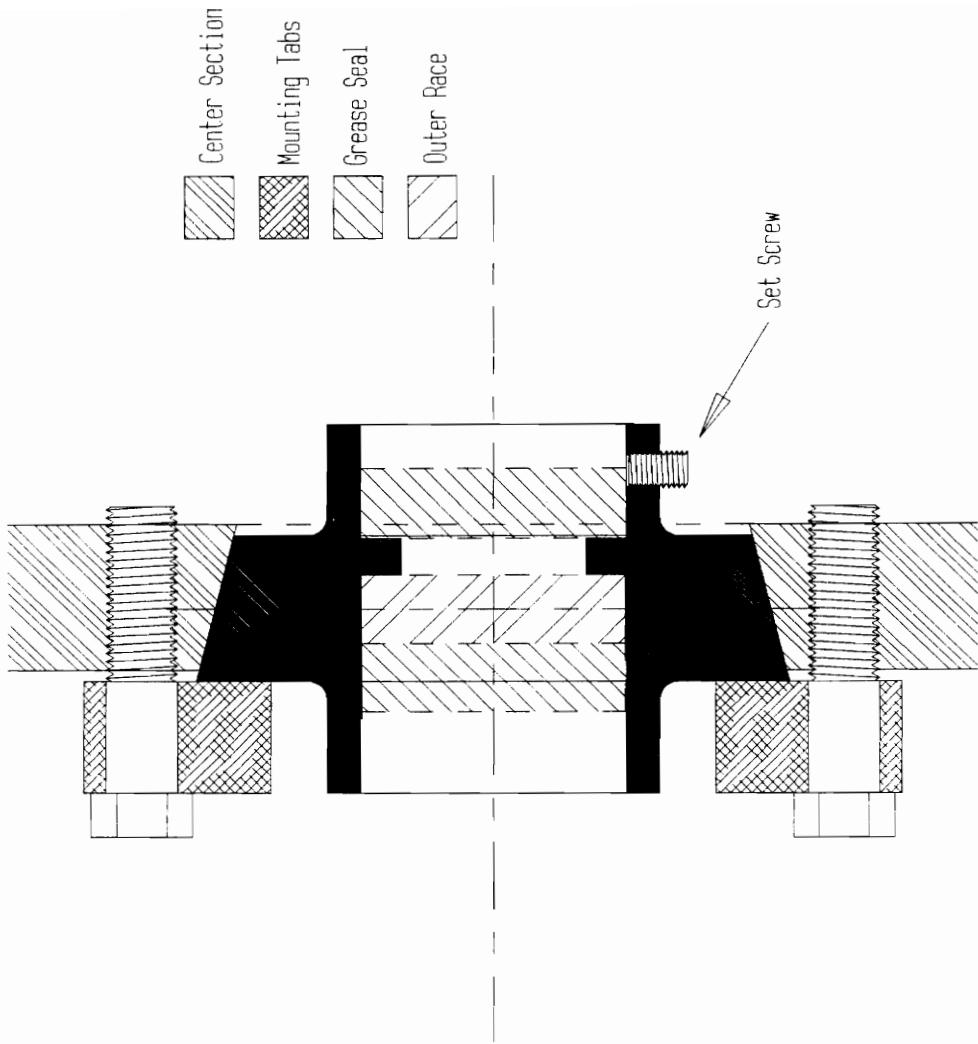
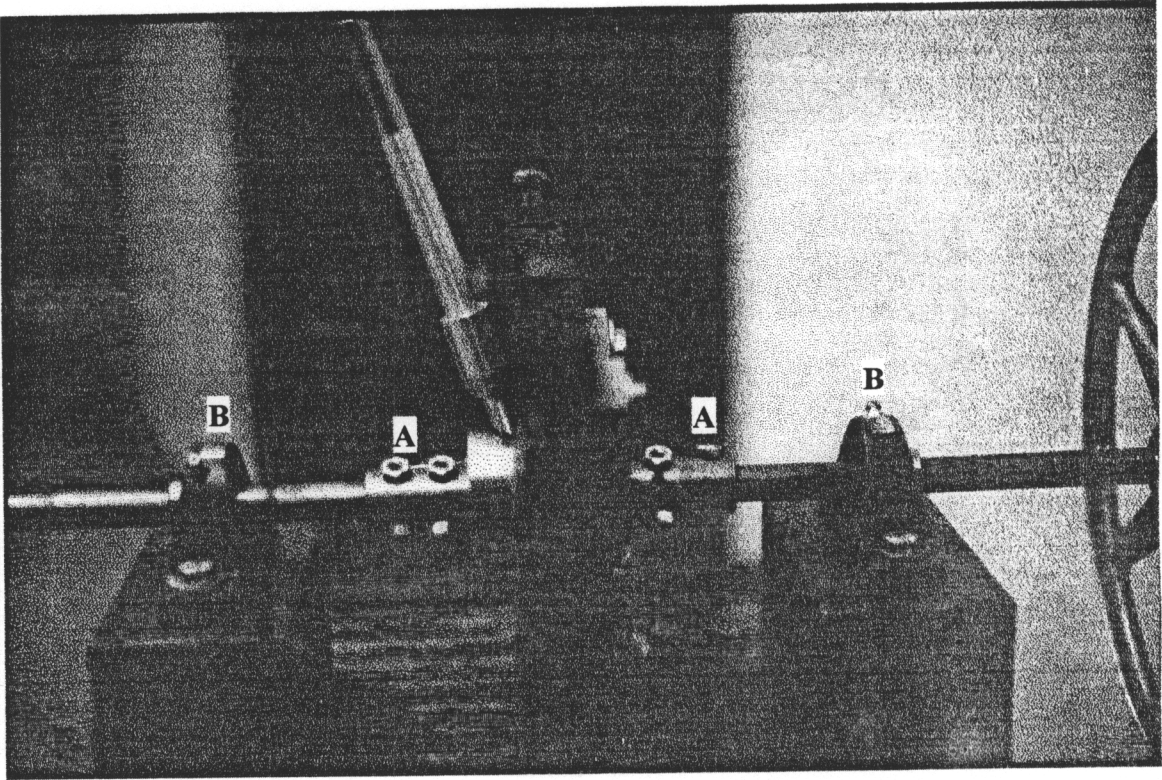


Figure 1. Test Jig Bearing Housing and Clamping Tabs

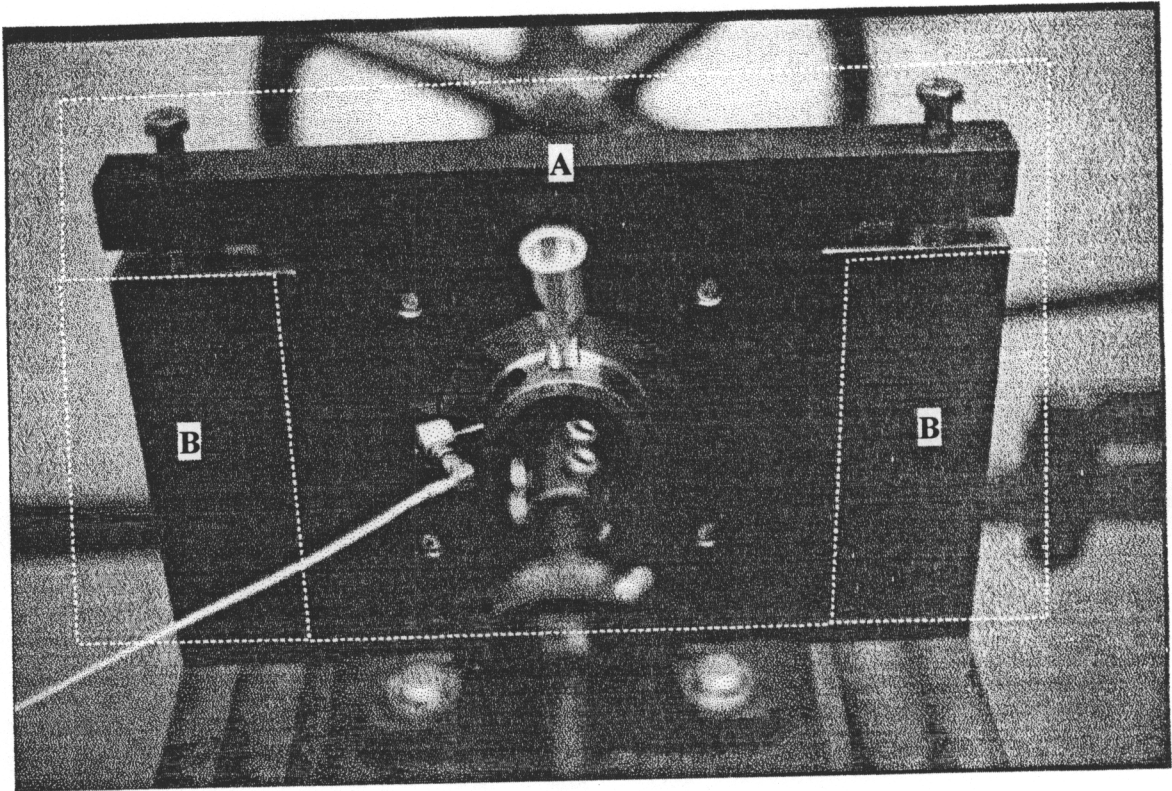


**LEGEND**

**A. Shaft Collar**

**B. Pillow Block Bearings**

**Figure 2. Test Jig Shaft Collars and Support Bearings**



**LEGEND**

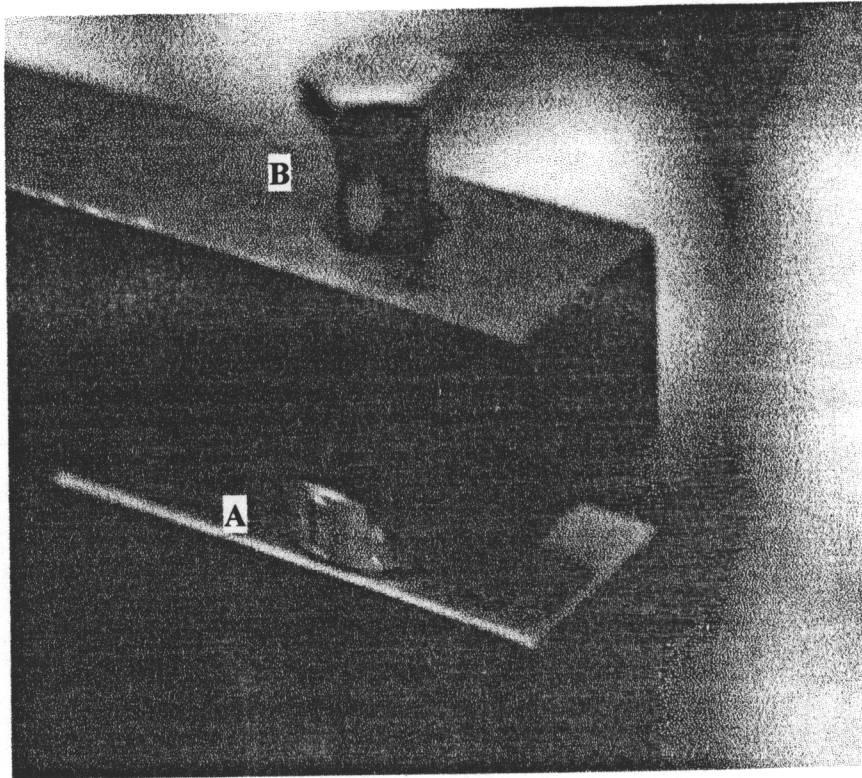
**A. Center Section**

**B. Supports**

**Figure 3. Test Jig Loading Mechanism**

load was controlled by two blocks (Figure 4) fabricated to allow shaft deflections corresponding to approximately 2228 and 4455 N (500 and 1000 lb).

The mounting holes for the accelerometer and microphone were drilled and tapped in the bearing housing 90 degrees apart (Figure 5). The mounting screw for the accelerometer was positioned to impact the outer race of the test bearing. An apparatus designed to hold the microphone was mounted to provide direct audio access to the cavity surrounding the test bearing. The test jig and drive motor were mounted to sub-frames that were bolted to the main frame (Figure 6). The drive motor sub-frame provided for belt tension adjustment. Both sub-frames were separated from the main frame by rubber blocks to minimize the direct transmission of motor noise. The shaft was driven a belt and pulleys sized to provide approximately 540 rpm based on the rated drive motor speed. Actual shaft speeds were 590 rpm ( $\pm 2.5$  rpm).

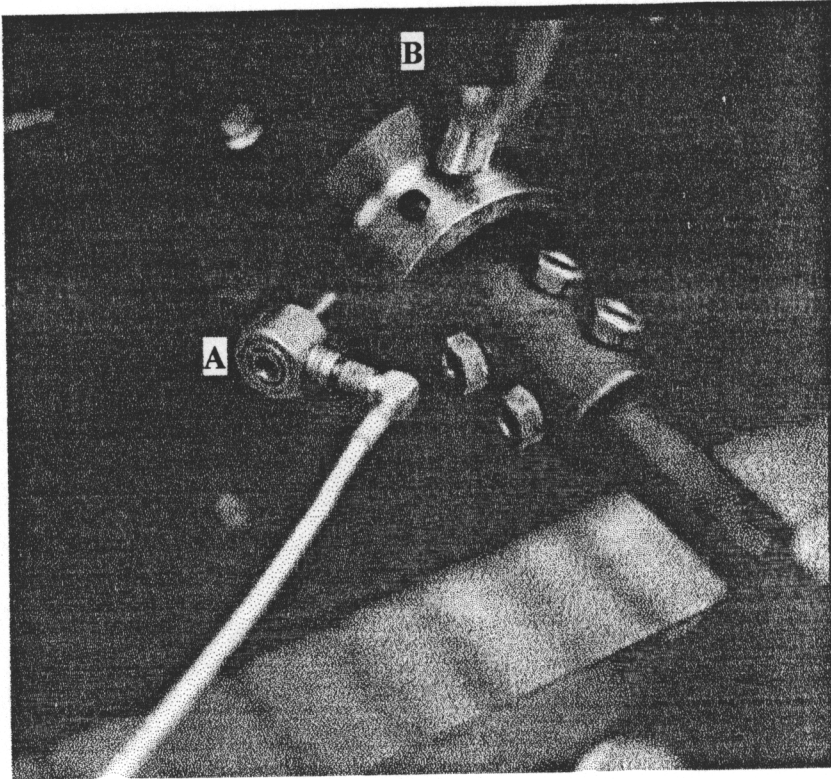


**LEGEND**

**A. Load Block**

**B. Loading Bolt**

**Figure 4. Test Jig Load Control Blocks and Loading Bolt**

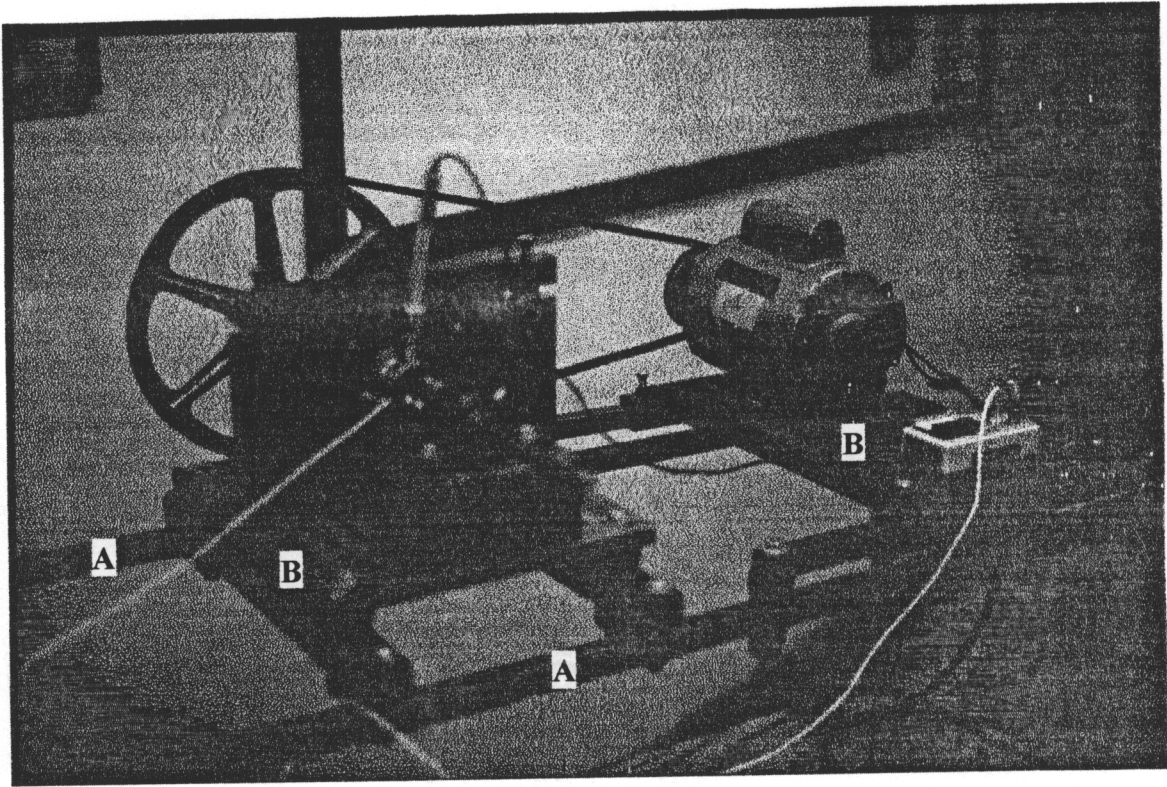


**LEGEND**

**A. Accelerometer**

**B. Microphone**

**Figure 5. Test Jig Sensor Mounting**



**LEGEND**

**A. Main Frame**

**B. Sub-Frames**

**Figure 6. Test Jig Main Frame and Sub-Frames Assembly**

## 4.2 Data Acquisition and Processing

A data acquisition system was developed to acquire and amplify the signal from both sensors, present the signal graphically in both the time and frequency domains, and digitize and store the time based signal for further processing and examination. Figure 7 is a block diagram of the data acquisition system. The signal from the accelerometer (Kistler\* 9712A5 Quartz Force Transducer) was amplified by a charge amplifier (Kistler Piezotron Coupler 5112). The signal from the microphone (Realistic Condenser Microphone) was amplified by an LM324 operational amplifier configured to provide a gain of approximately ten (Stout, 1976).

The amplified signal from both sensors was digitized and presented graphically by an oscilloscope (Tektronix 2232 100 MHz Digital Storage Oscilloscope). A Data 6000 Spectrum Analyzer and an ADC SA-1 Frequency Spectrum Analyzer were used to provide quick visual analysis during data collection. The digitized signal from the oscilloscope was transferred to an IBM PC through and IEEE-488 (GPIB) data acquisition card. Data received from the oscilloscope were in ASCII format containing

- \* Use of trade names in this publication does not imply endorsement by the authors of the products named.

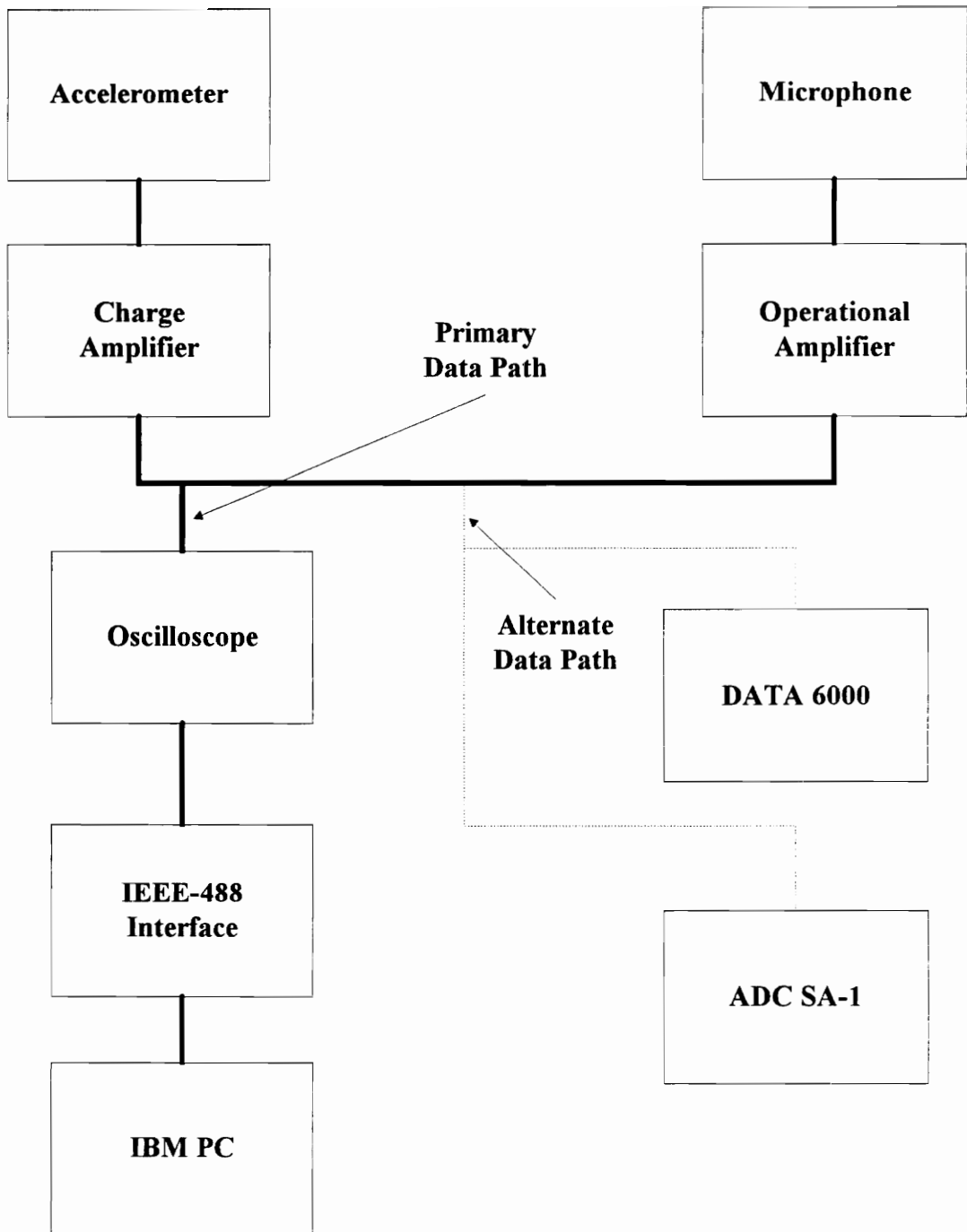


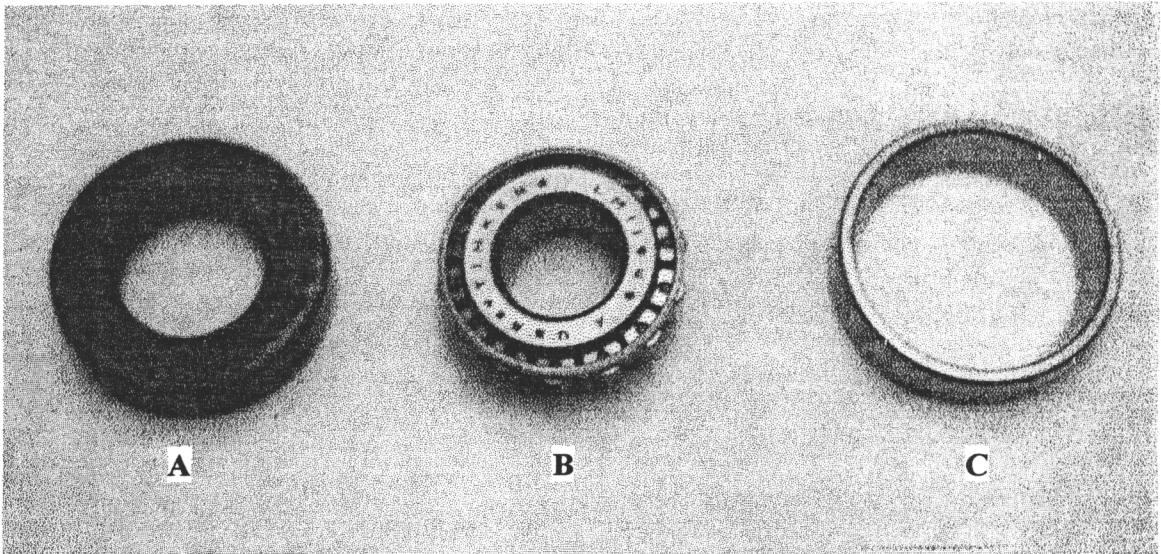
**Figure 7. Block Diagram of Data Acquisition System**

1024 time-voltage data points. A Fast Fourier Transform (FFT) function in the PSI-Plot software package (Poly Soft International) was used to transform the data to the frequency domain. The transformed data were transferred to Borland's Quattro Pro for Windows 5.0 for graphical presentation and statistical analysis. The FFT function in Quattro Pro was not used because the output is a text string of the complex number of the transform. This format makes it difficult to perform further analysis or present the data graphically. A two-sample paired t-test for means function in Quattro Pro was used to perform statistical analysis.

### **4.3 Experimental Procedure**

The test bearing was a single-row, straight-bore, tapered roller bearing (Timken LM11949 cone and LM11910 cup set, Figure 8). This bearing was chosen because it is of a type and specific geometry typical to agricultural applications and an example of this bearing had recently been replaced in a unit of farm machinery. Multiple types and sizes of bearings were not examined as the underlying principles of this type of monitoring have already been proven and are not specific to roller element bearing type or geometry.

Two separate experiments were performed. The first experiment compared the vibration signature of a bearing that had reached its useful life in a field environment with that of a new bearing. The purpose of this experiment was to determine the ability of the microphone to detect a significant difference in the vibration signatures of a new bearing and a bearing in an advanced stage of wear. Identical tests were performed using an accelerometer (Kistler 9712A5 Quartz Force Transducer) for sensor performance comparison. The second experiment used a set of new bearings altered to simulate an early stage of wear. Twelve new bearings were examined and their vibration signatures were recorded. The bearings were then altered by burning 0.005 inch (0.127 millimeter)



**LEGEND**

**A. CR Services 10034 Grease Seal**

**B. Timken LM11949 Cone**

**C. Timken LM11910 Cup**

**Figure8. Test Bearing: Timken LM11949 Cone and LM11910 Cup Set and CR Services 10034 Grease Seal**

diameter, 0.005 inch (0.127 millimeter) deep holes in their surfaces using electrical discharge machining equipment. Bearing samples 1 through 3 had defects placed on a single roller, bearing samples 4 through 6 had defects placed on three randomly selected rollers, bearing sample 7 through 9 had defects placed on the outer race, and bearing samples 10 through 12 were unaltered. Altered bearings were examined and their vibration signatures were recorded for comparison with the signatures obtained from the same bearing prior to alteration.

During all tests, the operational sensor was placed in the loaded zone directly above the shaft. Figure 5 shows the microphone in the operational position. During tests involving the bearing sample with outer race defects, the bearings were installed with the defects located in the loaded zone.

It was necessary to determine the gain factor for the operational amplifier used to amplify the signal from the microphone and the time base and data block size for the oscilloscope used to digitize the sensor signal prior to performing laboratory experiments. The gain factor for the charge amplifier was determined to be approximately ten by comparing the input and output waveforms from a 100 Hz sine wave generated by a signal generator (B&K Precision 3020 Sweep/Function Generator). The external components of the operational amplifier were then sized to obtain a gain factor of approximately ten using relationships for a non-inverting operational amplifier (Stout, 1976).

The time base and data block size settings on the oscilloscope control the frequency domain and resolution of the FFT output. The oscilloscope could be configured to provide data in 1024 (1K) or 4096 (4K) data point blocks. The time base was defined

in units of time per display unit. Since the oscilloscope displayed only 1K of data in both the 1K and 4K data storage modes, the sampling interval was independent of data block size. The larger data block increases the number of data points per frequency unit by increasing the size of the sampling window and does not affect the FFT frequency domain. Increasing the time base increases the sampling interval and therefore decreases the upper bound of the FFT frequency domain. The defect frequencies produced by the test bearing controlled the selection of the frequency domain limits and therefore the selection of the time base. The defect frequencies characteristic of the test bearing were estimated using equations [2] through [5] and are presented in Table 1.

As was discussed, harmonics (multiples), sums, differences, and averages of any or all defect frequencies may be present. Therefore, the upper limit of the frequency domain must exceed the highest defect frequency to prevent exclusion of the defect frequency harmonics. However, if the upper limit of the frequency domain is relatively high, the 4K sampling window must be used to maintain acceptable resolution in the processed signal. The larger sampling window requires considerably increased data storage and processing capabilities and might not be economically feasible in a mobile application. Furthermore, the increased detail obtained using the 4K sampling window only confuses graphical analysis of the processed signal. After consideration of these factors, the 1K sampling window and a time base of 50 milliseconds was chosen. This selection provided a frequency domain of 0 to 1000 Hz and a resolution of one data point for each 1.95 Hz.

**Table 1. Test Bearing Characteristic Defect Frequencies**

Defect Location		Frequency	
		(cycles/min)	(Hz)
Inner Race	BPFI	4921	82.0
Outer Race	BPFO	3339	55.7
Roller Element	BSF	1463	24.4
Roller Cage	FTF	239	4.0
Motor Noise	MF	590	9.8

Note: Defect frequencies only applicable for the selected bearing at 590 rpm.

The selected bearing was rated at 7930 N (1780 lb) radial load and 4080 N (917 lb) thrust load corresponding to an  $L_{10}$  life of 3000 hours at 500 rpm. Test loads of approximately 2228 and 4455 N (500 and 1000 lb) were selected, referred to in the remainder of this study as Load C and Load D, respectively. Both loads are significantly less than the rated load to allow for dynamic loading due to vibration without exceeding the rated loading. Shaft deflection corresponding to the test loads was estimated and load blocks were fabricated to provide the desired shaft deflections. The shaft, including the collars, was assumed to be one solid piece with a point load at the center of the test bearing and point loads at the centers of the support bearings. A modulus of elasticity of 200 GPa ( $30 \times 10^6$  psi) was used in shaft deflection estimates. Resulting loads applied to the test bearings are not exact values. However, the load magnitude is of little interest except that it should be consistent for comparison of results across a given group of test bearings.

The output from the oscilloscope represents a finite sample of the continuous signal acquired by the sensors. In order to obtain a representative sample of the sensor signal, ten sample data blocks were taken for each test case. Data acquisition required approximately 9 seconds per data block. A simple program was written in FORTRAN to provide a fixed length delay of approximately 30 seconds. The delay loop and waveform acquisition program were executed by a batch file to ensure equal spacing of the samples. Shaft speed was measured using a speed indicator (Hasler 71503 Type A) three times during the run and values were averaged.

Samples for each test bearing were taken for both the accelerometer and microphone for test loads C and D. The time-voltage data were transformed to the frequency domain and the ten samples were averaged. A two-sample paired t-test for means at an alpha level of 0.05 was performed on the transformed and averaged signal. The t-test was performed on the portion of the transformed and averaged signal from 0 to 250 Hz and the portion from 250 to 1000 Hz as well as on the entire signal for the data obtained from the comparison of new and field-worn bearings. The t-test was performed only on the portion of the transformed and averaged signal below 250 Hz for the data obtained from the comparison of new and artificially worn bearings. The data were also analyzed graphically to identify spikes in the difference between the transformed and averaged signal for the field-worn and new bearings at the defect frequencies.

## **Chapter V**

### **Results and Discussion**

#### **5.1 Comparison of New and Field-Worn Bearings**

Data were collected for new and field-worn bearings using the microphone and accelerometer under test loads C and D. Representative plots of the signals acquired from the new and field-worn bearings are illustrated in Figures 9 and 10. Representative plots of the difference in the transformed and averaged signal from the new and field-worn bearings are illustrated in Figures 11 and 12. Appendix A contains a graphical presentation of all data sets.

The data were analyzed using a two-sample, paired t-test for means and a null hypothesis of  $\mu_{\text{worn}} = \mu_{\text{new}}$  (Table 2). All comparisons of worn and new bearings resulted in statistically significant differences (maximum value of p was 0.0018).

# FFT for New and Field-Worn Bearings

Microphone, Load C

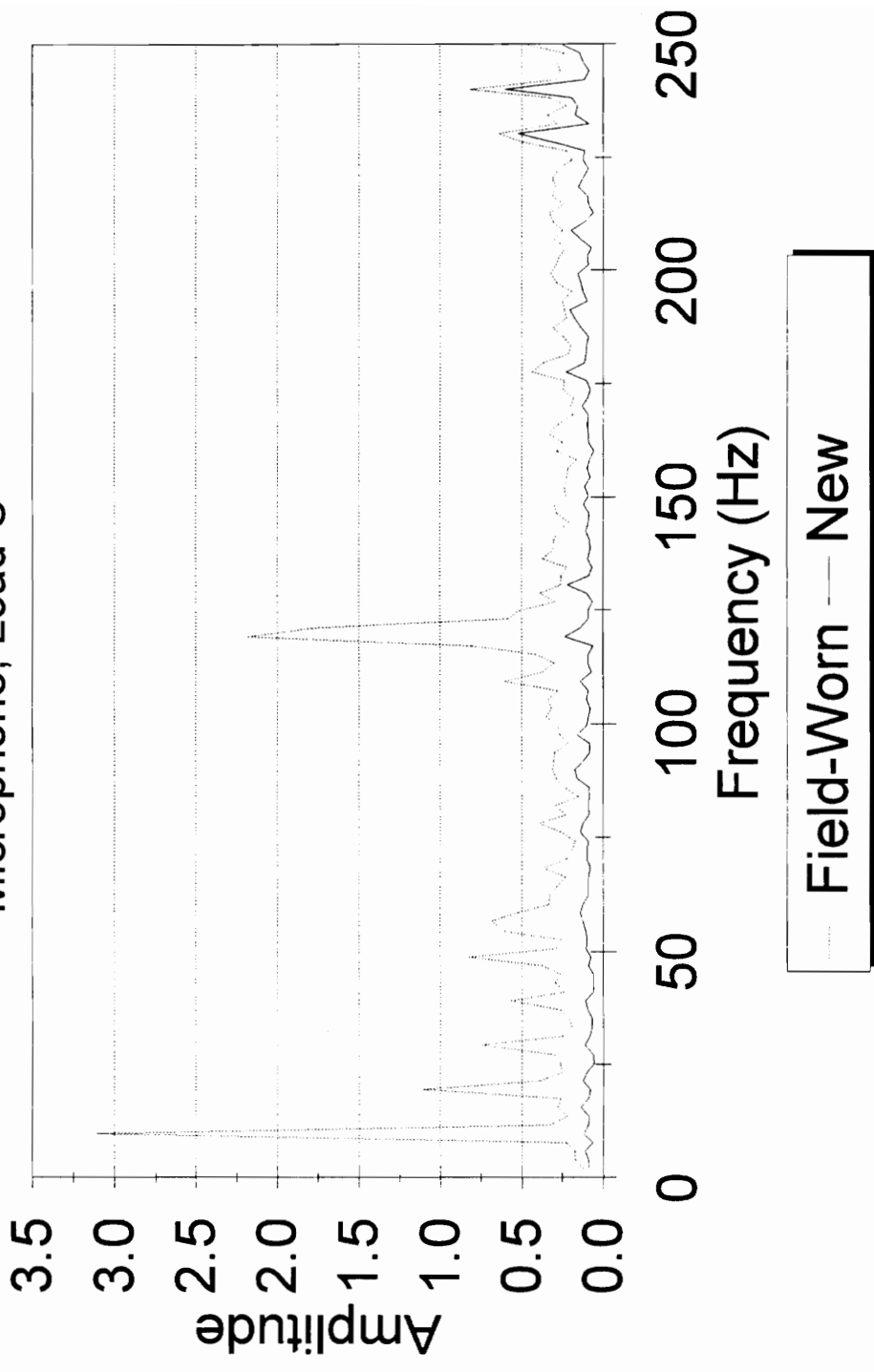


Figure 9. FFT for New and Field-Worn Bearings: Microphone, Load C

# FFT for New and Field-Worn Bearings

Accelerometer, Load D

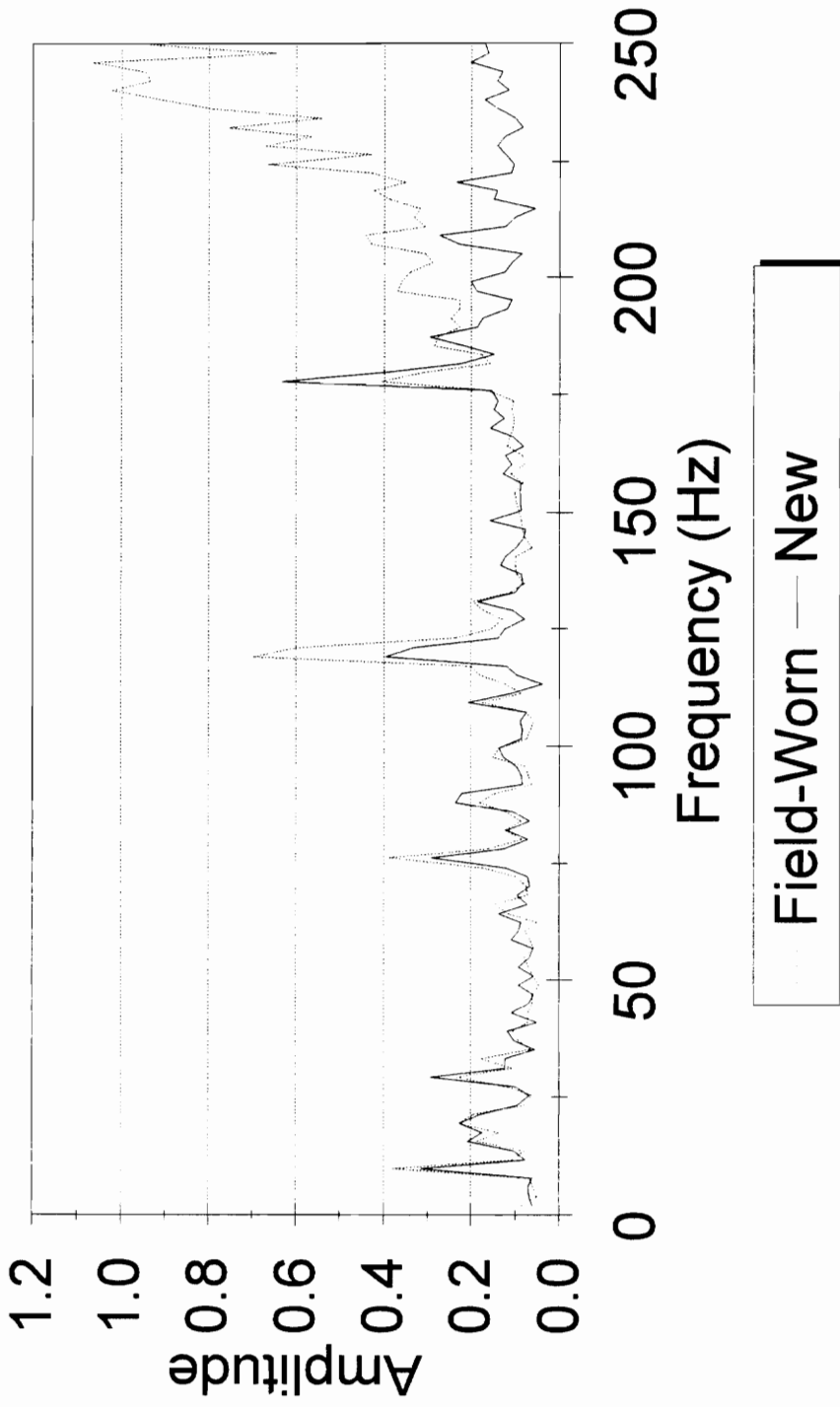


Figure 10. FFT for New and Field-Worn Bearings: Accelerometer, Load D

## Difference in New and Field-Worn FFT's

Microphone, Load C

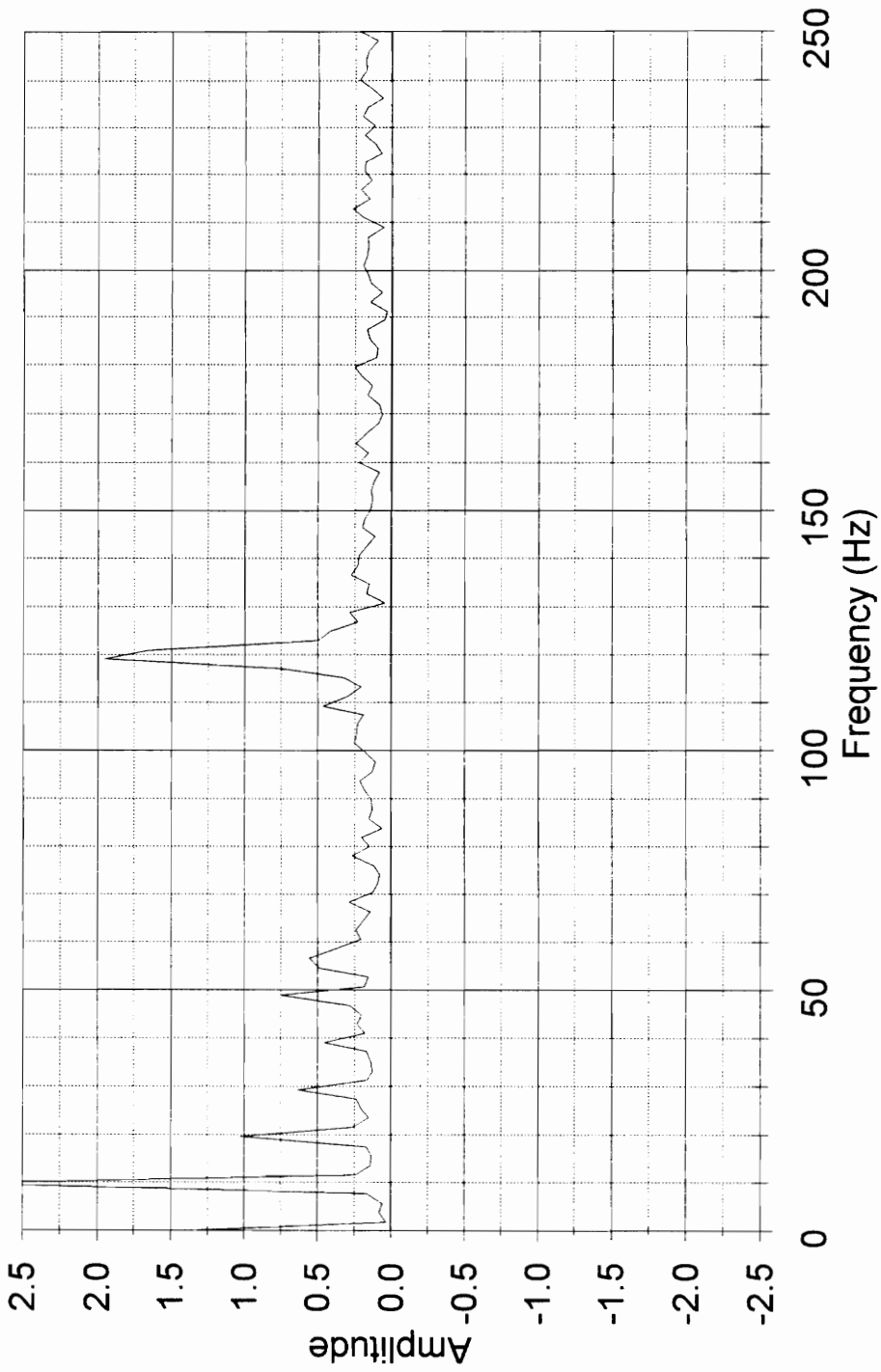


Figure 11. Difference in New and Field-Worn FFT's: Microphone, Load C

### Difference in New and Field-Worn FFT's Accelerometer, Load D

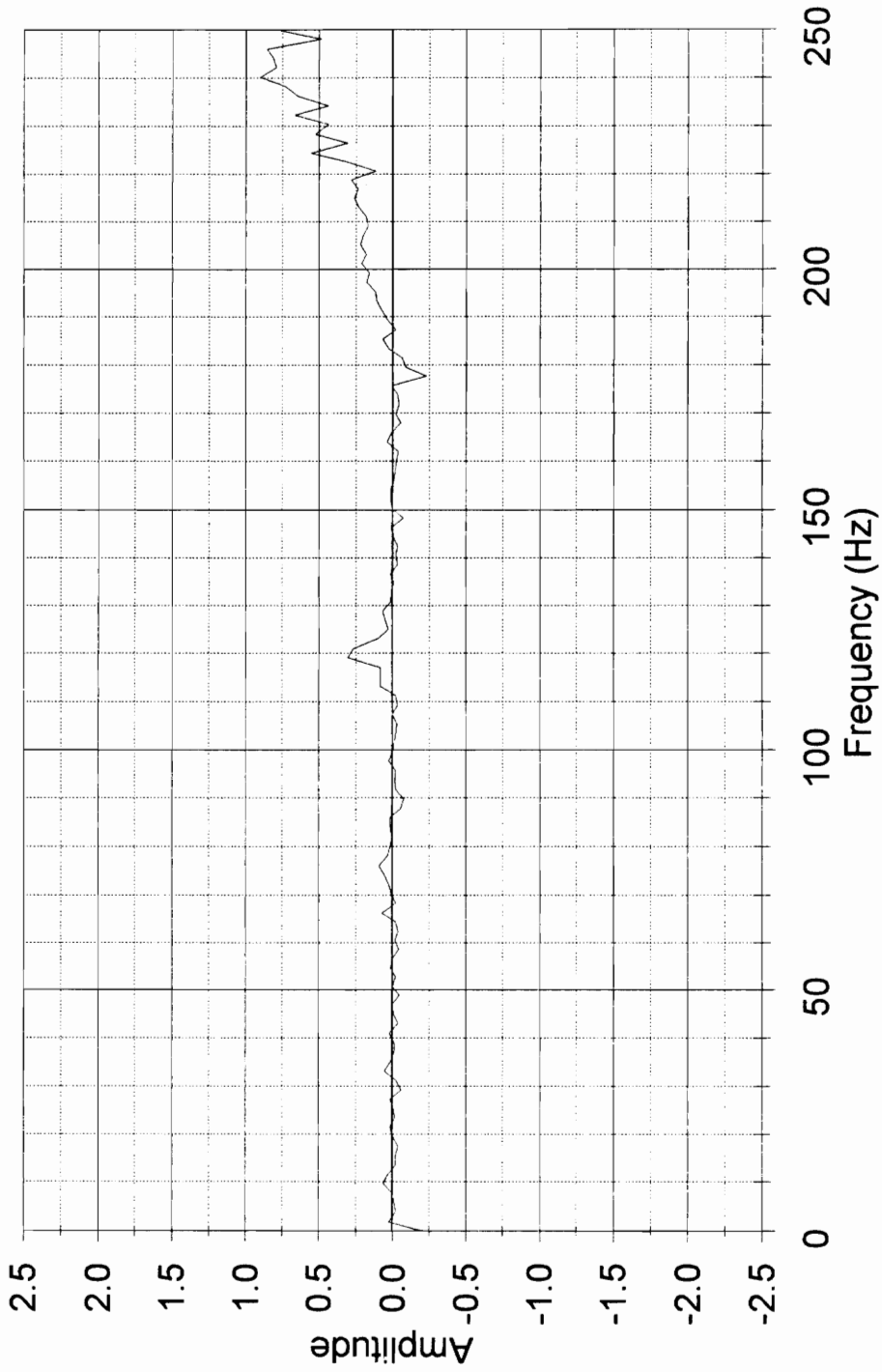


Figure 12. Difference in New and Field-Worn FFT's: Accelerometer, Load D

**Table 2. Statistical Results: Comparison of New and Field-Worn Bearings**

Load	Sensor	Frequency Range (Hz)	t	t-critical	p	Pearson's Correlation
C	Mic	0-1000	28.06	1.96	0.0000	0.72
		0-250	8.18	1.98	0.0000	0.87
		250-1000	29.63	1.97	0.0000	0.37
D	Mic	0-1000	14.92	1.96	0.0000	0.43
		0-250	3.64	1.98	0.0004	0.73
		250-1000	16.03	1.97	0.0000	0.23
C	Accel	0-1000	4.26	1.96	0.0000	0.26
		0-250	3.18	1.98	0.0018	0.41
		250-1000	14.15	1.97	0.0000	0.41
D	Accel	0-1000	8.27	1.96	0.0000	0.27
		0-250	5.00	1.98	0.0000	0.36
		250-1000	6.71	1.97	0.0000	0.21

However, results for the accelerometer may be misleading. The desired outcome is a definite trend of increasing signal strength as wear progresses, especially in the frequency range that contains the defect frequencies and the first few multiples of the defect frequencies. The difference in the signals (worn minus new) acquired by the microphone (Figure 11) exhibits the desired trend. However, the difference in the signal acquired using the accelerometer (Figure 12) does not exhibit the desired trend.

The Pearson's Correlation Coefficient (PCC) is a measure of the validity of pairing data: the higher the coefficient, the more closely the data follows the same general trend. The values of the PCC for the data acquired using the microphone indicate a strong trend in the data at frequencies below 250 Hz and a much weaker trend in the data above 250 Hz. These results are desirable as the defect frequencies and the first few multiples of the defect frequencies are below 250 Hz. The values of the PCC for the data acquired using the accelerometer are similar in that the strongest trends are evident below 250 Hz, but the trends in general are much weaker than the trends indicated in the microphone data. As a result, further examination of the data were restricted to the 0 to 250 Hz frequency range.

Results of the statistical comparison are confirmed by graphical analysis of the difference in the FFT for worn and new bearings (Figures 11 and 12). The data acquired using the microphone indicates a stronger signal from the worn bearing at nearly every frequency (Figures 9 and 11). Defect frequencies can be found in Table 1. Closer examination reveals distinct peaks in the microphone data at 10,20,30, and 40 Hz. These peaks represent the first four multiples of the motor noise (MF). Another peak at slightly less than 50 Hz is twice the BSF. A peak between 50 and 60 Hz corresponds to the

BPFO and another peak slightly less than 120 Hz corresponds to twice the BPFO. Small peaks at approximately 110 and 130 Hz may be developing sidebands of  $\pm MF$ . In contrast, it is difficult to identify any discernible pattern in the data acquired from the accelerometer (Figure 12). There is a single peak in the defect frequency range, but absence of a motor noise signal casts considerable doubt on its significance. The path of vibration to the accelerometer was through the material in the bearing housing. The damping of the vibration signature by the surrounding material may have prevented significant acquisition by the accelerometer. The path of the vibration to the microphone was through the air surrounding the bearing as well as the bearing housing. This path difference could explain the discrepancies between the signals acquired by the microphone and the accelerometer. Another possible explanation is that the measurement of acceleration as a means of vibration signature acquisition tends to overemphasize the higher frequencies (Berry, 1991). However, the microphone was able to identify defect frequencies in the lower end of the spectrum.

## 5.2 Comparison of New and Artificially Worn Bearings

Ninety-six data sets were collected, forty-eight for new bearings and forty-eight for artificially worn bearings (twelve bearing samples, two sensors, and two test loads). The data were sorted into forty-eight groups consisting of the new and altered bearing data for each treatment (bearing sample, sensor, and load). The data within each group were analyzed using a two-sample, paired t-test for means and a null hypothesis of  $\mu_{\text{worn}} = \mu_{\text{new}}$  (Tables 3 through 6).

Most comparisons of worn and new bearings resulted in statistically significant differences (p-value less than 0.01). Six data sets did not exhibit significant differences in the transformed and averaged signal for new and altered bearings. Table 7 illustrates the composition of these six data sets. Forty-two data sets exhibited statistically significant differences based on the p-value. Table 8 illustrates the composition of these forty-two data sets. Of these forty-two, thirteen of the data sets also had reasonably significant values for the PCC (greater than 0.6). Table 9 illustrates the composition of these thirteen data sets. These thirteen data sets were divided among the treatments: one from the single roller defect group, three from the multiple roller defect group, four from the single race

**Table 3. Statistical Results: Comparison of New and Artificially Worn Bearings, Bearings 1-3**

	Sensor	Load	t	p	Pearson's Correlation
Bearing 1	Accel.	C	23.46	0.0000	0.0690
		D	3.73	0.0003	0.0654
	Mic.	C	37.48	0.0000	0.0578
		D	31.79	0.0000	0.0243
Bearing 2	Accel.	C	13.04	0.0000	0.4644
		D	15.47	0.0000	0.6827
	Mic.	C	46.63	0.0000	0.1071
		D	44.70	0.0000	-0.0360
Bearing 3	Accel.	C	2.25	0.0259	0.3861
		D	1.85	0.0672	0.2634
	Mic.	C	32.49	0.0000	0.2282
		D	11.81	0.0000	0.0214

Results for Paired Two-sample t-test for Means

128 Observations per set

t-critical (two-tailed) = 1.98

Bearing Samples 1-3: One roller defect

**Table 4. Statistical Results: Comparison of New and Artificially Worn Bearings, Bearings 4-6**

	Sensor	Load	t	p	Pearson's Correlation
Bearing 4	Accel.	C	7.35	0.0000	0.7357
		D	0.03	0.9791	0.7643
	Mic.	C	19.25	0.0000	-0.1893
		D	26.75	0.0000	-0.2923
Bearing 5	Accel.	C	14.00	0.0000	0.5144
		D	7.76	0.0000	0.3031
	Mic.	C	16.82	0.0000	-0.0650
		D	22.65	0.0000	-0.3280
Bearing 6	Accel.	C	12.05	0.0000	0.8686
		D	-4.98	0.0000	0.8518
	Mic.	C	19.42	0.0000	-0.2856
		D	25.31	0.0000	-0.4016

Results for Paired Two-sample t-test for Means

128 Observations per set

t-critical (two-tailed) = 1.98

Bearing Samples 4-6: Three roller defects

**Table 5. Statistical Results: Comparison of New and Artificially Worn Bearings, Bearing 7-9**

	Sensor	Load	t	p	Pearson's Correlation
Bearing 7	Accel.	C	-0.47	0.6365	0.6786
		D	-7.05	0.0000	0.6393
	Mic.	C	31.57	0.0000	0.2904
		D	10.94	0.0000	0.0318
Bearing 8	Accel.	C	2.86	0.0050	0.6383
		D	-0.42	0.6758	0.4680
	Mic.	C	21.48	0.0000	0.3322
		D	16.52	0.0000	0.7107
Bearing 9	Accel.	C	-18.58	0.0000	0.6557
		D	-18.51	0.0000	0.5808
	Mic.	C	43.79	0.0000	0.2127
		D	8.32	0.0000	-0.0444

Results for Paired Two-sample t-test for Means

128 Observations per set

t-critical (two-tailed) = 1.98

Bearing Samples 7-9: One outer race defect

**Table 6. Statistical Results: Comparison of New and Artificially Worn Bearings, Bearings 10-12**

	Sensor	Load	t	p	Pearson's Correlation
Bearing 10	Accel.	C	-18.09	0.0000	0.6477
		D	-32.03	0.0000	0.4879
	Mic.	C	12.53	0.0000	0.6255
		D	9.81	0.0000	0.3943
Bearing 11	Accel.	C	2.05	0.0427	0.1885
		D	-23.09	0.0000	0.1883
	Mic.	C	11.66	0.0000	-0.1766
		D	9.30	0.0000	-0.0378
Bearing 12	Accel.	C	-7.67	0.0000	0.8360
		D	-6.79	0.0000	0.8840
	Mic.	C	16.65	0.0000	0.4836
		D	15.66	0.0000	0.9310

Results for Paired Two-sample t-test for Means

128 Observations per set

t-critical (two-tailed) = 1.98

Bearing Samples 10-12: Unaltered

**Table 7. Statistical Results: Test Cases with No Significant Difference Between New and Altered Bearings**

Bearing Sample	Sensor(s)	Load(s)
3	Accelerometer	C and D
4	Accelerometer	D
7	Accelerometer	C
8	Accelerometer	D
11	Accelerometer	C

Note:

- Bearing Samples 1-3: One roller defect
- Bearing Samples 4-6: Three roller defects
- Bearing Samples 7-9: One outer race defect
- Bearing Samples 10-12: Unaltered

**Table 8. Statistical Results: Test Cases with Significant Differences Between New and Altered Bearings**

Bearing Sample	Sensor(s)	Load(s)
1	Accelerometer Microphone	C and D C and D
2	Accelerometer Microphone	C and D C and D
3	Microphone	C and D
4	Accelerometer Microphone	C C and D
5	Accelerometer Microphone	C and D C and D
6	Accelerometer Microphone	C and D C and D
7	Accelerometer Microphone	D C and D
8	Accelerometer Microphone	C C and D
9	Accelerometer Microphone	C and D C and D
10	Accelerometer Microphone	C and D C and D
11	Accelerometer Microphone	D C and D
12	Accelerometer Microphone	C and D C and D

Note:

- Bearing Samples 1-3: One roller defect
- Bearing Samples 4-6: Three roller defects
- Bearing Samples 7-9: One outer race defect
- Bearing Samples 10-12: Unaltered

**Table 9. Statistical Results: Test Cases with Significant Differences Between New and Altered Bearings and Significant PCC's**

Bearing Sample	Sensor(s)	Load(s)	p	Pearson's Correlation
2	Accelerometer	D	0.0000	0.6827
4	Accelerometer	C	0.0000	0.7357
6	Accelerometer	C	0.0000	0.8686
		D	0.0000	0.8518
7	Accelerometer	D	0.0000	0.6393
8	Accelerometer	C	0.0050	0.6363
	Microphone	D	0.0000	0.7107
9	Accelerometer	C	0.0000	0.6557
10	Accelerometer	C	0.0000	0.6477
	Microphone	C	0.0000	0.6255
12	Accelerometer	C	0.0000	0.8360
		D	0.0000	0.8840
		D	0.0000	0.9310

Note:

- Bearing Samples 1-3: One roller defect
- Bearing Samples 4-6: Three roller defects
- Bearing Samples 7-9: One outer race defect
- Bearing Samples 10-12: Unaltered

defect group, and five from the unaltered group. Ten of these twelve data sets were obtained using the accelerometer and three were obtained using the microphone.

Graphical analyses was also performed on the data. Representative plots (one from each treatment group) of the difference in the transformed and averaged signal from the new and altered worn bearings can be found in Figures 13 through 20. Appendix B contains a graphic presentation of all data sets. Several of the example plots have a spike at approximately 120 Hz. Another spike at approximately 80 Hz is evident in Figure 13. Examples of the first few harmonics of the motor frequency noise appear in Figures 14 and 18. The graphical analyses did not consistently confirm the statistical analyses as the graphical analyses in the first experiment did. Five of the thirteen test cases listed in Table 9 were confirmed by graphical analyses and are listed in Table 10. A positive test result was defined as one in which statistical or graphical results indicate a significant difference in the data set and an identifiable trend in that difference. The eight test cases that were not confirmed by graphical analyses are listed in Table 11 with the proposed reason for rejection by graphical analysis. All eight test cases that were not confirmed by graphical analysis were rejected on the basis of a general negative trend (reduction in bearing vibration signal) or low variability of the signal. A general negative trend is contrary to the desired trend. The PCC is sensitive to low variability and may indicate a significant trend exists in low variability data when a general trend is not present. Table 12 contains a list of thirteen additional test cases that were rejected by the statistical analysis, but show

### Difference in New and Altered FFT's Accelerometer, Load C, Bearing 1

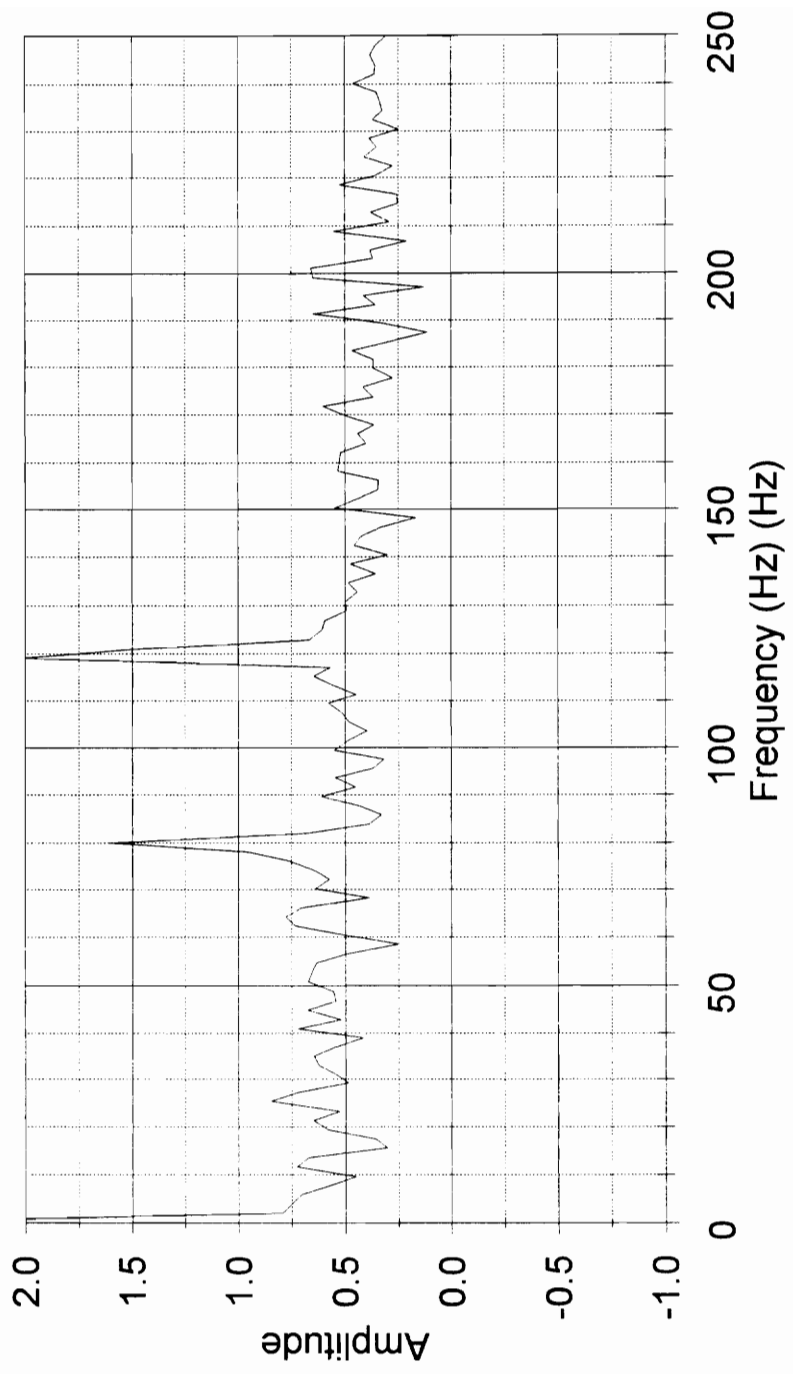


Figure 13. Difference in New and Altered FFT's:  
Accelerometer, Load C, Bearing 1

## Difference in New and Altered FFT's Microphone, Load C, Bearing 3

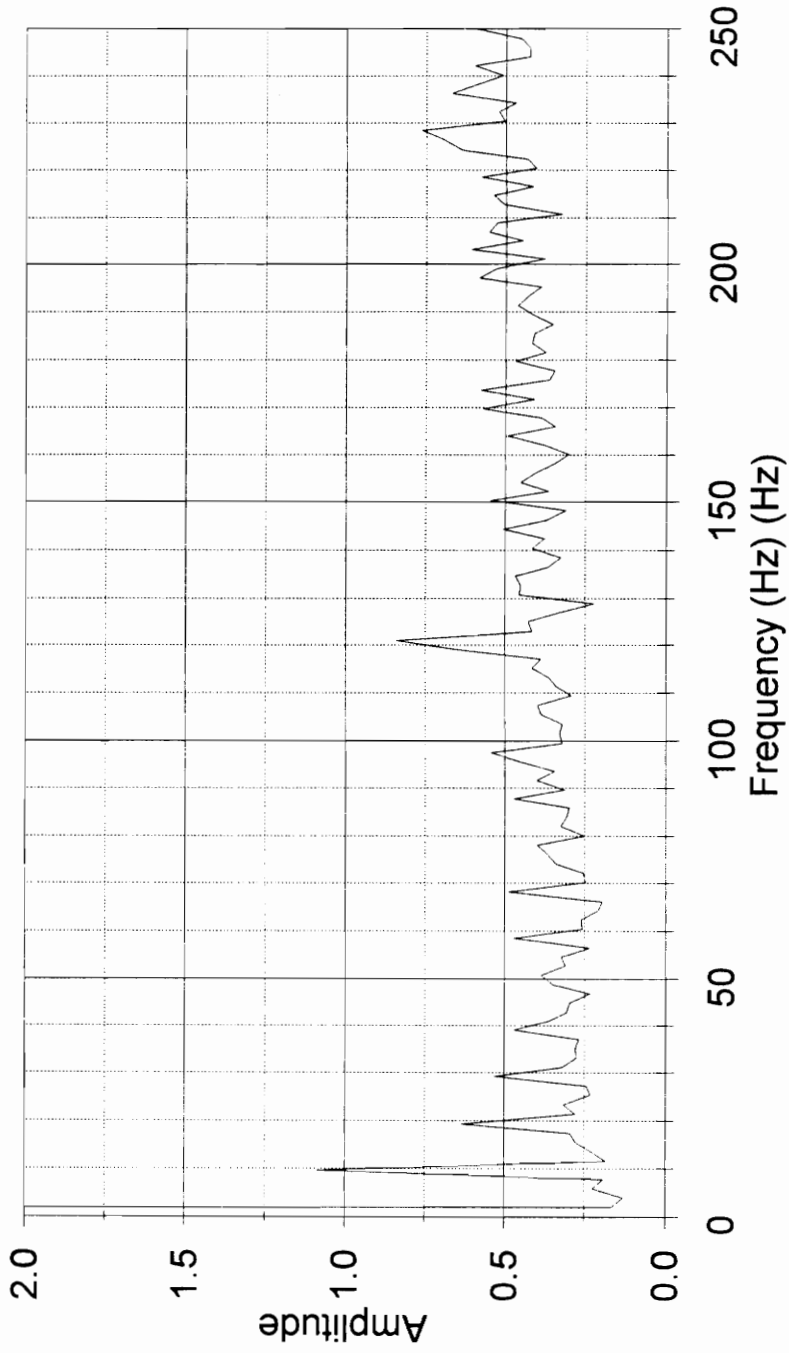


Figure 14. Difference in New and Altered FFT's:  
Microphone, Load C, Bearing 3

### Difference in New and Altered FFT's Accelerometer, Load D, Bearing 4

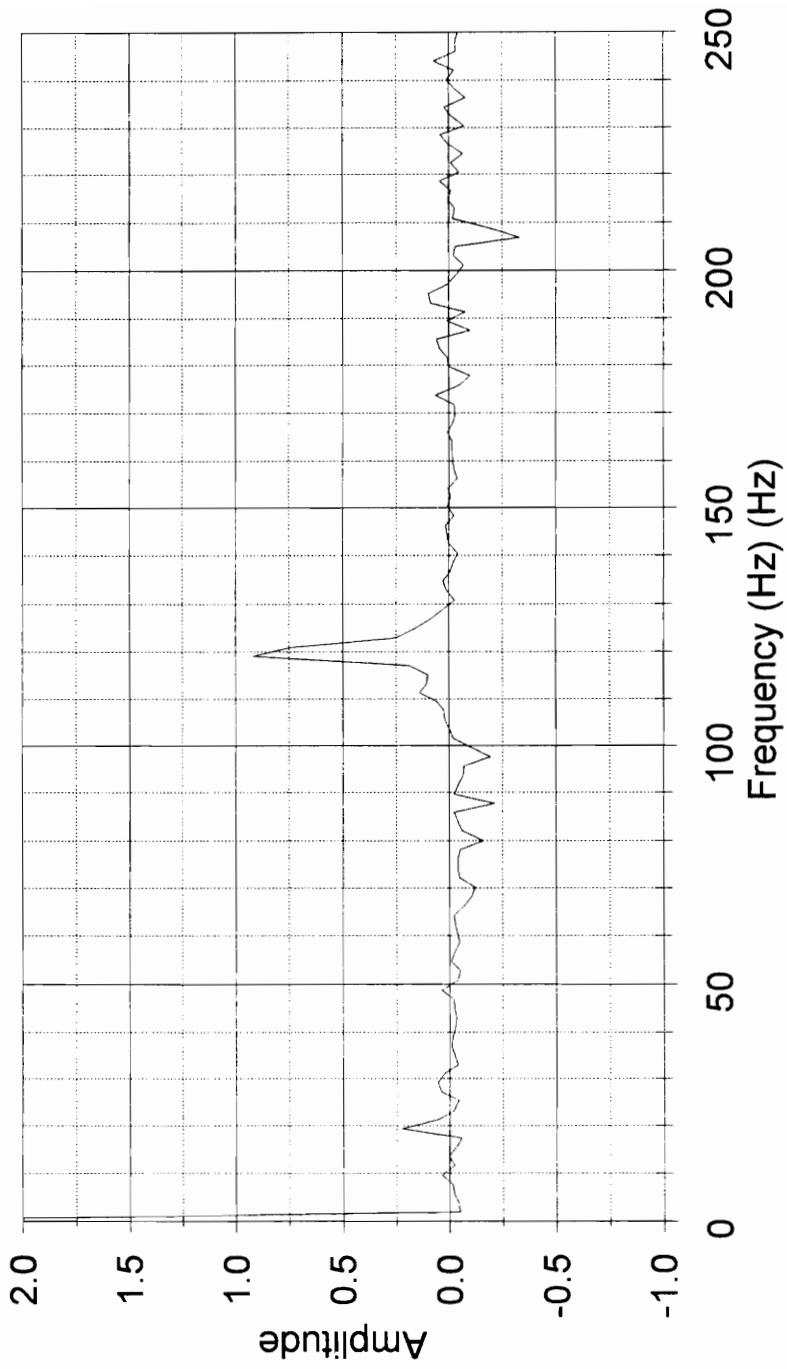


Figure 15. Difference in New and Altered FFT's:  
Accelerometer, Load D, Bearing 4

# Difference in New and Altered FFT's

## Microphone, Load D, Bearing 5

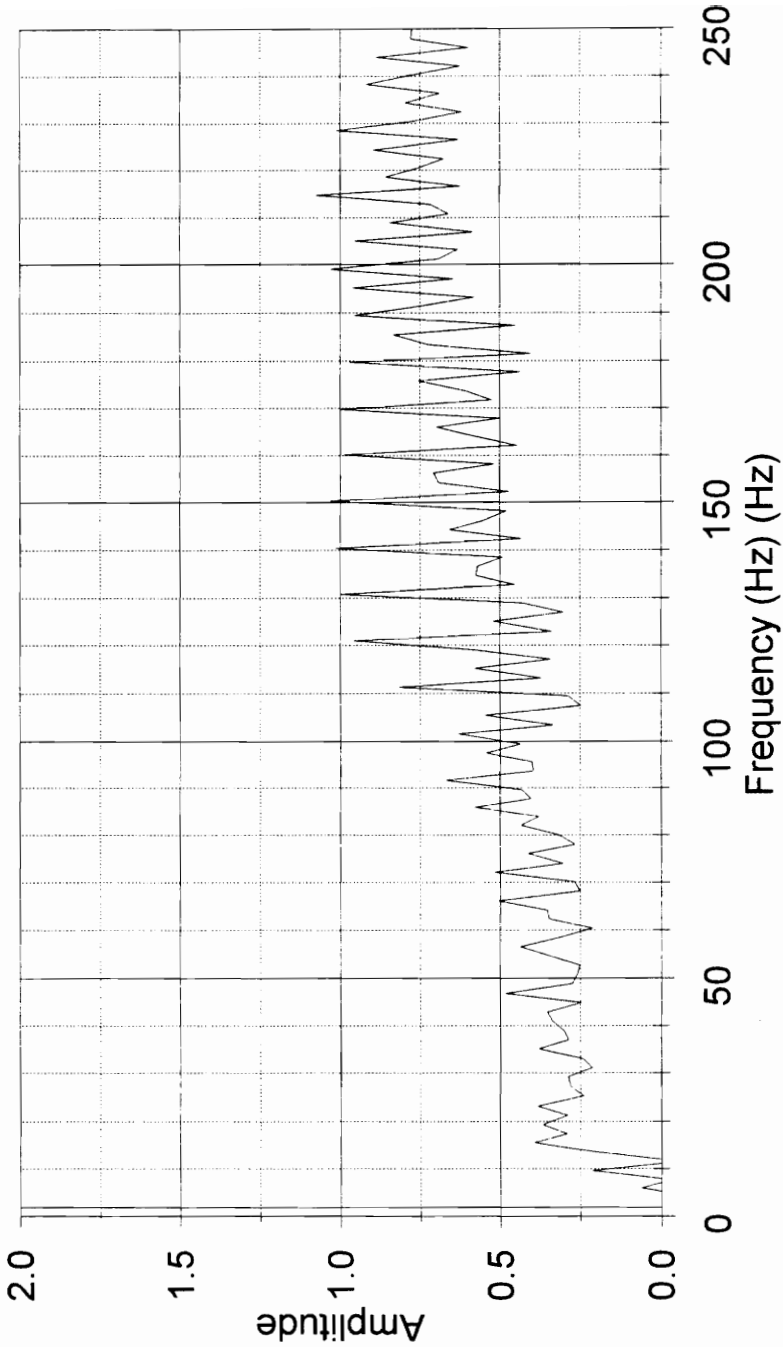


Figure 16. Difference in New and Altered FFT's:  
Microphone, Load D, Bearing 5

## Difference in New and Altered FFT's Accelerometer, Load C, Bearing 8

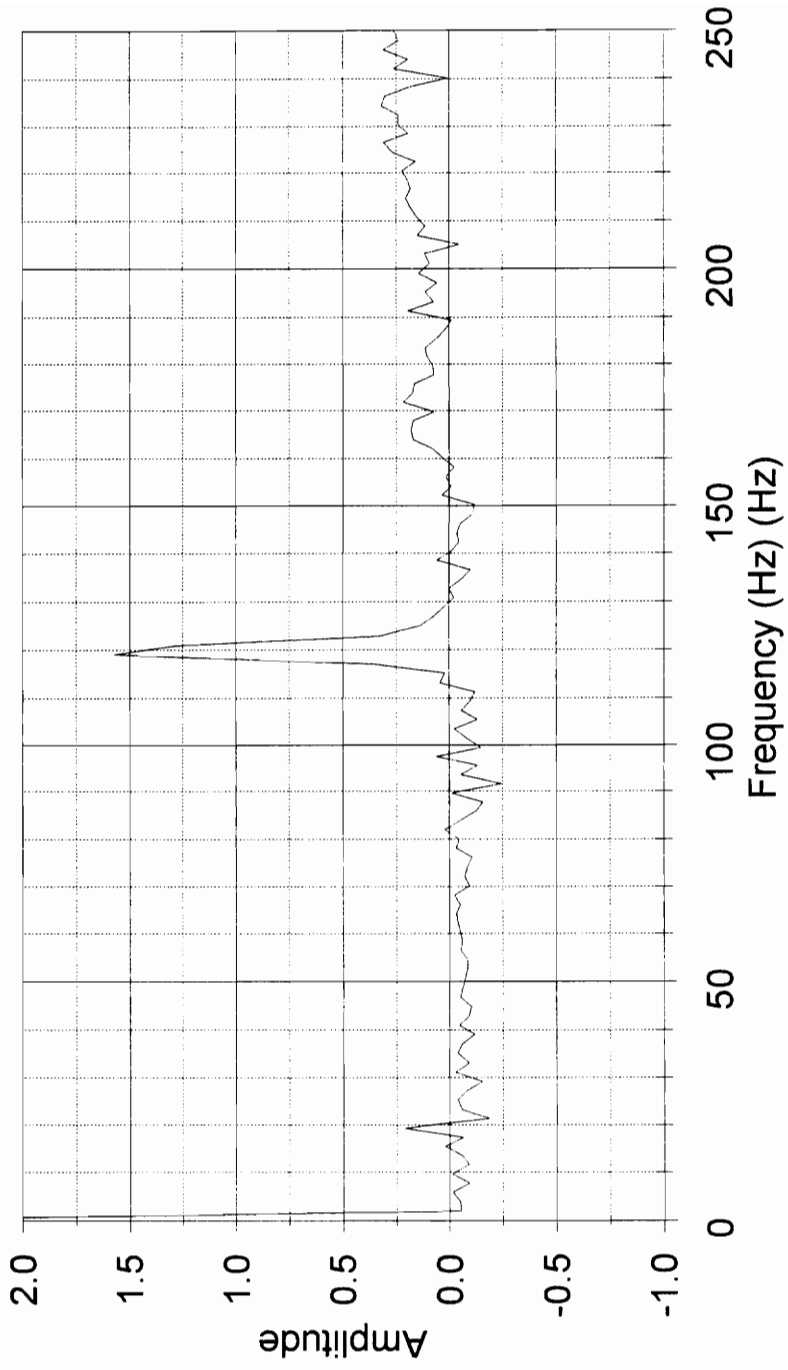


Figure 17. Difference in New and Altered FFT's:  
Accelerometer, Load C, Bearing 8

## Difference in New and Altered FFT's Microphone, Load D, Bearing 7

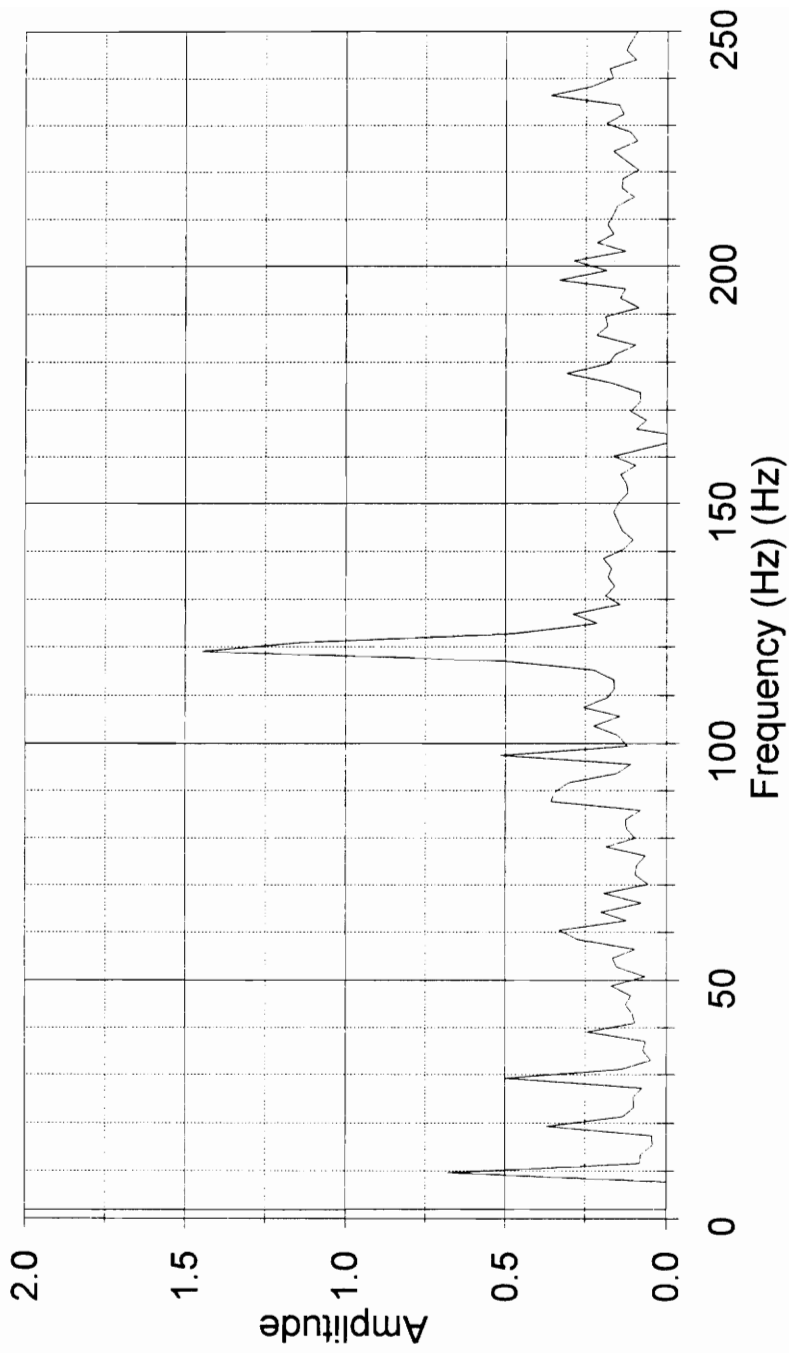


Figure 18. Difference in New and Altered FFT's:  
Microphone, Load D, Bearing 7

### Difference in New and Altered FFT's Accelerometer, Load C, Bearing 11

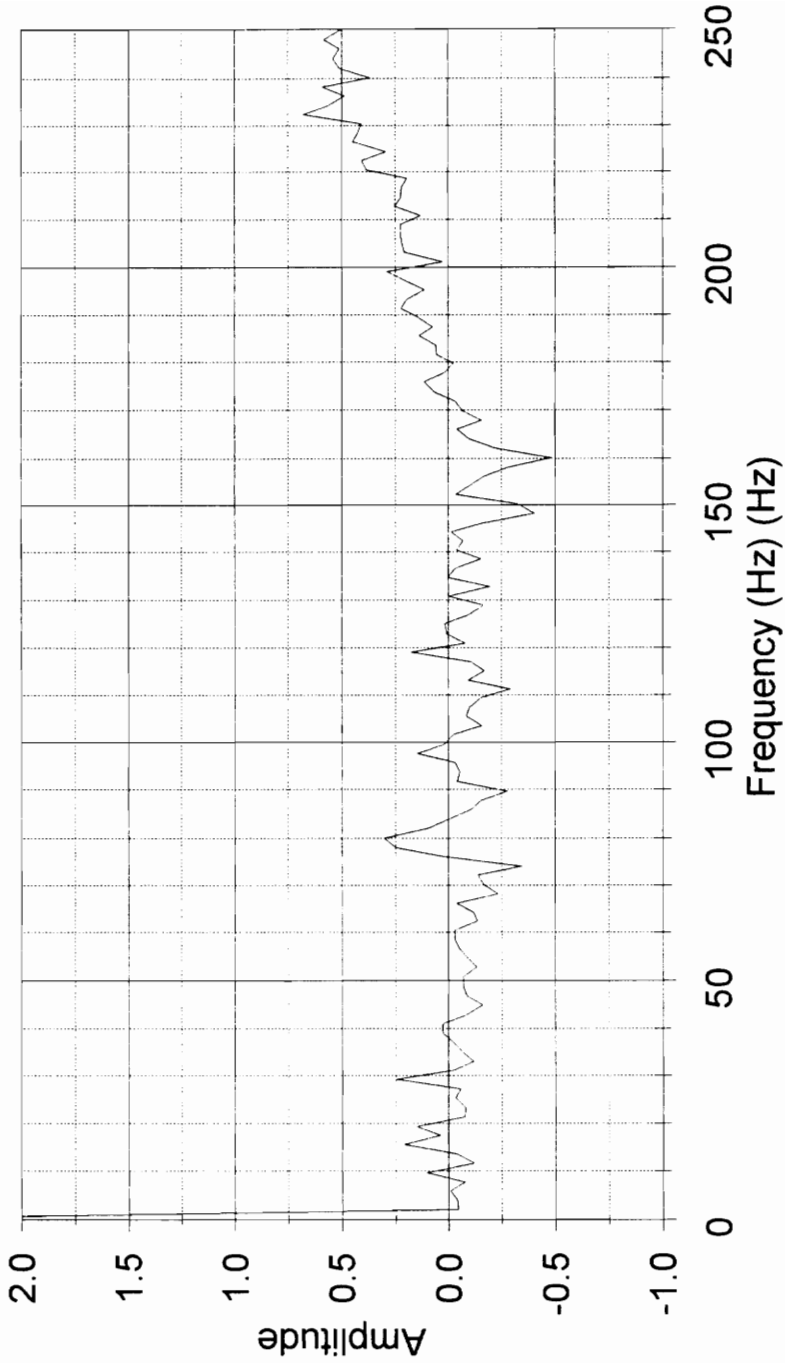


Figure 19. Difference in New and Altered FFT's:  
Accelerometer, Load C, Bearing 11

## Difference in New and Altered FFT's Microphone, Load D, Bearing 12

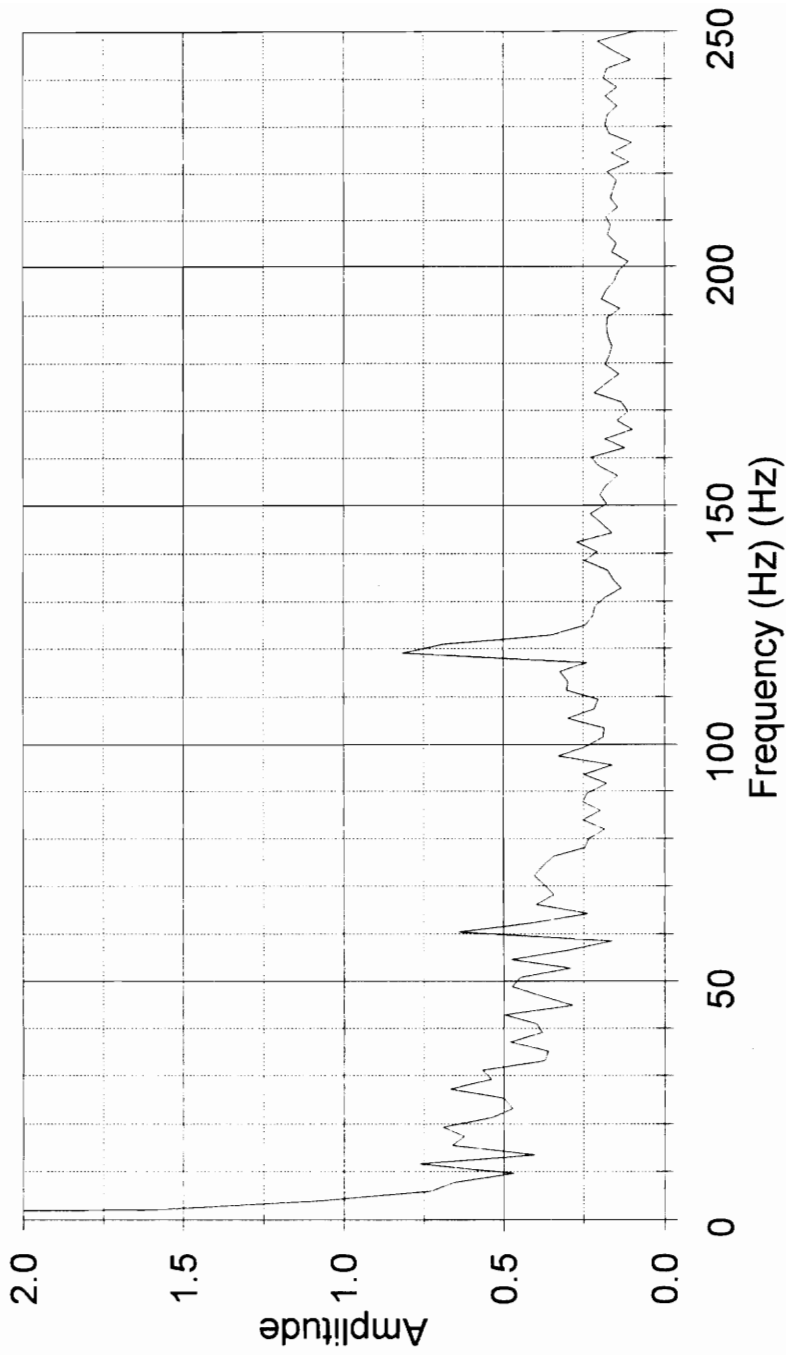


Figure 20. Difference in New and Altered FFT's:  
Microphone, Load D, Bearing 12

**Table 10. Statistical Results and Graphical Results: Test Cases where Positive Graphical Analysis Confirms Positive Statistical Analysis**

Bearing Sample	Sensor(s)	Load(s)
8	Accelerometer	C
	Microphone	D
9	Accelerometer	C
10	Microphone	C
12	Microphone	D

Note:

- Bearing Samples 1-3: One roller defect
- Bearing Samples 4-6: Three roller defects
- Bearing Samples 7-10: One outer race defect
- Bearing Samples 11-12: Unaltered

**Table 11. Statistical Results and Graphical Results: Test Cases where Negative Graphical Analysis Contradicts Positive Statistical Analysis**

Bearing Sample	Sensor(s)	Load(s)	Reason for Rejection
2	Accelerometer	D	Low variability
4	Accelerometer	C	Low variability
6	Accelerometer	C	Low variability
		D	Low variability
7	Accelerometer	D	Low variability, Negative trend
10	Accelerometer	C	Low variability
12	Accelerometer	C	Low variability, Negative trend
		D	

Note:

- Bearing Samples 1-3: One roller defect
- Bearing Samples 4-6: Three roller defects
- Bearing Samples 7-10: One outer race defect
- Bearing Samples 11-12: Unaltered

**Table 12. Statistical Results and Graphical Results: Test Cases where Positive Graphical Analysis Contradicts Negative Statistical Analysis**

Bearing Sample	Sensor(s)	Load(s)
1	Accelerometer	C and D
	Microphone	D
2	Accelerometer	C
3	Microphone	C
4	Accelerometer	D
7	Microphone	C and D
9	Accelerometer	D
	Microphone	C and D
11	Microphone	C and D

Note:

Bearing Samples 1-3: One roller defect

Bearing Samples 4-6: Three roller defects

Bearing Samples 7-10: One outer race defect

Bearing Samples 11-12: Unaltered

more promising results when analyzed graphically. The values of the PCC from data using the microphone and confirmed by statistical and graphical analyses (0.63, 0.71, and 0.93) were comparable to the values of the PCC obtained for the microphone data in the first experiment (0.87, and 0.73). The values of the PCC from data using the accelerometer and confirmed by statistical and graphical analyses (0.63 and 0.66) were considerably higher than the values of the PCC obtained for the accelerometer data in the first experiment (0.36 and 0.41).

While conducting the experiments on the altered bearings, difficulties were encountered with the shaft and support bearings. Due to the shaft design, the shaft bent around an axis defined by the hole used to secure one of the collars. The support bearings were self-centering and, as the shaft turned, the support bearings were constantly re-centering. This re-centering produced strong vibrations which overpowered the signal from the bearing in some test cases. Examples of this phenomena can be found in Figure 16 and in Appendix B.

Despite the problems encountered during data collection, evidence is available to show that the microphone functioned poorly when used with bearings at a simulated early stage of wear. However, the microphone performed better than the accelerometer when used with a bearing that was at an advanced stage of wear. The accelerometer seemed to perform better with the artificially worn bearings than with the field-worn bearings showing an increase in the PCC values for the second experiment. The discrepancy in the performance of the two sensors may be due to their relative sensitivity. The accelerometer was more sensitive, and therefore could acquire weak signals more readily than the

microphone. The microphone was less sensitive and was not “confused” by the signal from the bearings at an advanced stage of wear.

## **Chapter VI**

### **Conclusions and Recommendations**

The ability of the microphone to identify defect frequencies in a range typical to agricultural applications is encouraging. The data indicates that the microphone performs well when monitoring bearings at an advanced stage of wear. However, the data do not confirm the ability of the microphone to function when monitoring bearings at an early stage of wear. Additional study is needed to determine a threshold level of wear that is required for the microphone to detect the defect frequencies produced by a bearing as it wears. Experiments need to be conducted to test the function of the microphone as a transducer for bearing failure detection while operating a bearing until failure. Time constraints in this study preclude this type of experimentation. However, data presented gives an indication of the performance of the microphone at both early and advanced stages of wear.

Laboratory experiments required the bearings be installed, removed, reinstalled, and finally removed again. It is possible that the bearings may have been damaged in the installation or removal process. For example, the outer race may have been scratched during installation. Such damage was not considered, but no evidence of any impact on the results was found. Ideally one would like to have a separate housing for each of the test bearings to allow both new and altered tests to be conducted with identical installation. However, implementation would require considerable fabrication expense.

The most severe difficulty encountered during experimentation was that of the noise created by the support bearing continuously attempting to re-center itself. The cause of this difficulty was a shaft that was slightly undersized for the applied load. The experimental procedure required repeated disassembly of the test apparatus and removal of the test bearing. A shaft one standard size smaller (0.625 in. or 15.875 mm) than the inner bore of the bearing (0.750 in. or 19.050 mm) was used. The collars were used to increase the shaft diameter, creating a shoulder on which the test bearing was pressed. This eliminated the need to press the bearing along half the shaft length. A hole was drilled through the shaft and the collar was bolted to the shaft. The hole caused the shaft to bend eccentrically. The effect was similar to that of shaft whirl. The collar was braised onto the shaft in the original design. The heat treatment effect of the brazing coupled with the cyclic nature of the loading caused a catastrophic failure of one shaft used. Attempts were made to secure the collar with set screws, but this configuration could not transmit the thrust load from the test bearing to the shaft without slippage.

The problem with the non-uniform shaft flexure could be solved through redesign of the test jig. Moving the loading mechanism to one end of the shaft in a cantilever configuration would allow use of a larger shaft. The diameter of the end of the shaft could be reduced to match the inner bore of the test bearing and grease seal. Such a configuration would eliminate the collar that resists the thrust load. One collar would still be necessary to provide a sealing surface for the grease seal. This design would incorporate a larger shaft with a solid cross-section while still allowing easy bearing installation and removal.

The noise produced by the support bearings, while detrimental to the laboratory experiments, represented background noise that would likely be present in a field application. Both the accelerometer and microphone encountered similar problems with background noise interference. It is therefore logical that signal conditioning technology similar to that currently used in bearing monitoring systems utilizing accelerometers could be used in a system incorporating microphones.

An advantage of using a cost-effective microphone-operational amplifier sensor package is that sensors can be multiplexed to allow “time-sharing” of a single data processing and storage unit. The cost of much more expensive sensor packages overshadows the cost of the data processing and storage unit. Increasing the number of bearings monitored would result in more efficient use of data processing and storage capabilities.

Some on-board processing may be advantageous. Transforming the data to the frequency domain reduces the storage requirement by approximately one-half. Acceptable

results may be possible using band-pass filters to dissect the sensor signal and measure only magnitudes in certain frequency ranges. Periodic time averaging could further reduce storage requirements. The reduction in storage requirements could effect a significant reduction in system cost, especially if all data processing and storage were conducted on-board the mobile equipment. A reduction in the storage requirements would decrease the frequency of data down-loading if the data were periodically transferred to a personal computer.

Periodic down-loading of the data to a personal computer has become a more viable option as more agricultural producers gain access to PC's. Data transfer to PC's would facilitate the use of artificial intelligence pattern recognition techniques for vibration spectra analysis. Liu and Mengel (1991) report a 91% success rate for pattern recognition techniques and a 100% success rate for neural networks (3x12x1) in classifying defective bearings. Neural networks could be used in on-board processing of the vibration spectra. Processing speed should not be a great concern because only periodic sampling would be required and bearing deterioration usually occurs over an extended period of time.

Data transfer to and storage on personal computers would provide a vibration spectra history. Such a history would also provide the owner with a descriptive record of bearing condition and wear over time. These records could be a useful management tool if used, for example, to schedule bearing replacement to coincide with other maintenance operations.

## REFERENCES

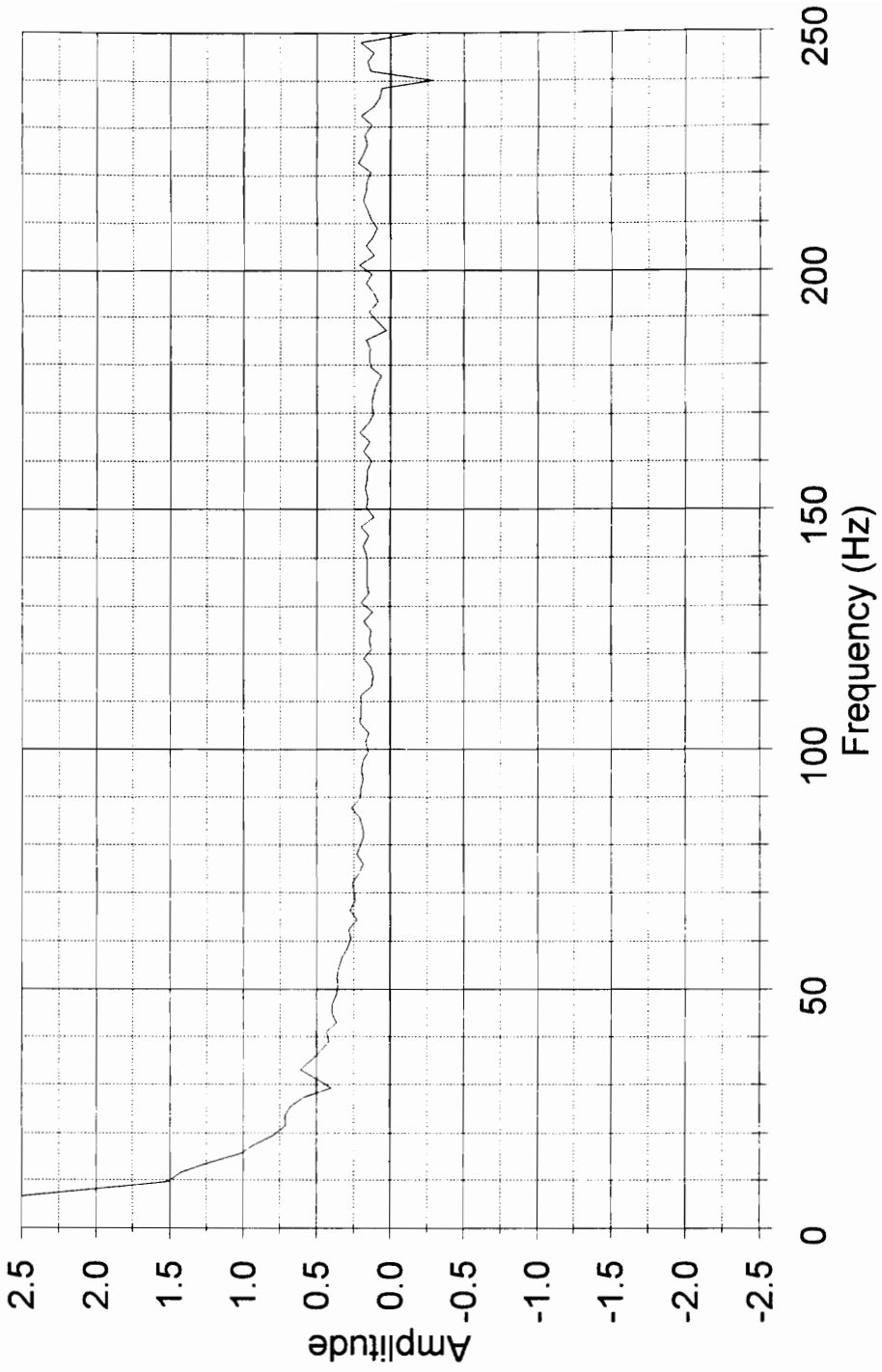
- Berry, James E., "How to Track Rolling Element Bearing Health with Vibration Signature Analysis," *Sound and Vibration*, November 1991, Vol. 25 No. 11, p.24-35.
- Braun, S. and B. Datner, "Analysis of Roller/Ball Bearing Vibrations," *ASME Journal of Mechanical Design*, Jan. 1979, Vol. 101, p. 121.
- Dyer, D. and R.M. Stewart, "Detection of Rolling Element Bearing Damage by Statistical Vibration Analysis," *ASME Journal of Mechanical Design*, Vol. 100, 1978, p.229.
- Ehrich, E.F., "Sum and Difference Frequencies in Vibration of High Speed Rotating Machinery," *ASME Journal of Engineering for Industry*, Vol. 94, No. 1, Feb. 1972, p. 181.
- Harker, R.G. and J.L. Sandy, "Rolling Element Bearing Monitoring and Diagnostics Techniques," *Journal of Engineering for Gas Turbines and Power (Transactions of the ASME)*, April 1989, Vol. 111 No. 2, p 251-256.
- Li, C. James and S.M. Wu, "On-Line Detection of Localized Defects in Bearings by Pattern Recognition Analysis," *Journal of Engineering for Industry (Transactions of ASME)*, November 1989, Vol. 111 No. 4, p. 331-336.
- Liu, T.I. and J.M. Mengel, "Detection of Ball Bearing Conditions by an A.I. Approach," *Sensors, Controls, and Quality Issues in Manufacturing, Production Engineering Division Publication*, ASME, 1991, Vol. 55, p. 13-21.

Stout, David F., *Handbook of Operational Amplifier Circuit Design*, McGraw-Hill Book Company, 1976, p. 4.1-4.21.

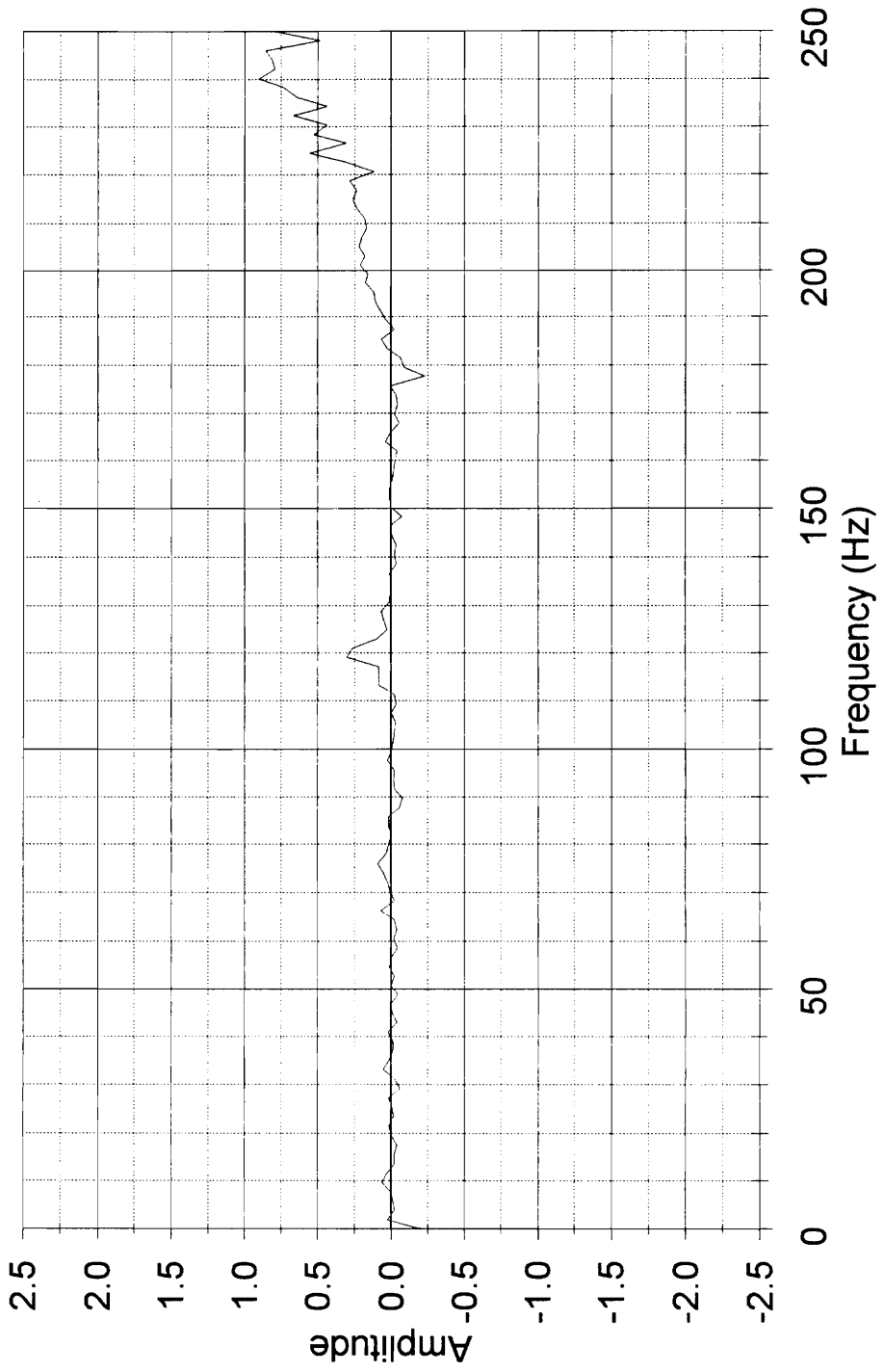
## **APPENDIX**

**Appendix A.**  
**Graphical Presentation of Data:**  
**Comparison of New and Field-Worn Bearing**

# Difference in New and Field-Worn FFT's Accelerometer, Load C

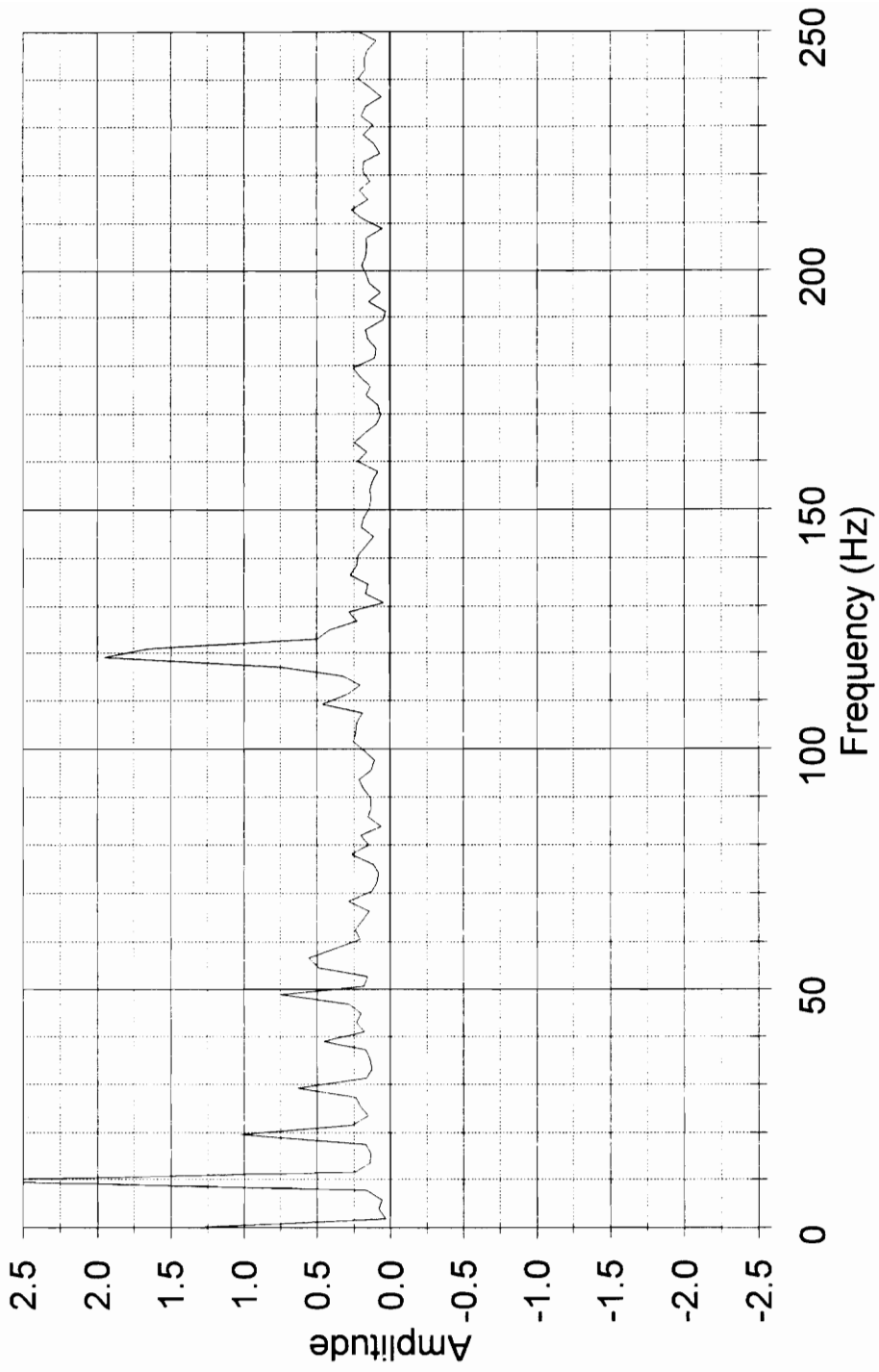


# Difference in New and Field-Worn FFT's Accelerometer, Load D



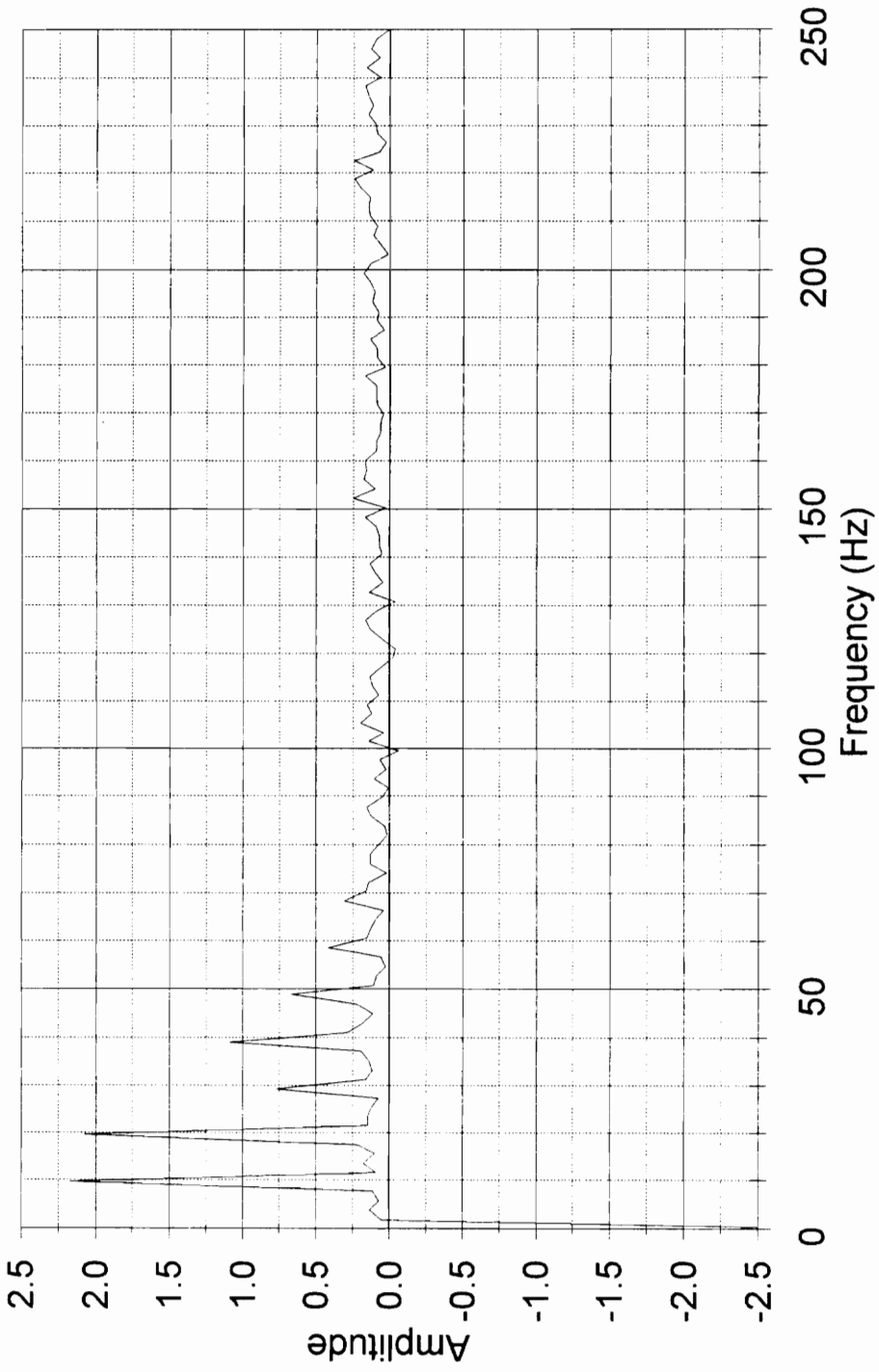
# Difference in New and Field-Worn FFT's

Microphone, Load C



# Difference in New and Field-Worn FFT's

Microphone, Load D

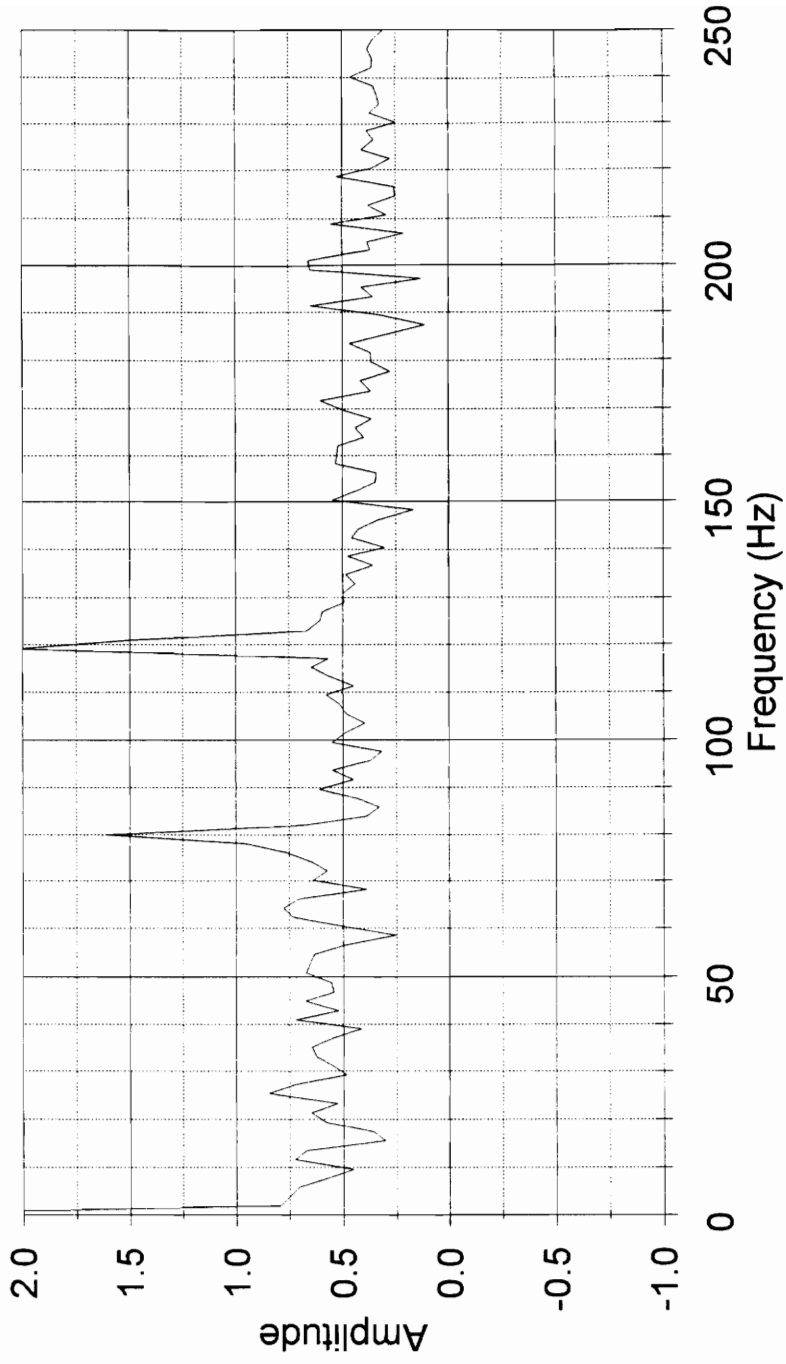


**Appendix B.**

**Graphical Presentation of Data:**

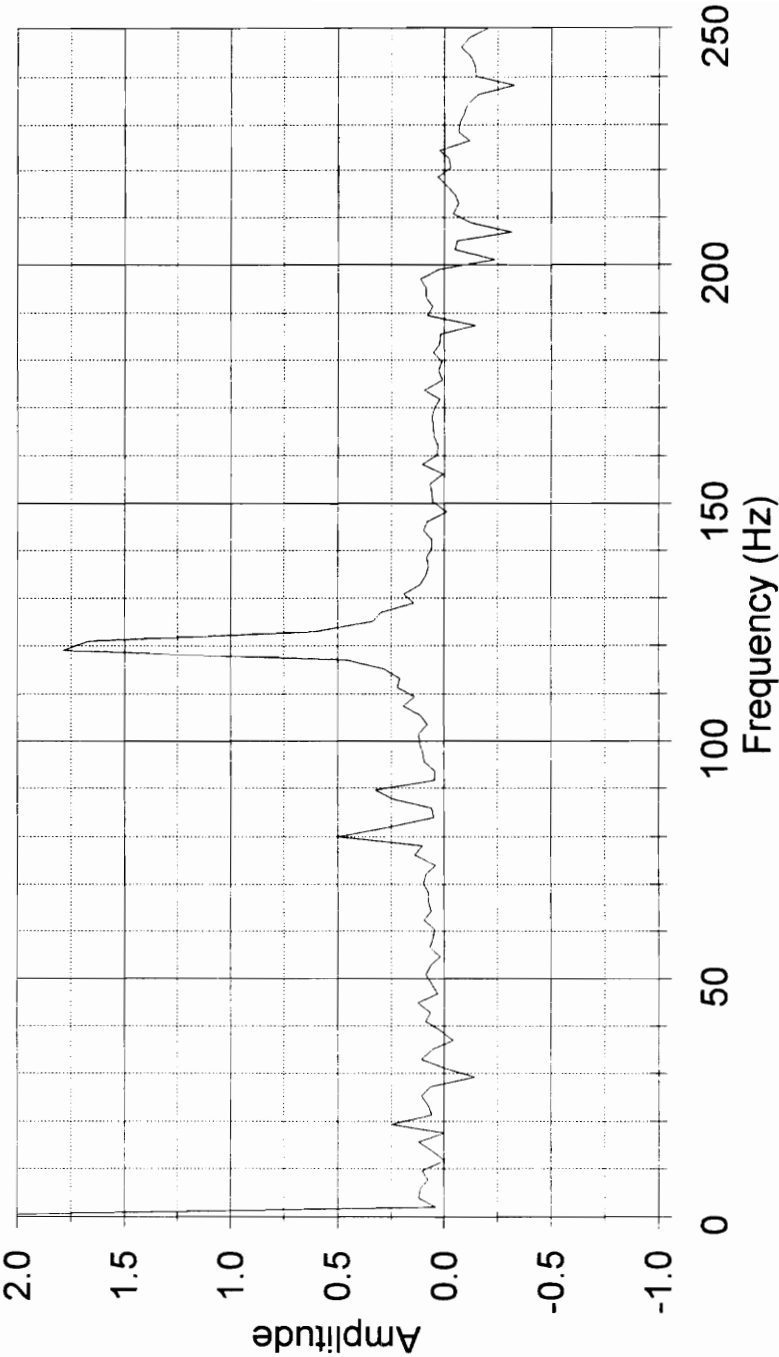
**Comparison of New and Artificially Worn Bearings**

# Difference in New and Altered FFT's Accelerometer, Load C, Bearing 1



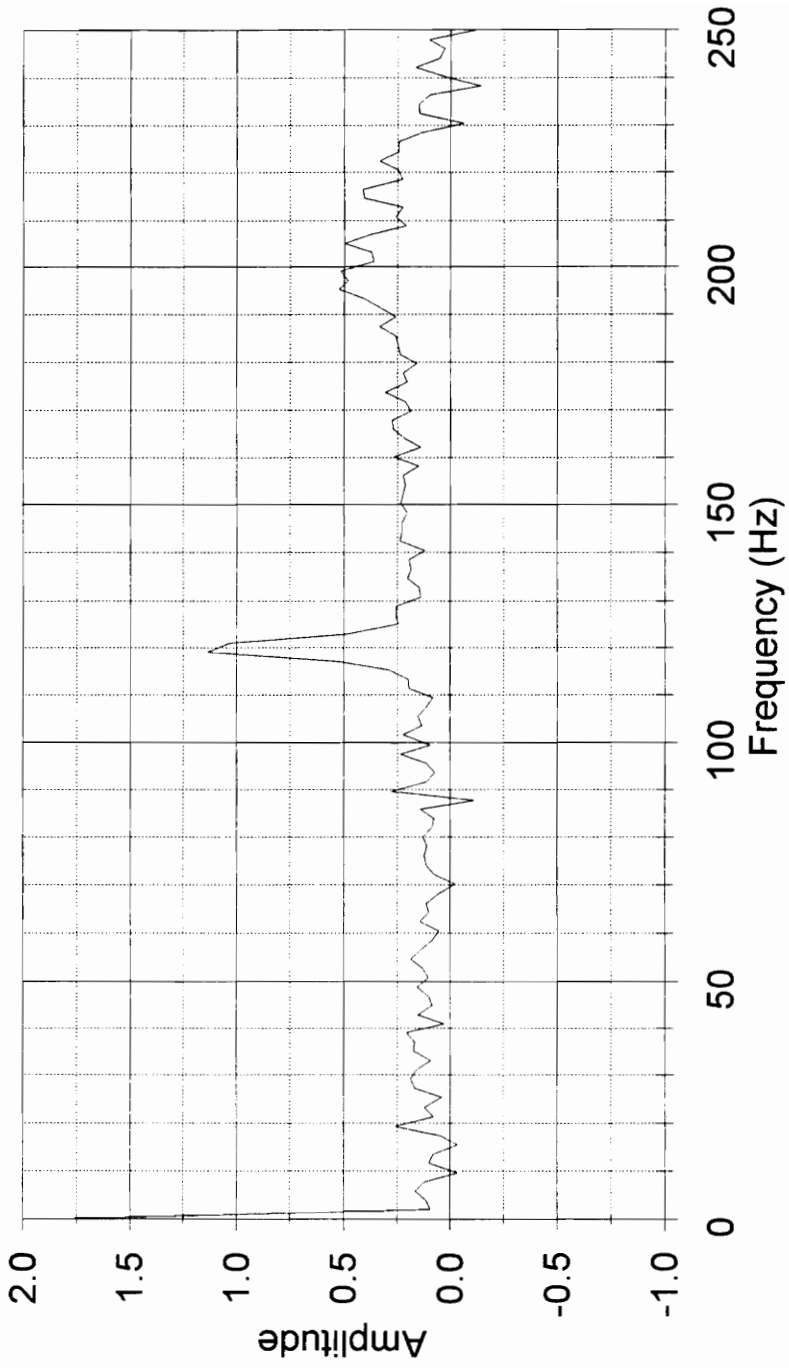
# Difference in New and Altered FFT's

## Accelerometer, Load D, Bearing 1



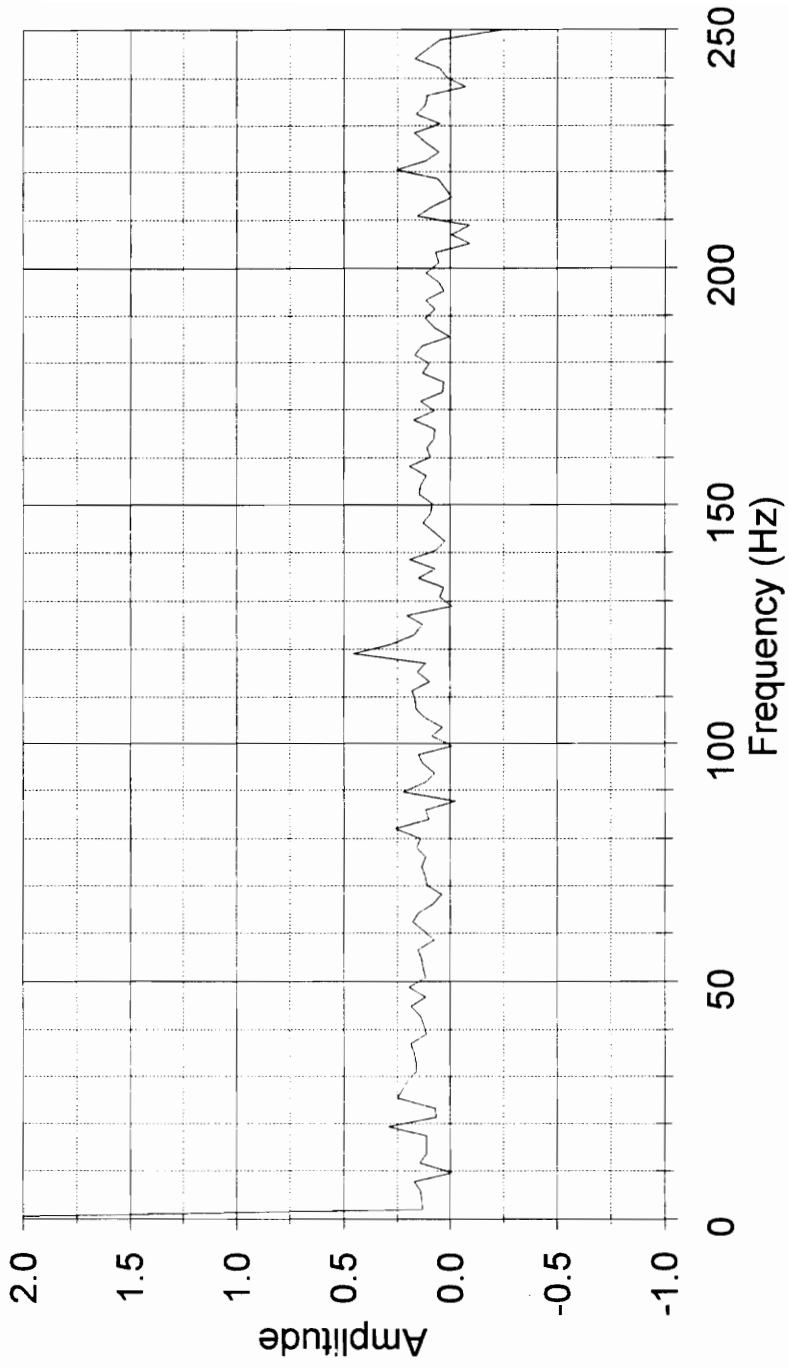
# Difference in New and Altered FFT's

## Accelerometer, Load C, Bearing 2

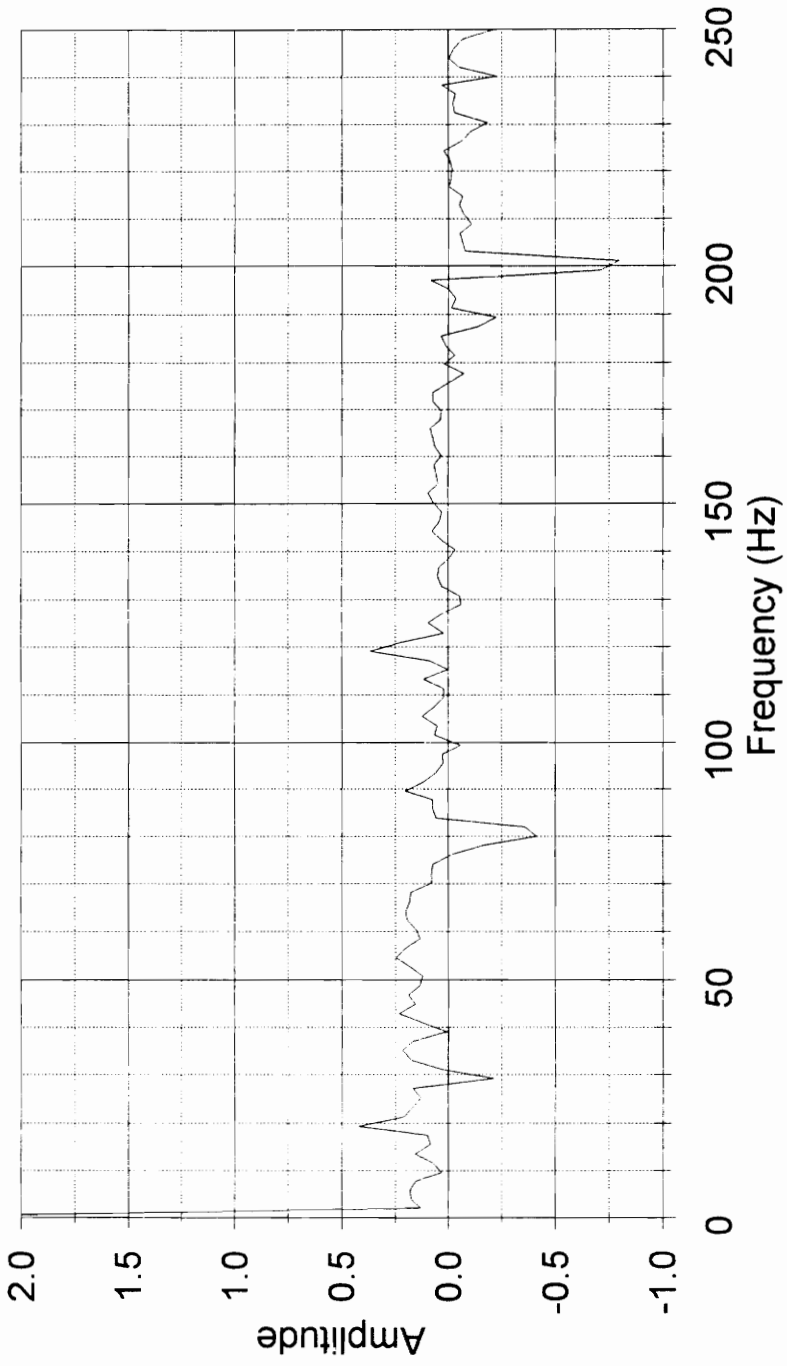


# Difference in New and Altered FFT's

## Accelerometer, Load D, Bearing 2

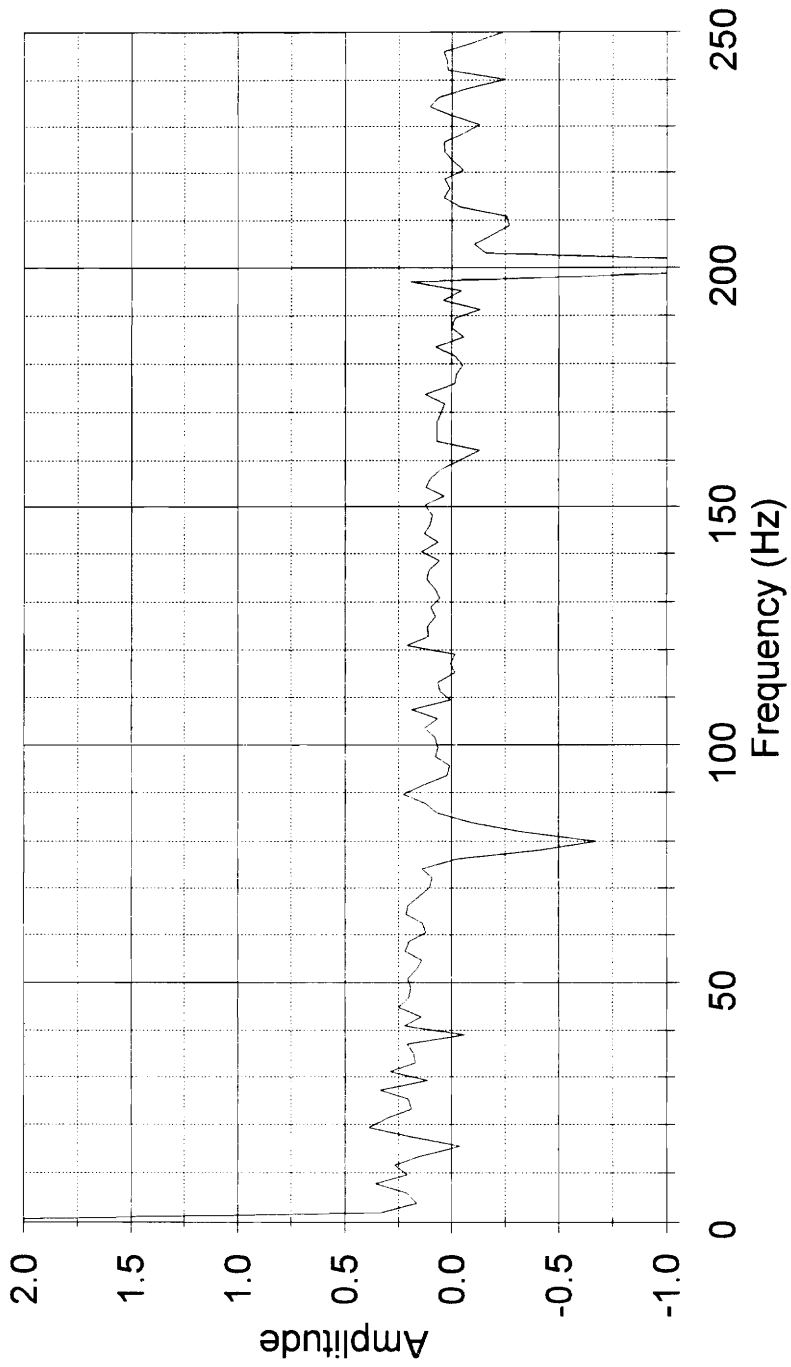


# Difference in New and Altered FFT's Accelerometer, Load C, Bearing 3

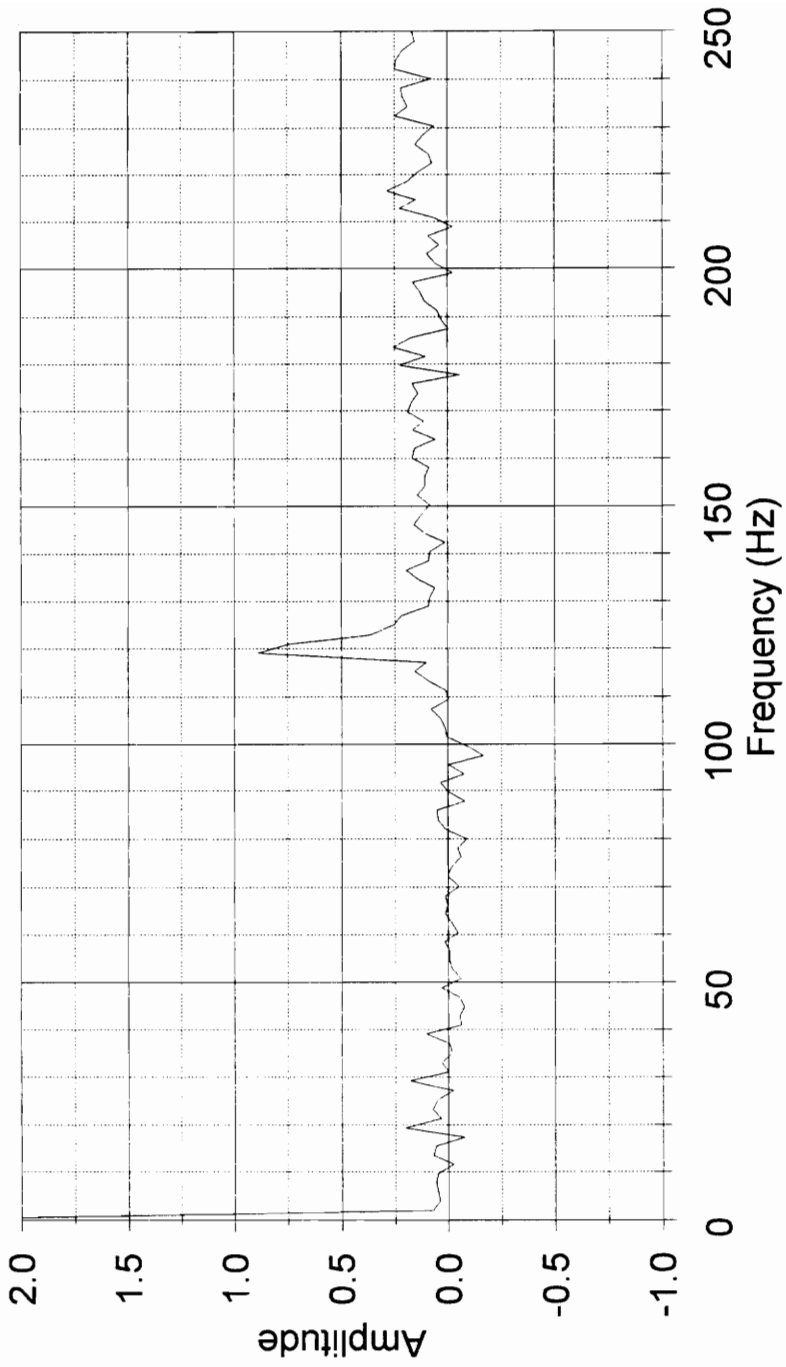


# Difference in New and Altered FFT's

## Accelerometer, Load D, Bearing 3

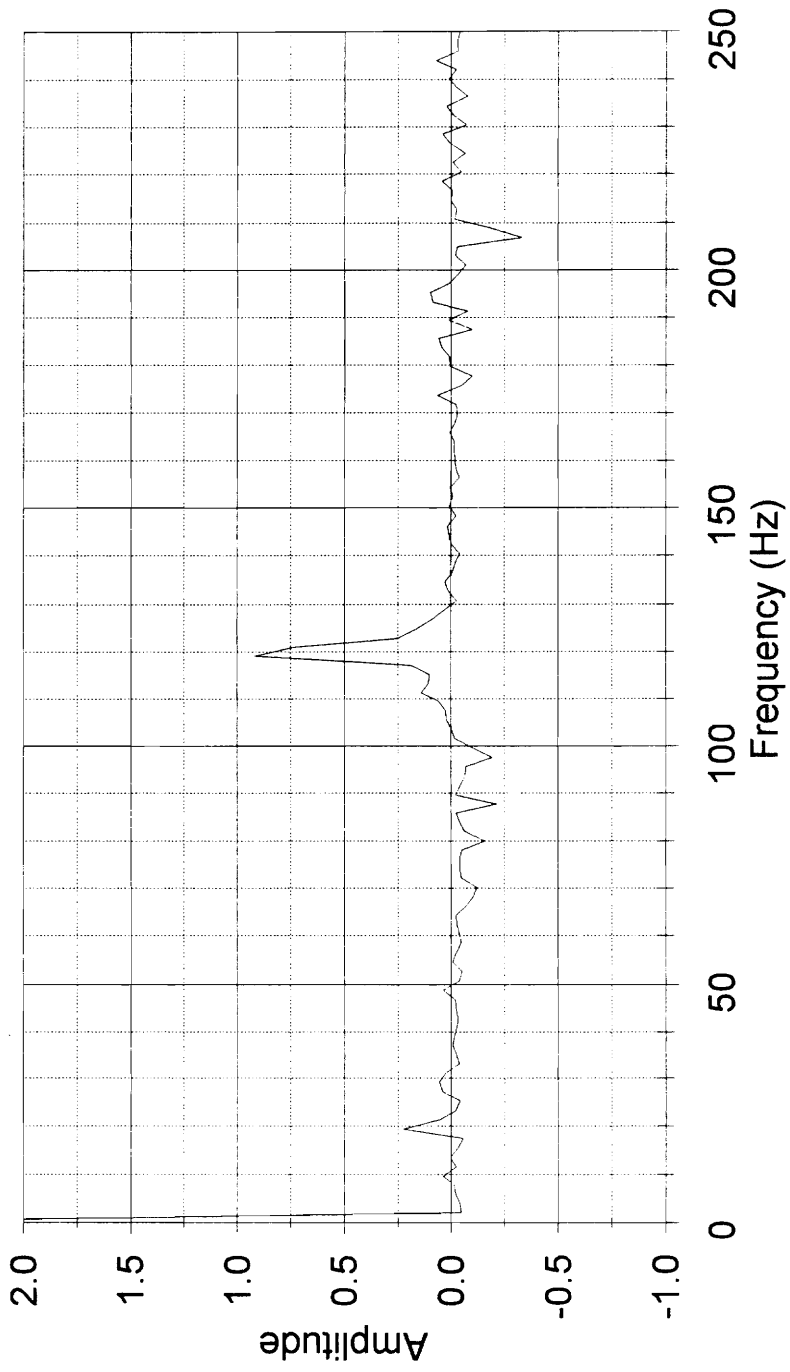


### Difference in New and Altered FFT's Accelerometer, Load C, Bearing 4



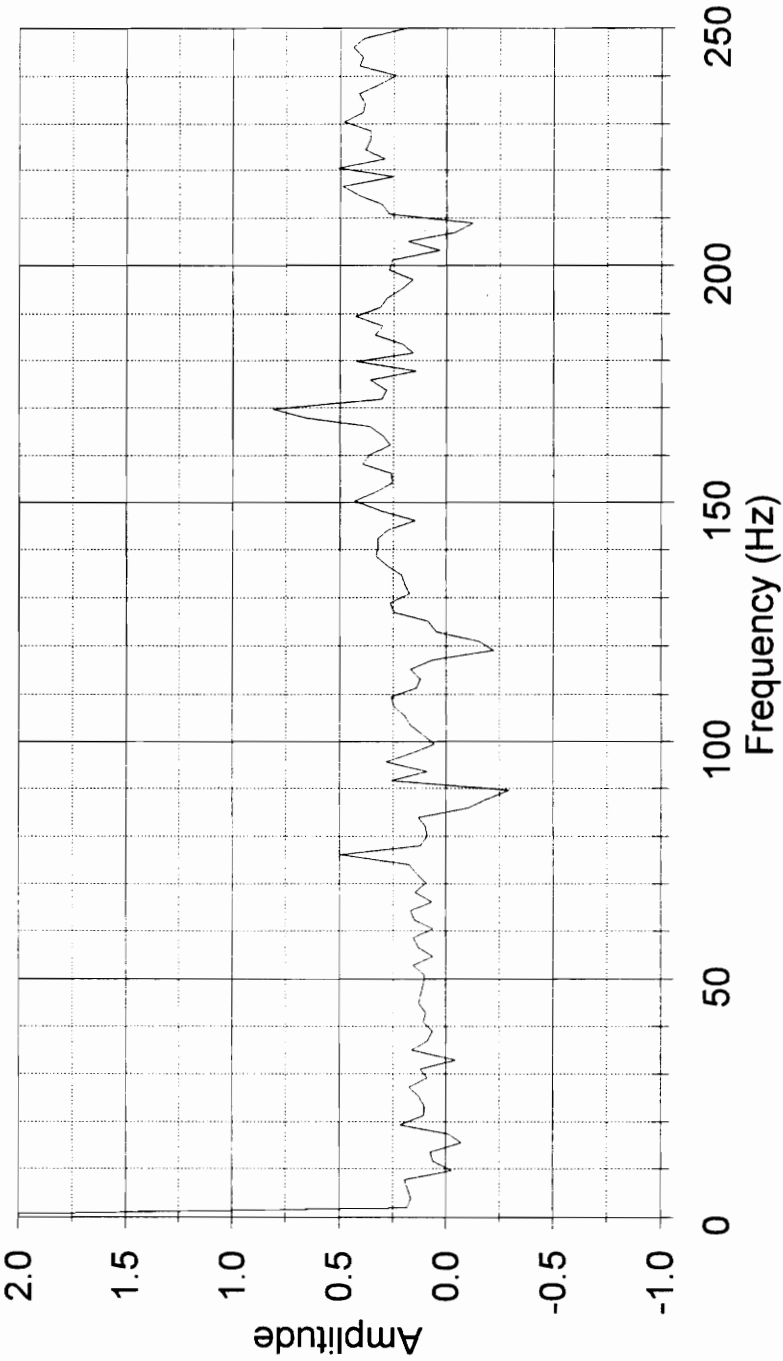
# Difference in New and Altered FFT's

## Accelerometer, Load D, Bearing 4



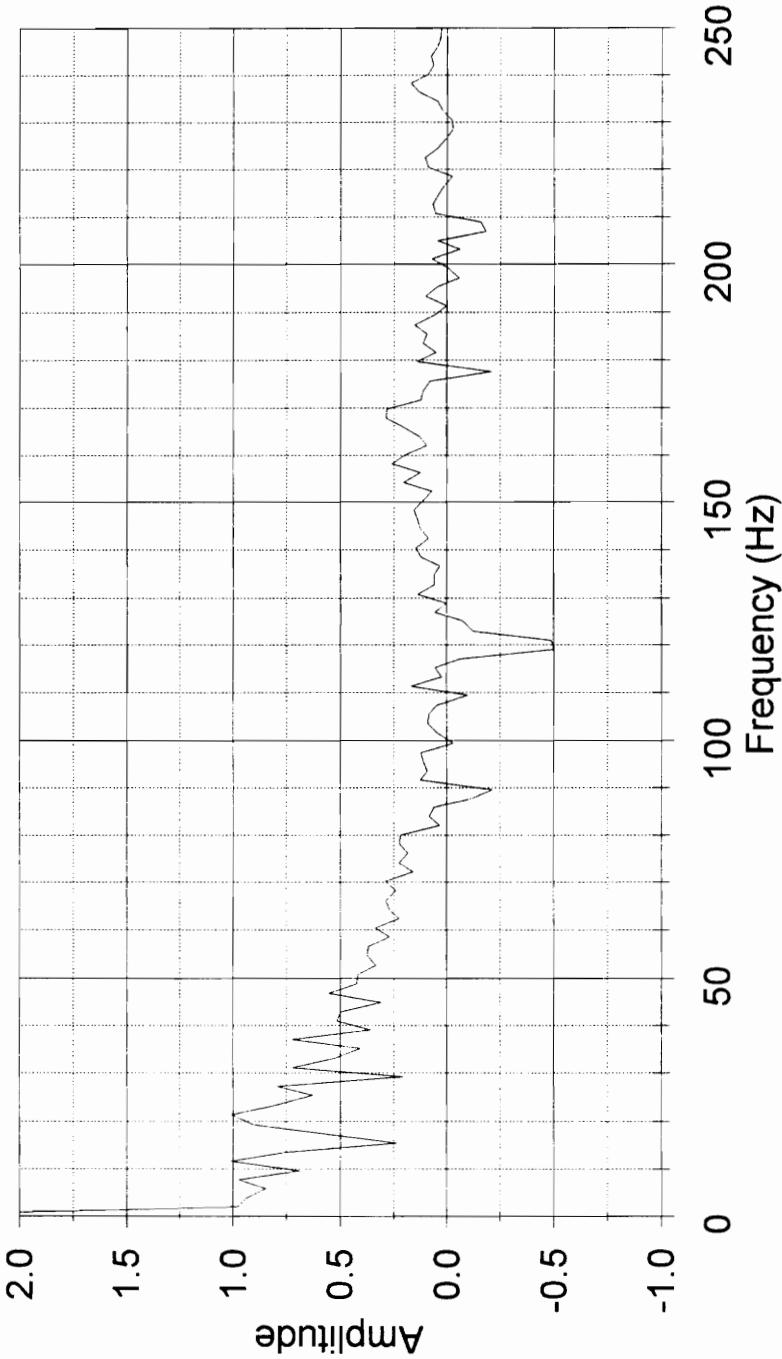
# Difference in New and Altered FFT's

Accelerometer, Load C, Bearing 5



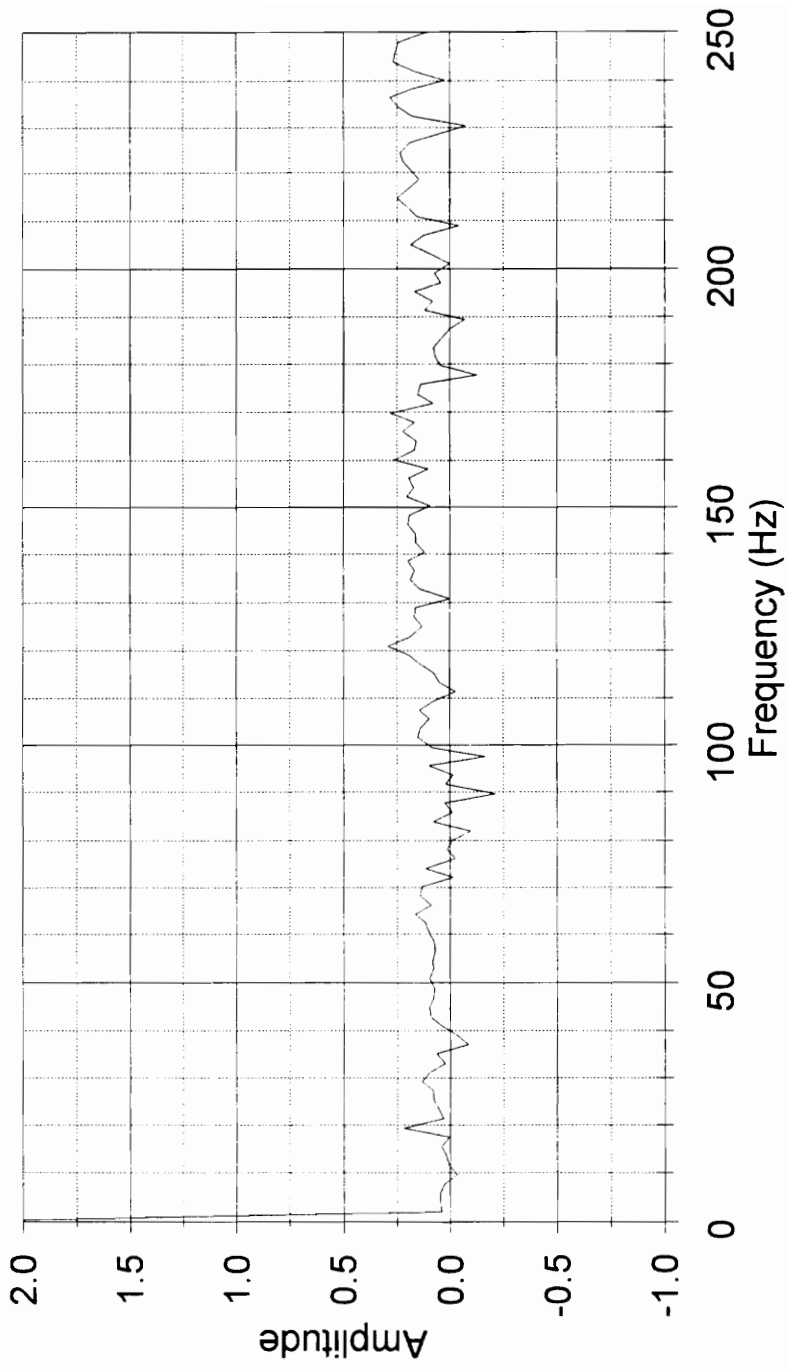
# Difference in New and Altered FFT's

Accelerometer, Load D, Bearing 5



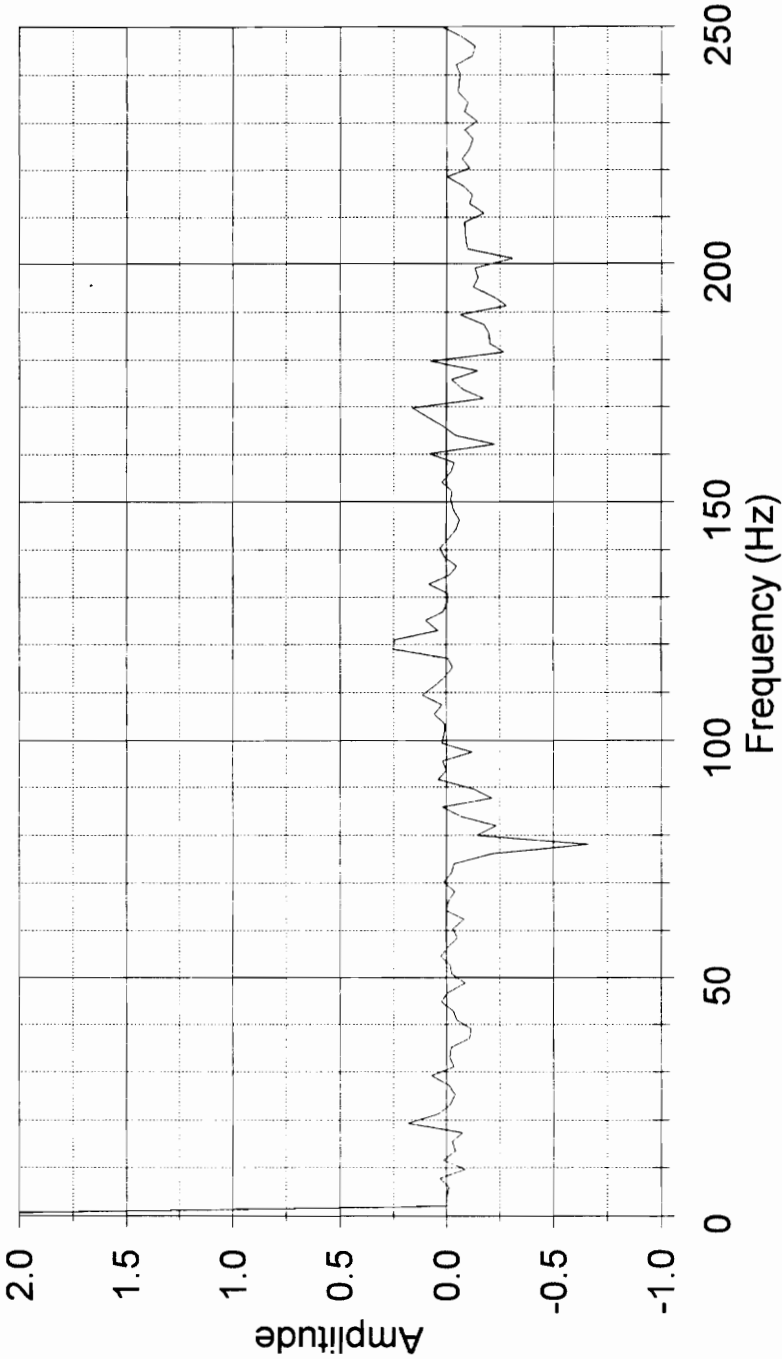
# Difference in New and Altered FFT's

## Accelerometer, Load C, Bearing 6

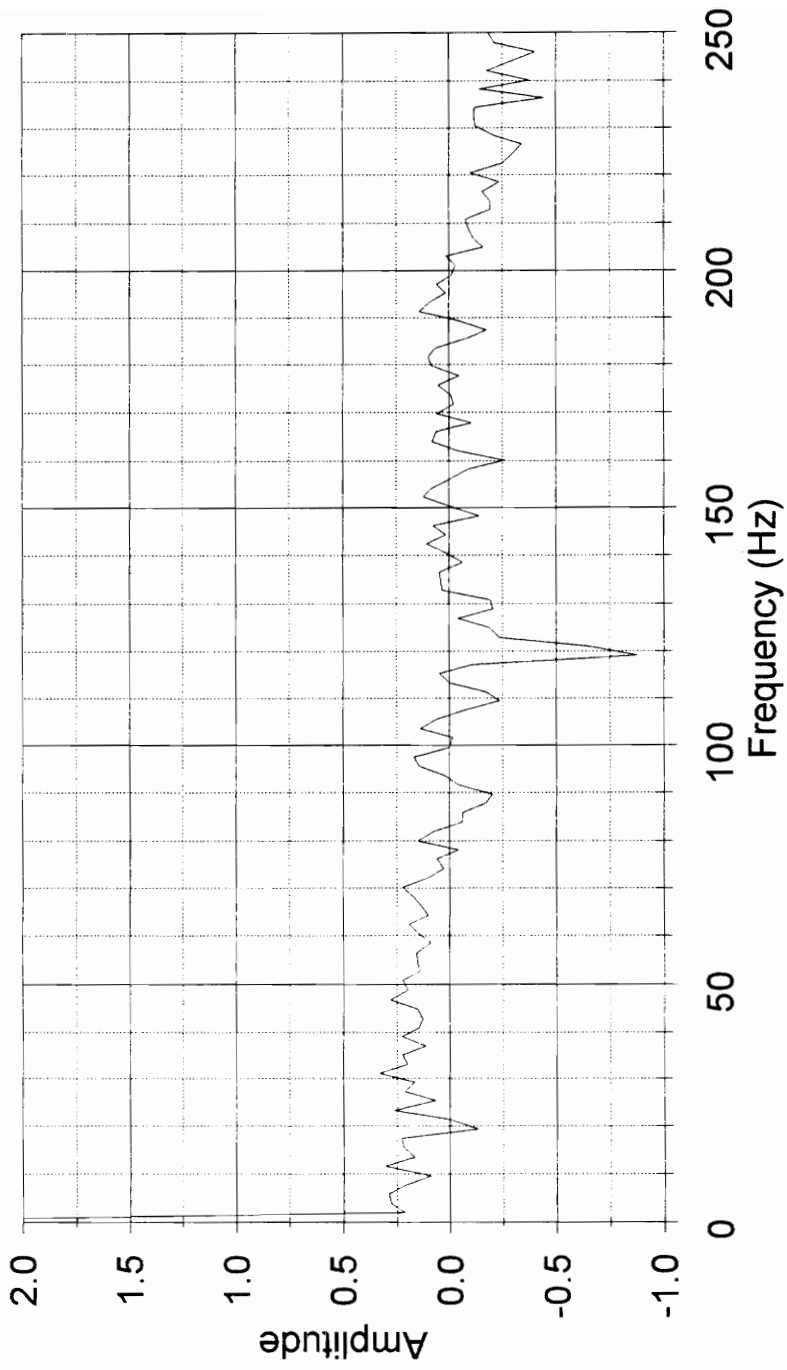


# Difference in New and Altered FFT's

## Accelerometer, Load D, Bearing 6

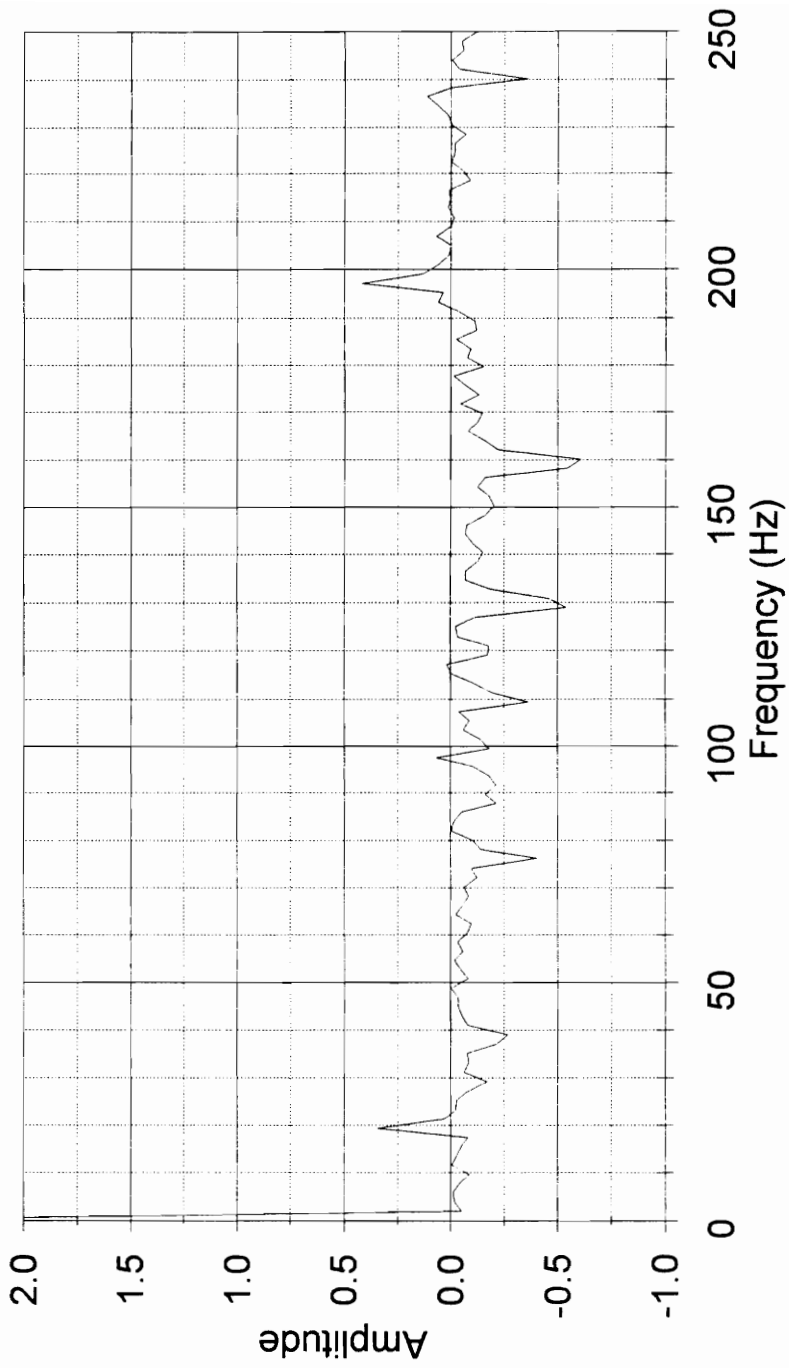


### Difference in New and Altered FFT's Accelerometer, Load C, Bearing 7



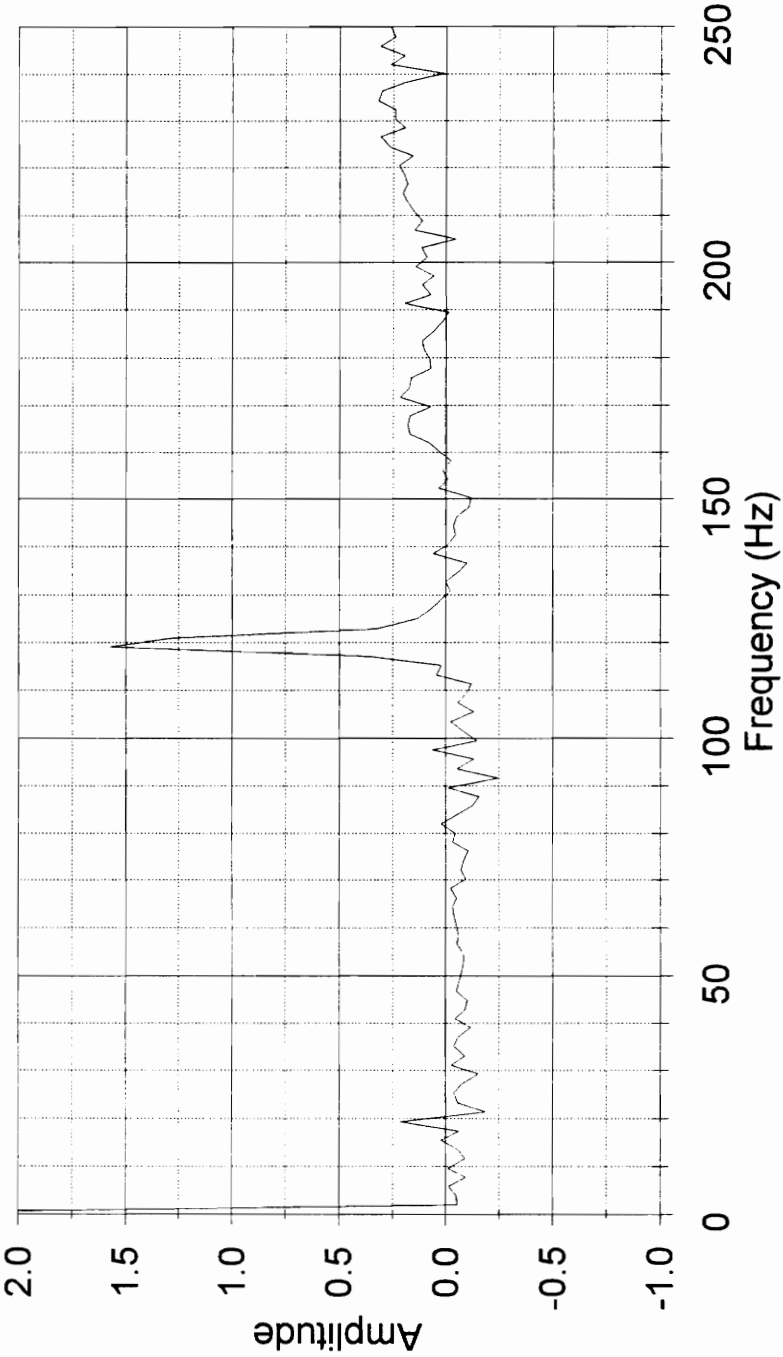
# Difference in New and Altered FFT's

## Accelerometer, Load D, Bearing 7



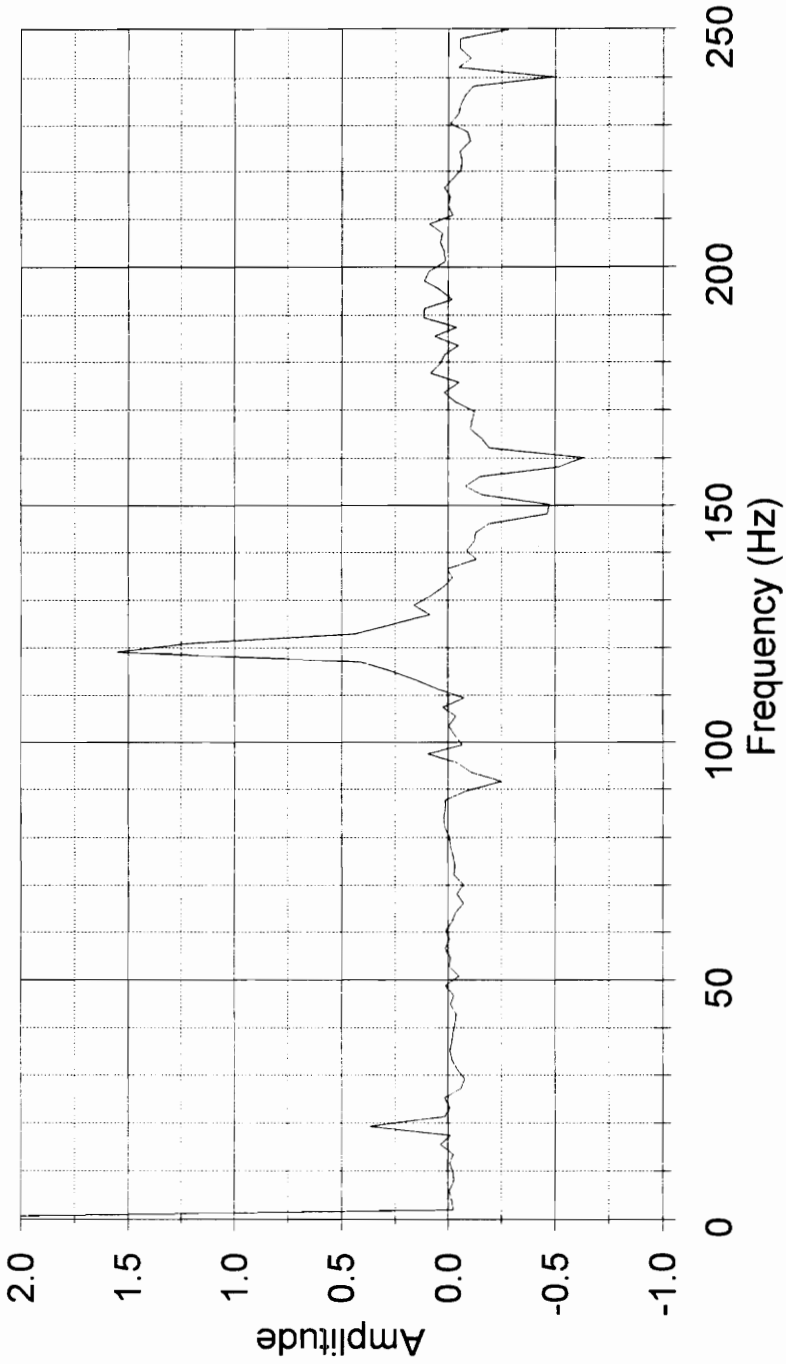
# Difference in New and Altered FFT's

Accelerometer, Load C, Bearing 8

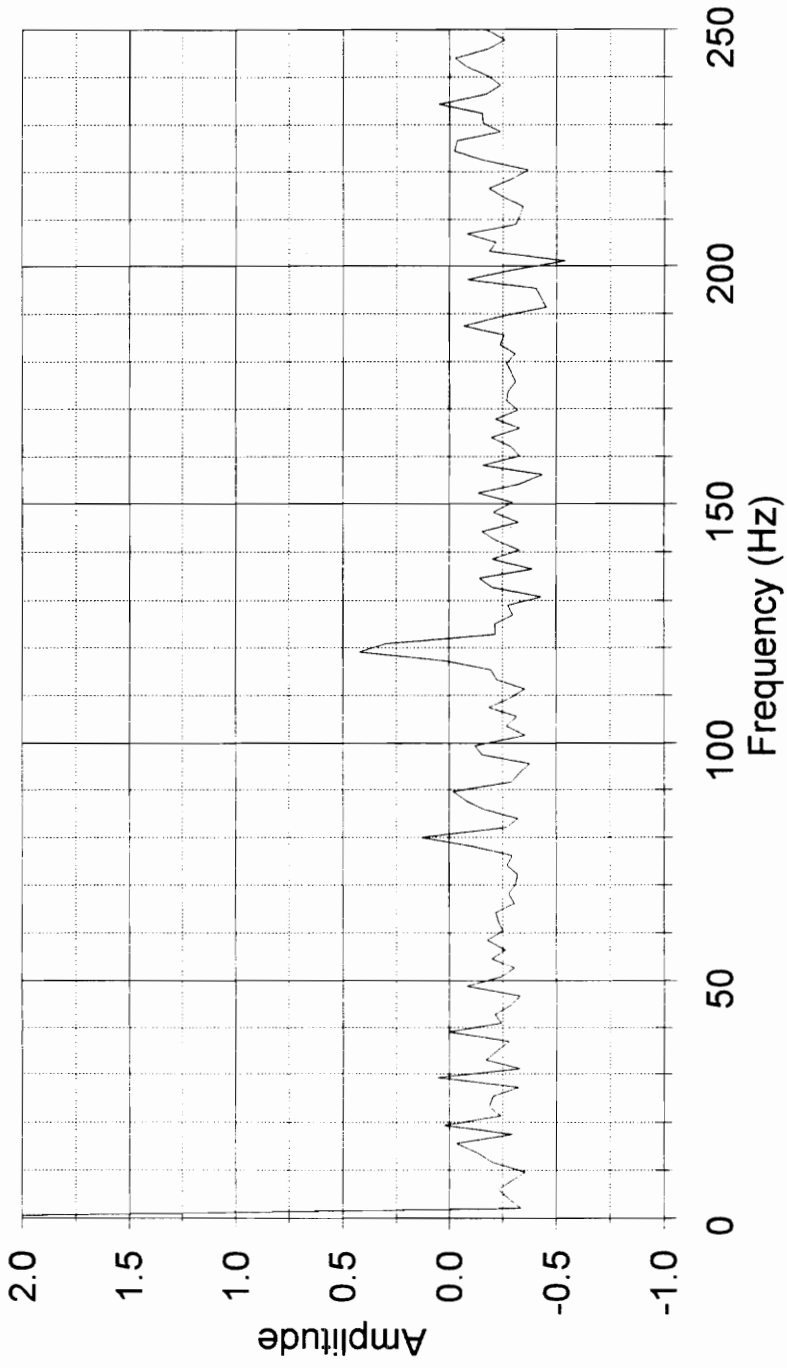


# Difference in New and Altered FFT's

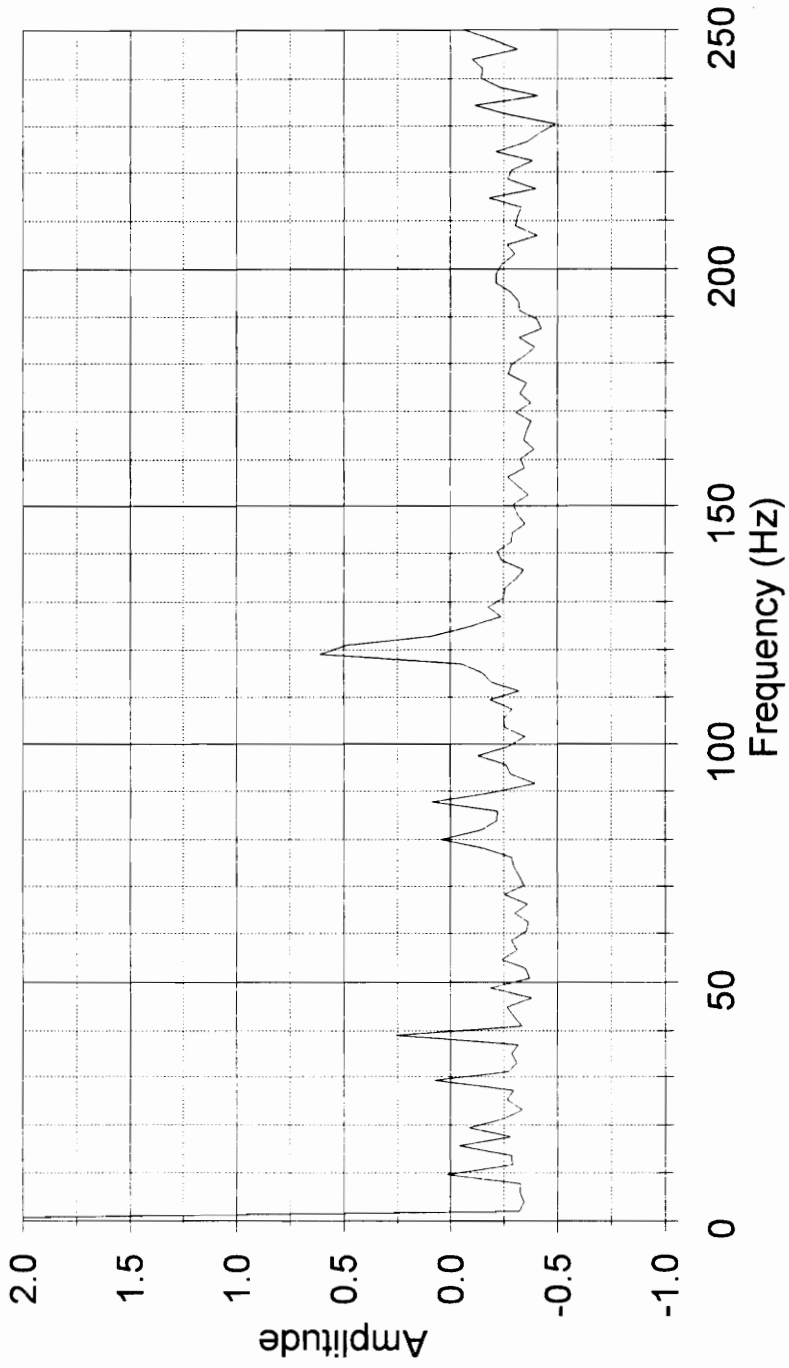
## Accelerometer, Load D, Bearing 8



# Difference in New and Altered FFT's Accelerometer, Load C, Bearing 9

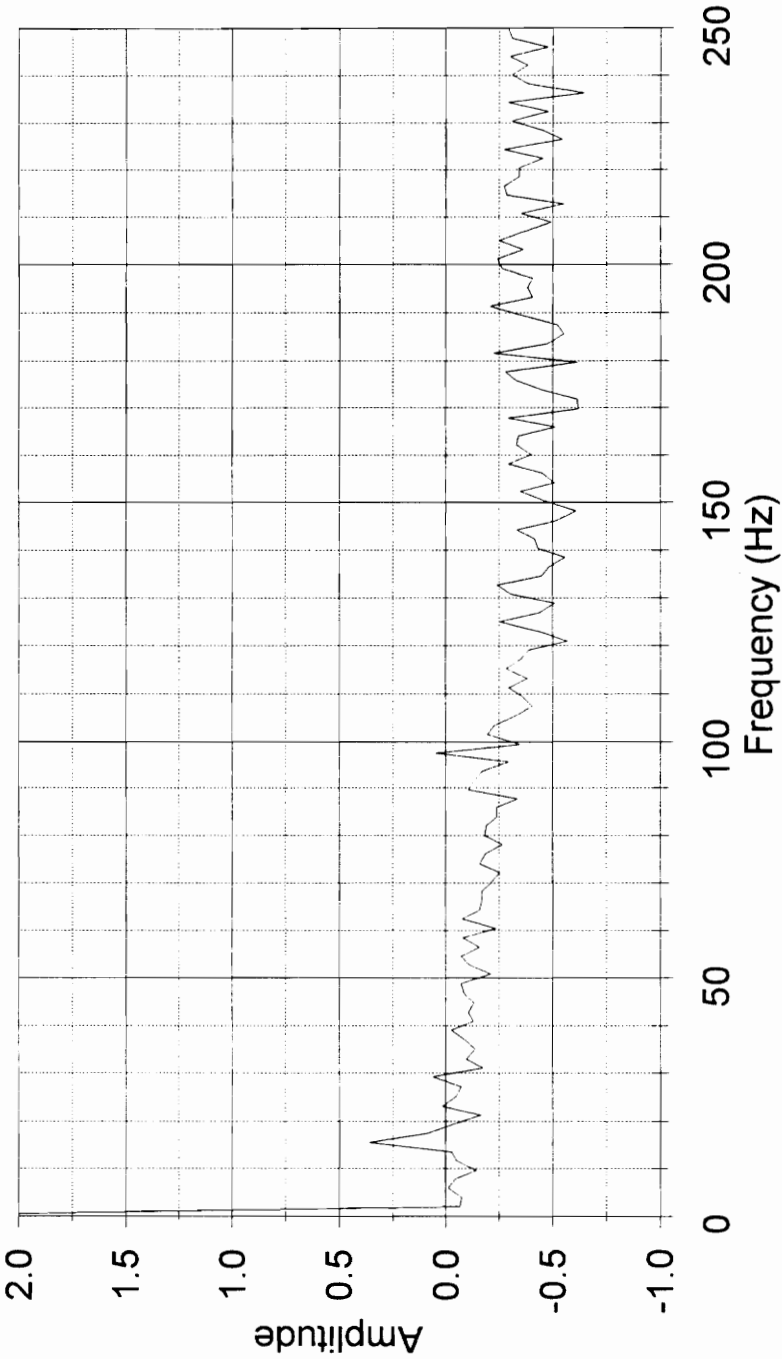


# Difference in New and Altered FFT's Accelerometer, Load D, Bearing 9



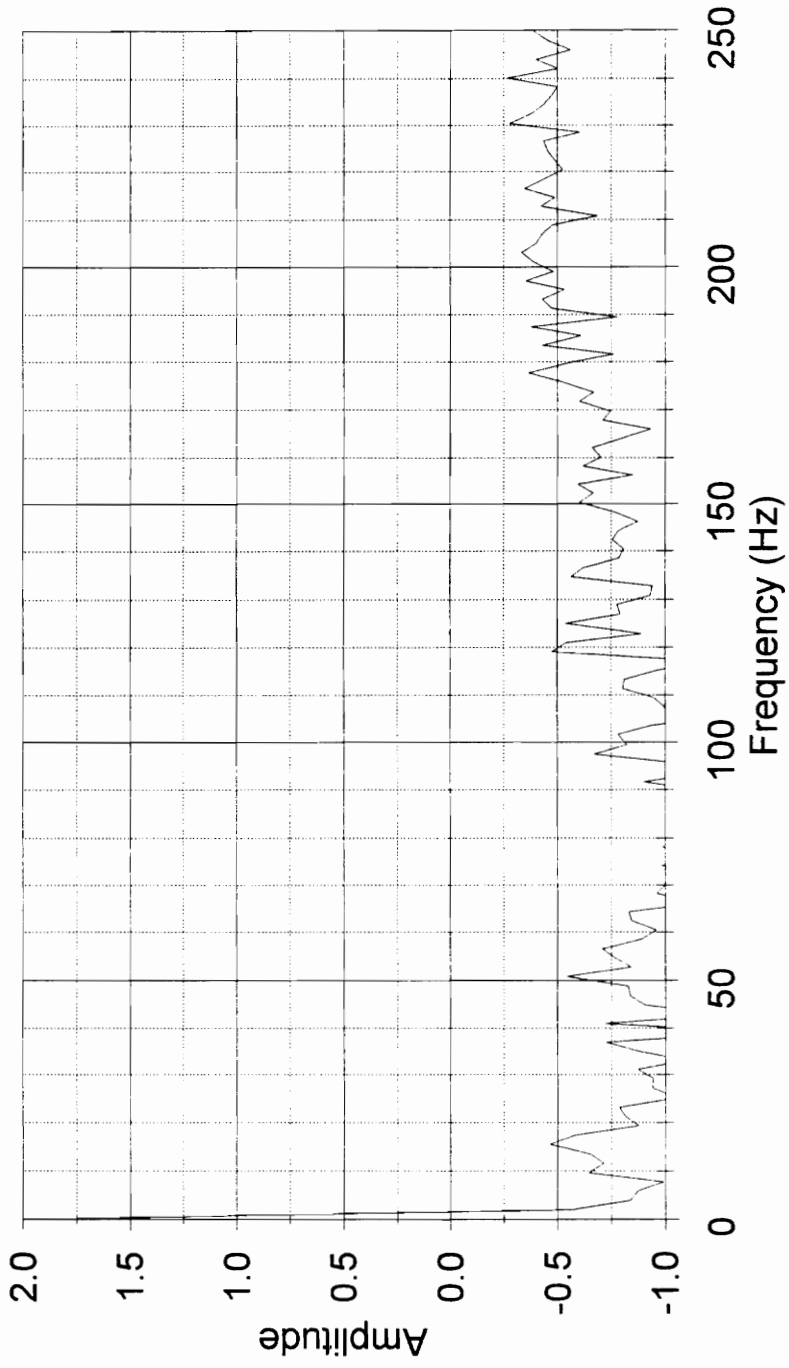
# Difference in New and Altered FFT's

## Accelerometer, Load C, Bearing 10

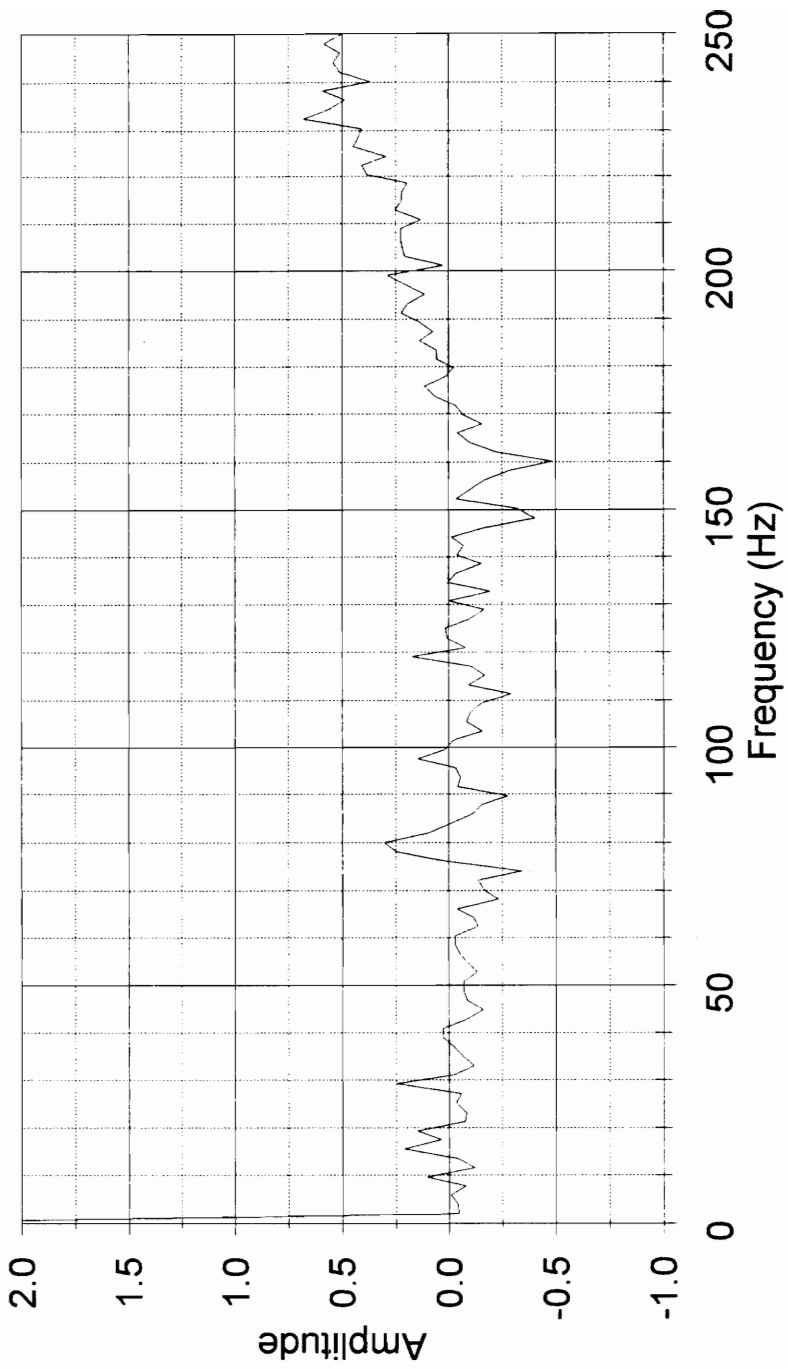


# Difference in New and Altered FFT's

## Accelerometer, Load D, Bearing 10

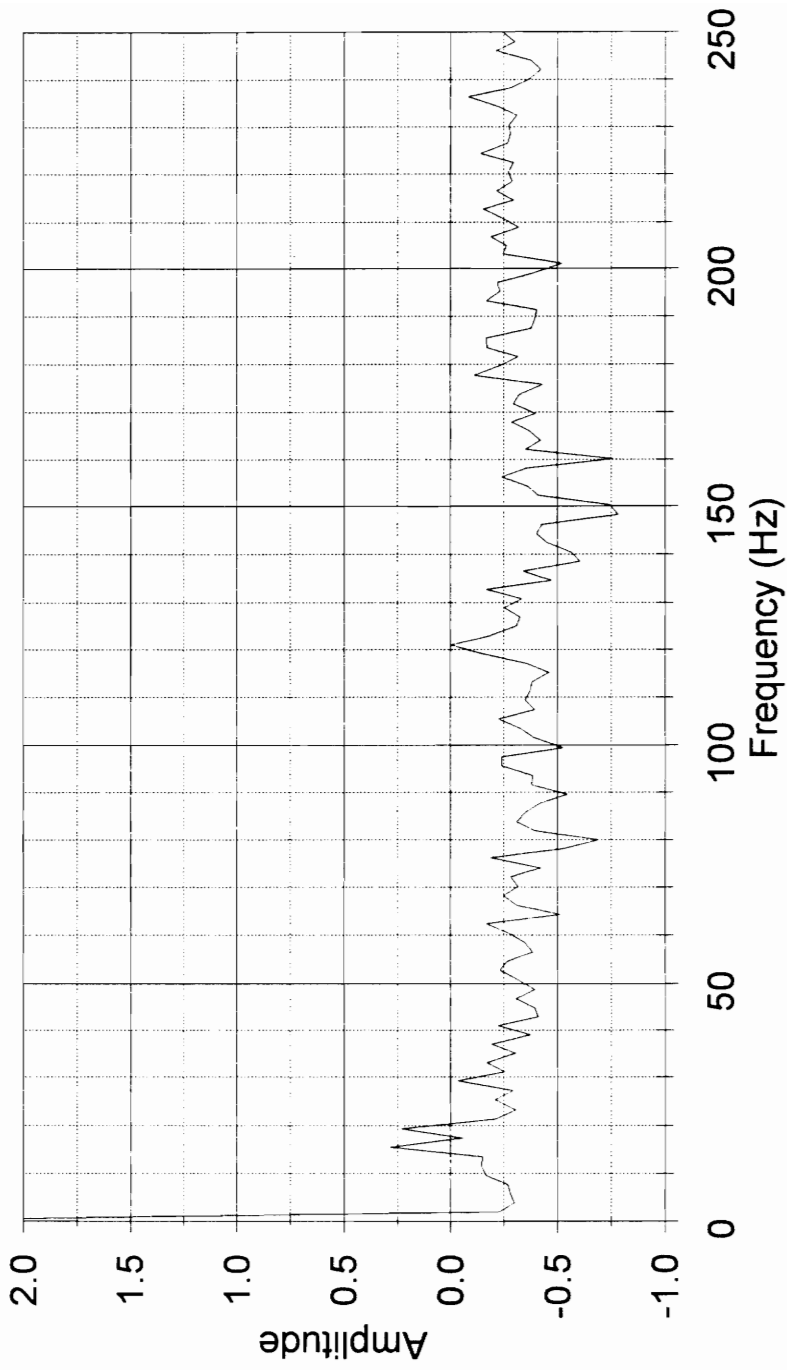


### Difference in New and Altered FFT's Accelerometer, Load C, Bearing 11

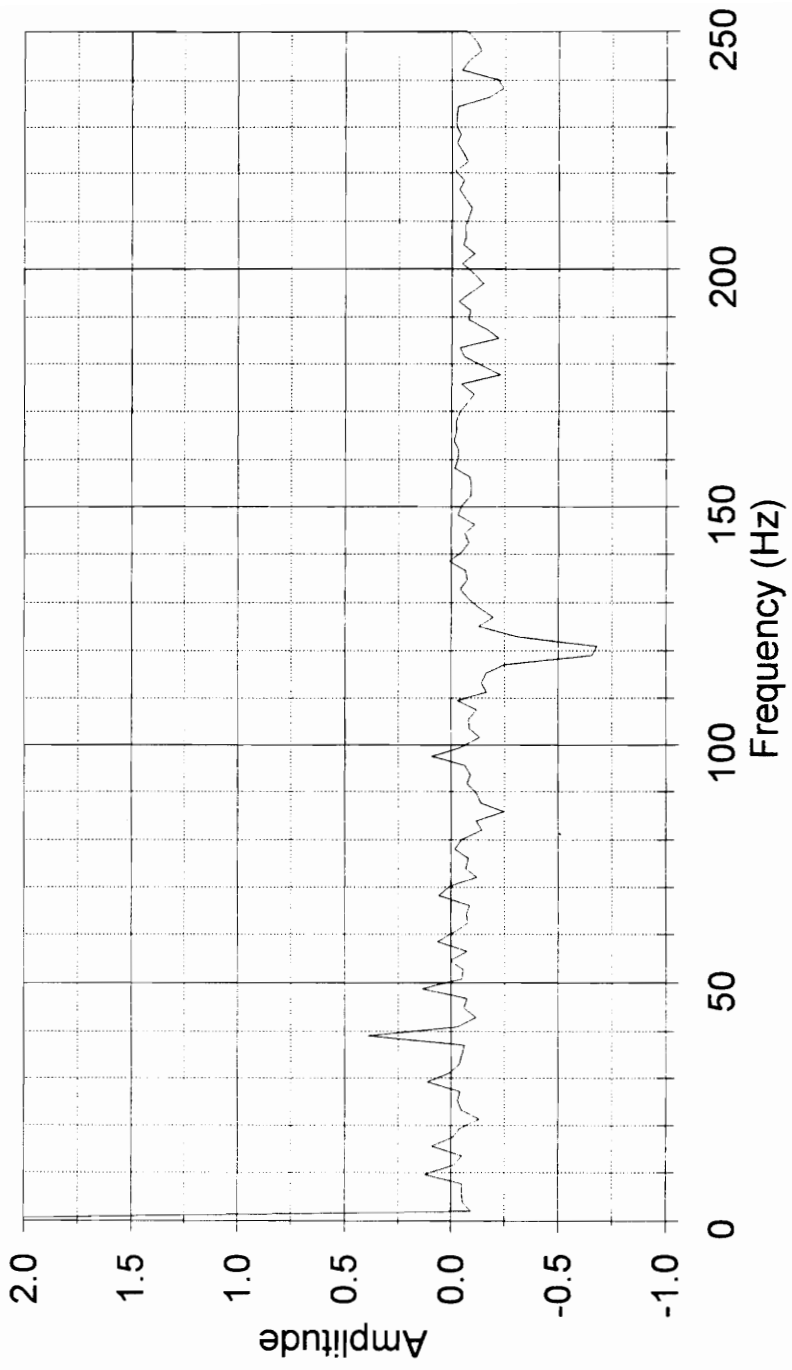


# Difference in New and Altered FFT's

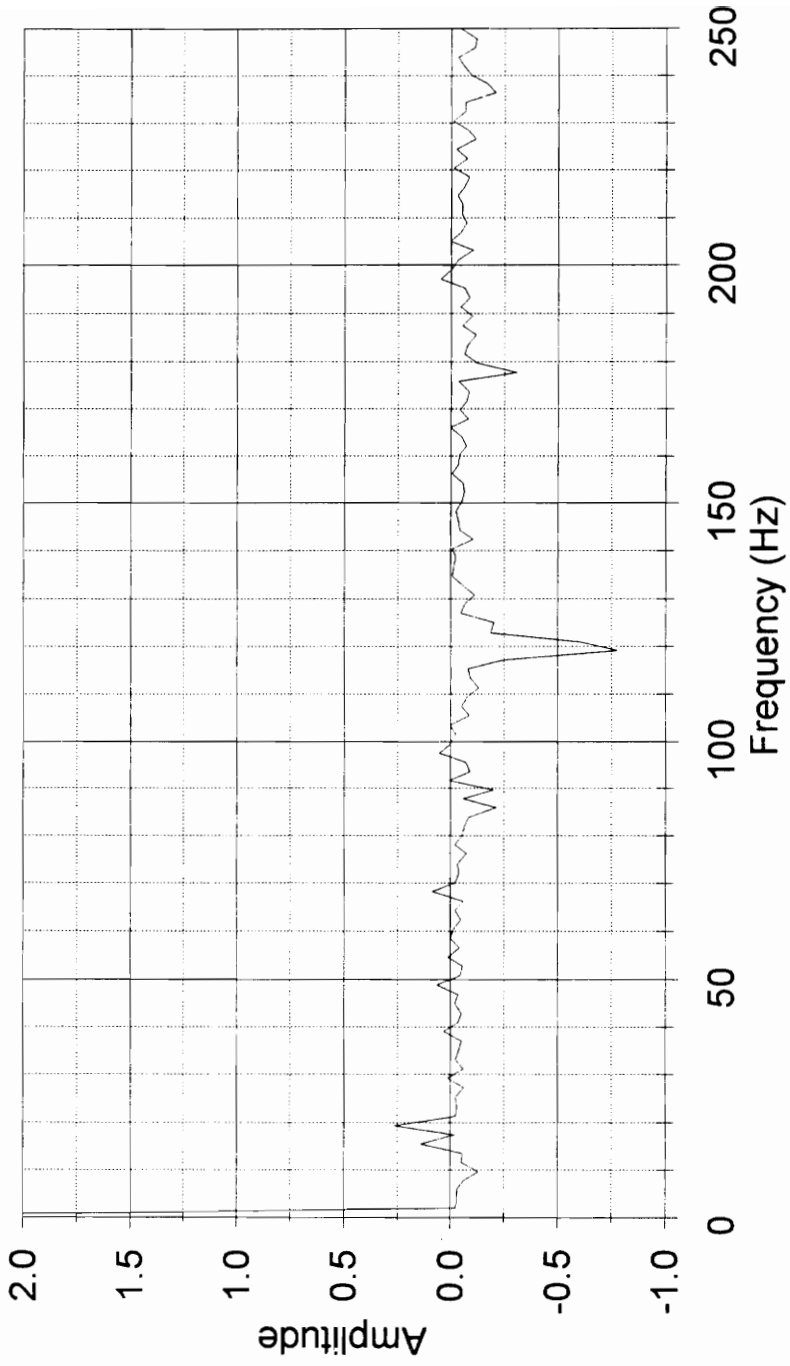
## Accelerometer, Load D, Bearing 11



## Difference in New and Altered FFT's Accelerometer, Load C, Bearing 12

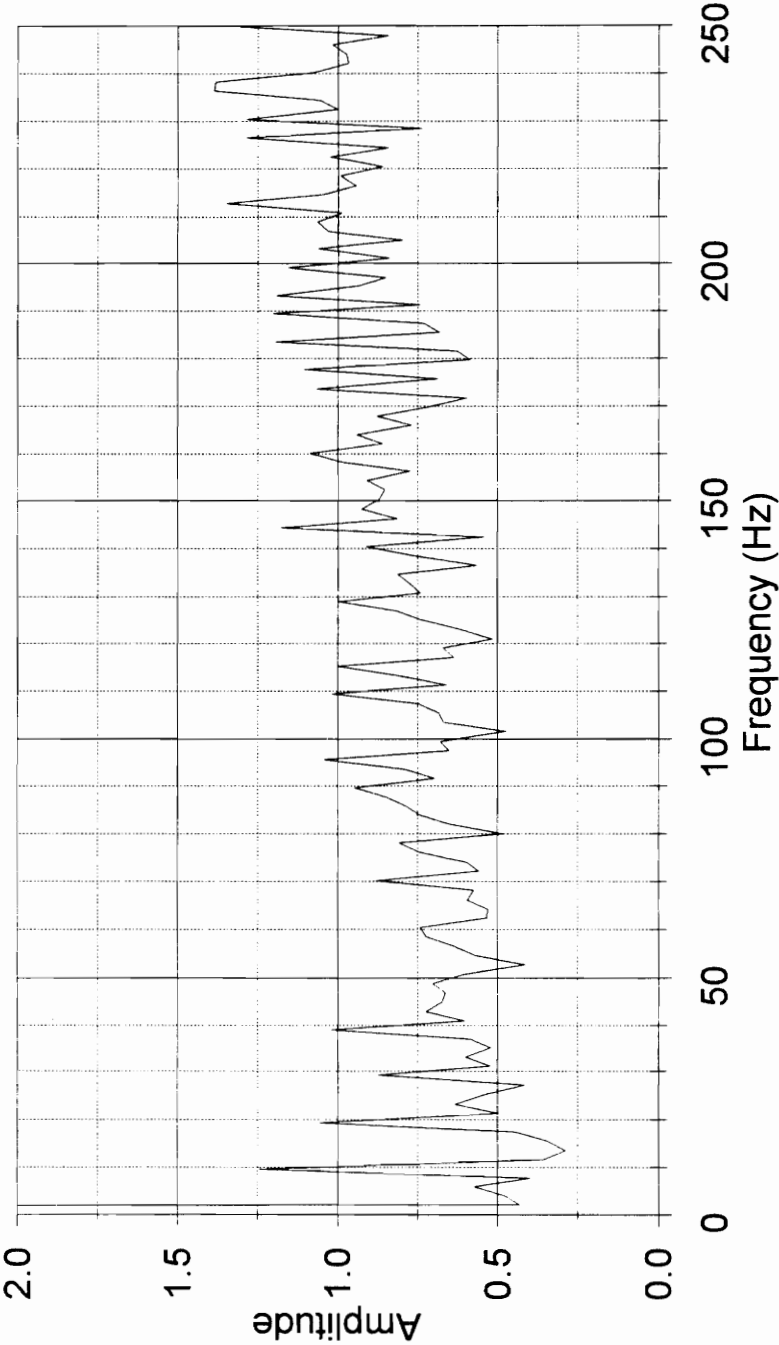


# Difference in New and Altered FFT's Accelerometer, Load D, Bearing 12



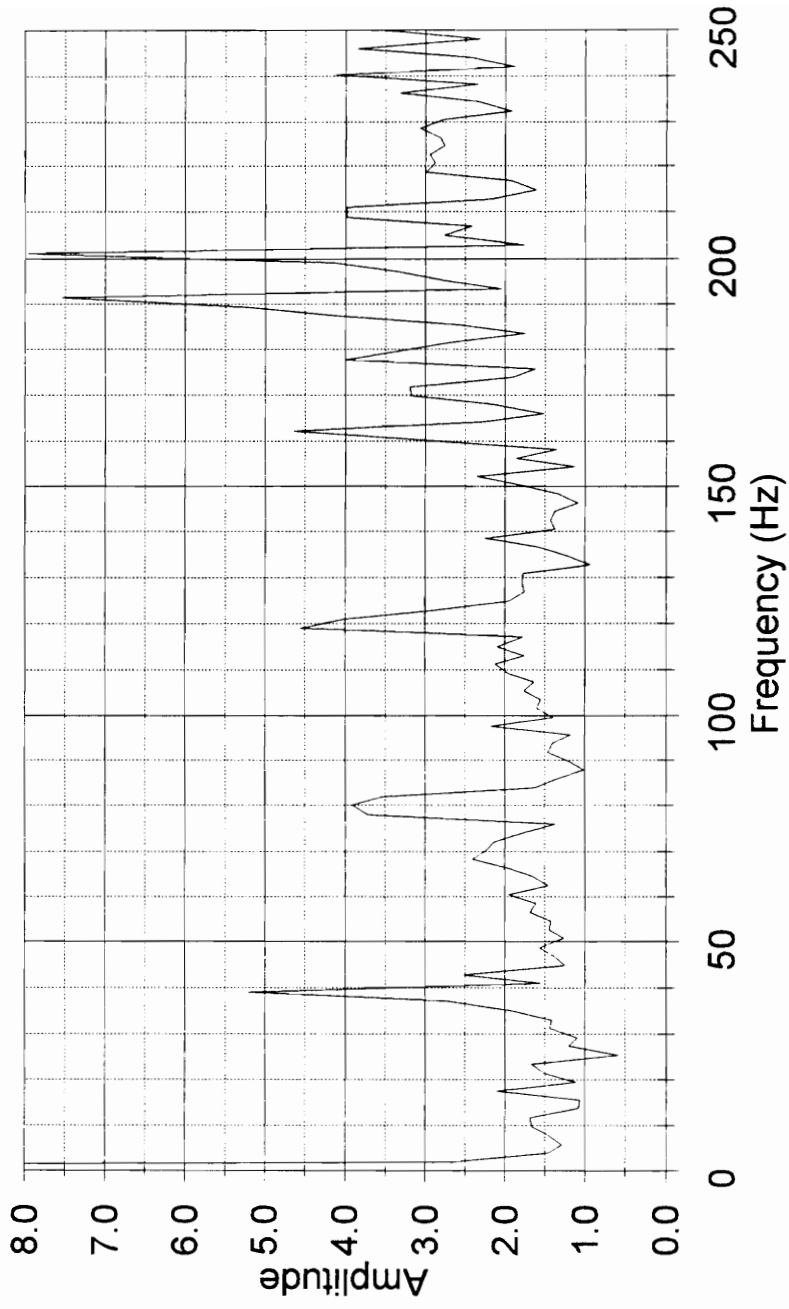
# Difference in New and Altered FFT's

Microphone, Load C, Bearing 1



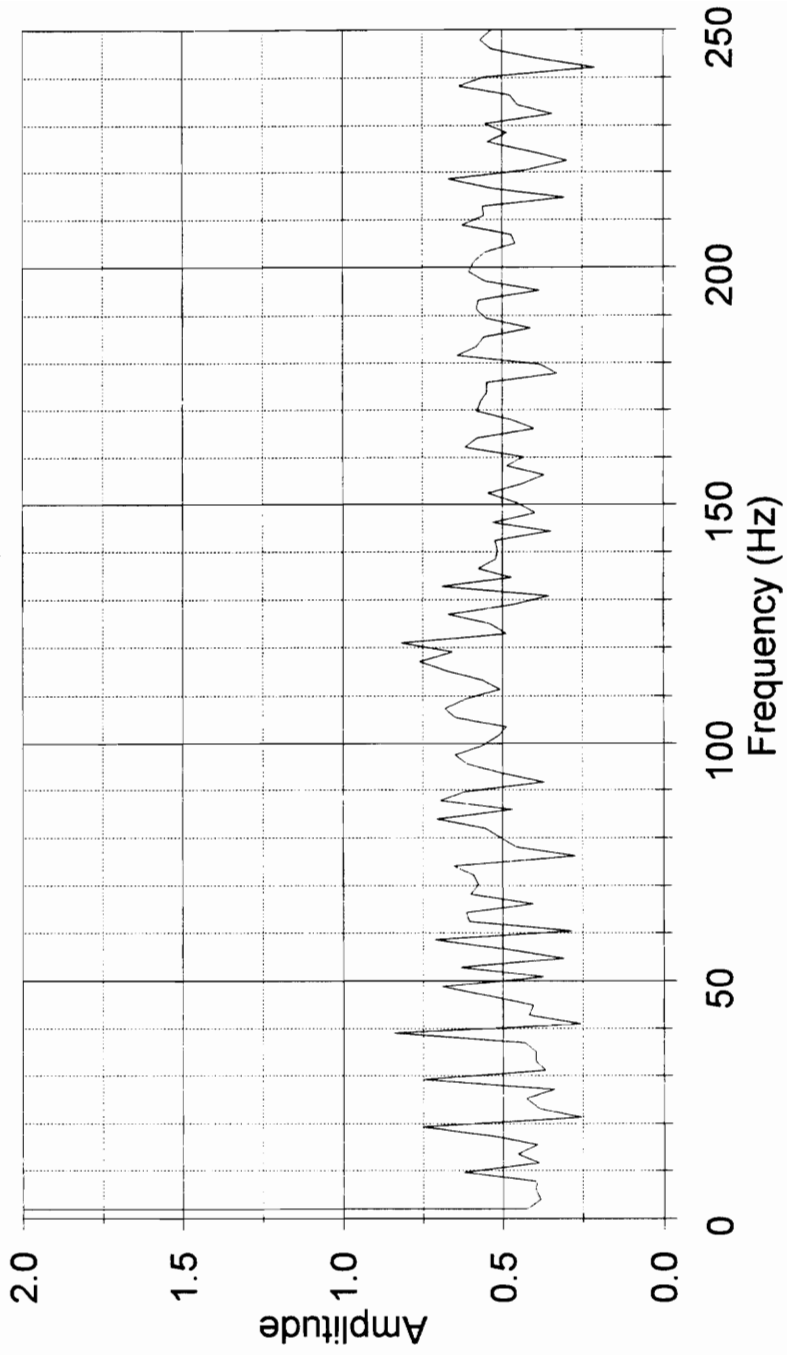
# Difference in New and Altered FFT's

Microphone, Load D, Bearing 1



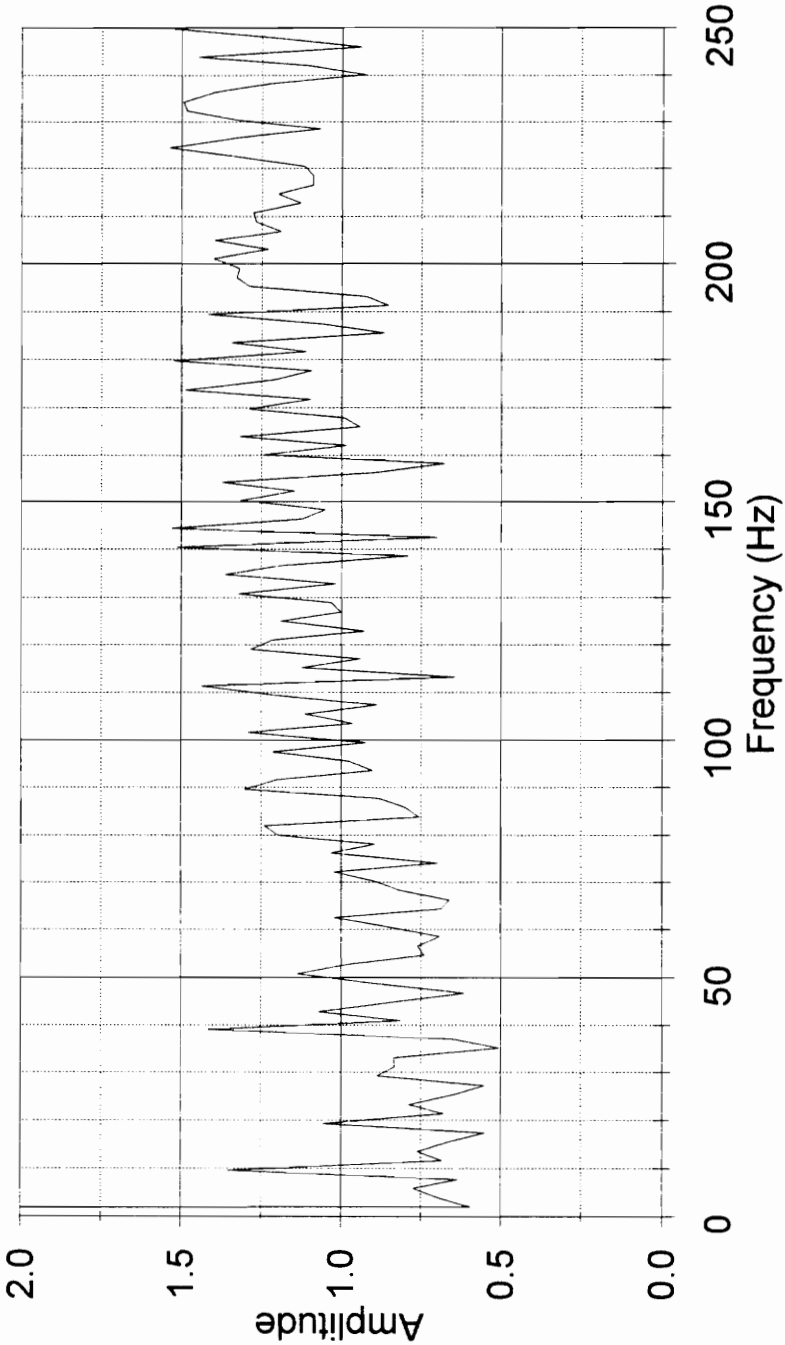
# Difference in New and Altered FFT's

## Microphone, Load C, Bearing 2

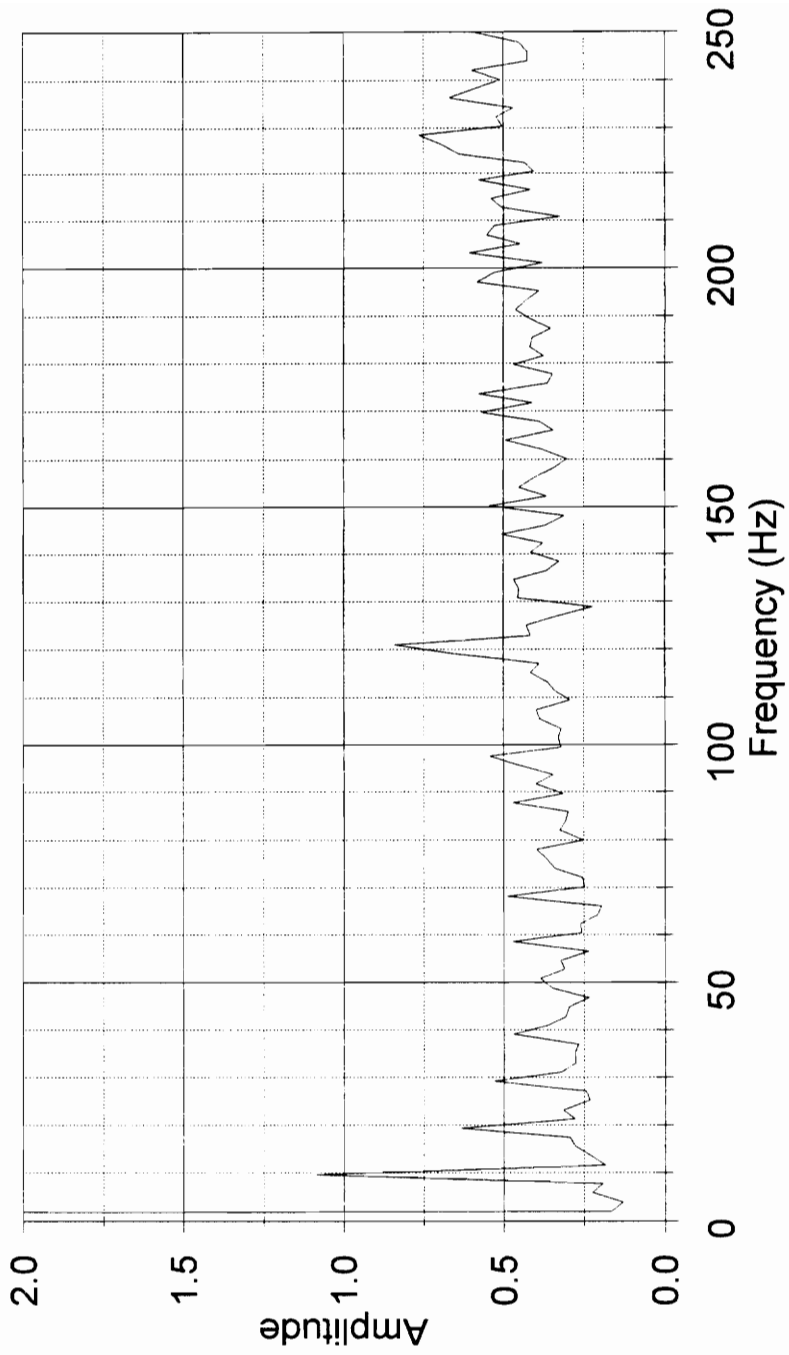


# Difference in New and Altered FFT's

Microphone, Load D, Bearing 2

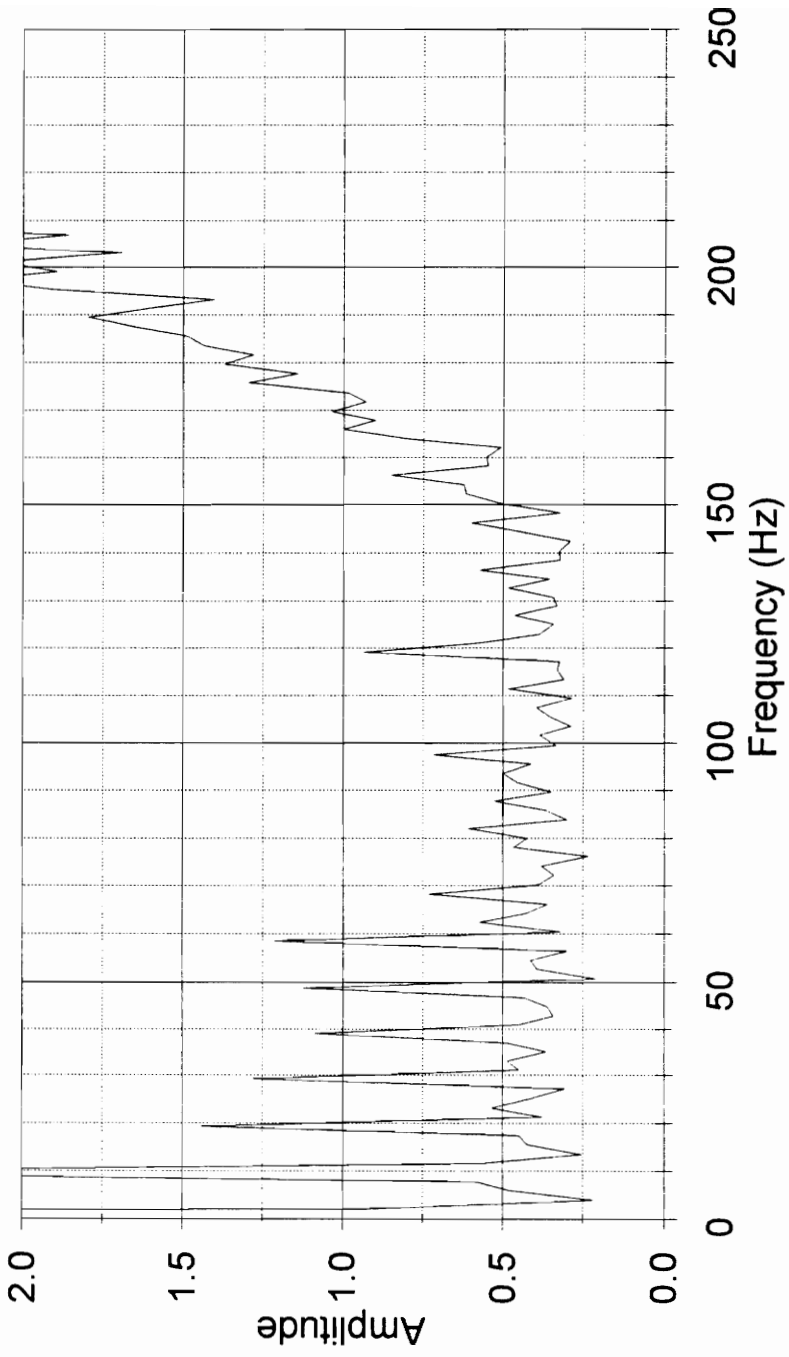


### Difference in New and Altered FFT's Microphone, Load C, Bearing 3

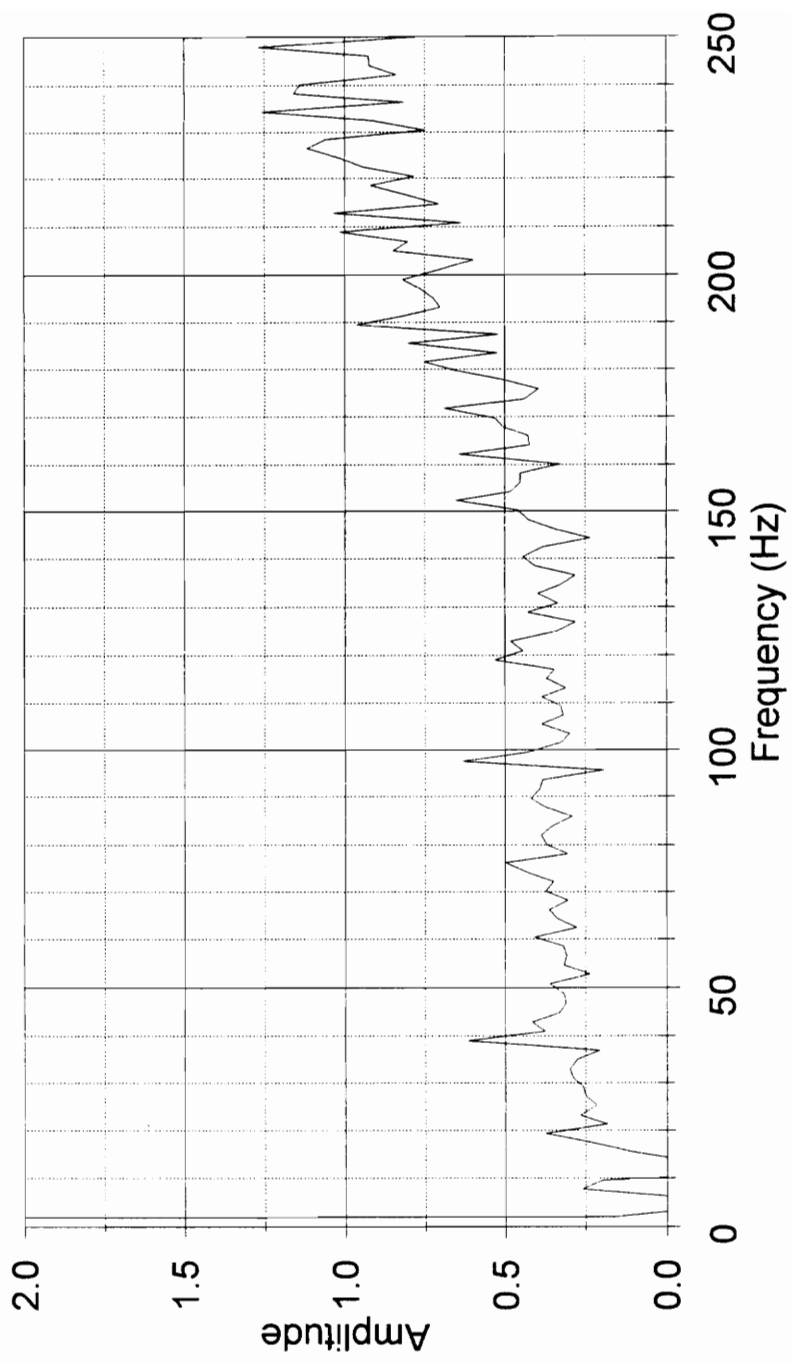


# Difference in New and Altered FFT's

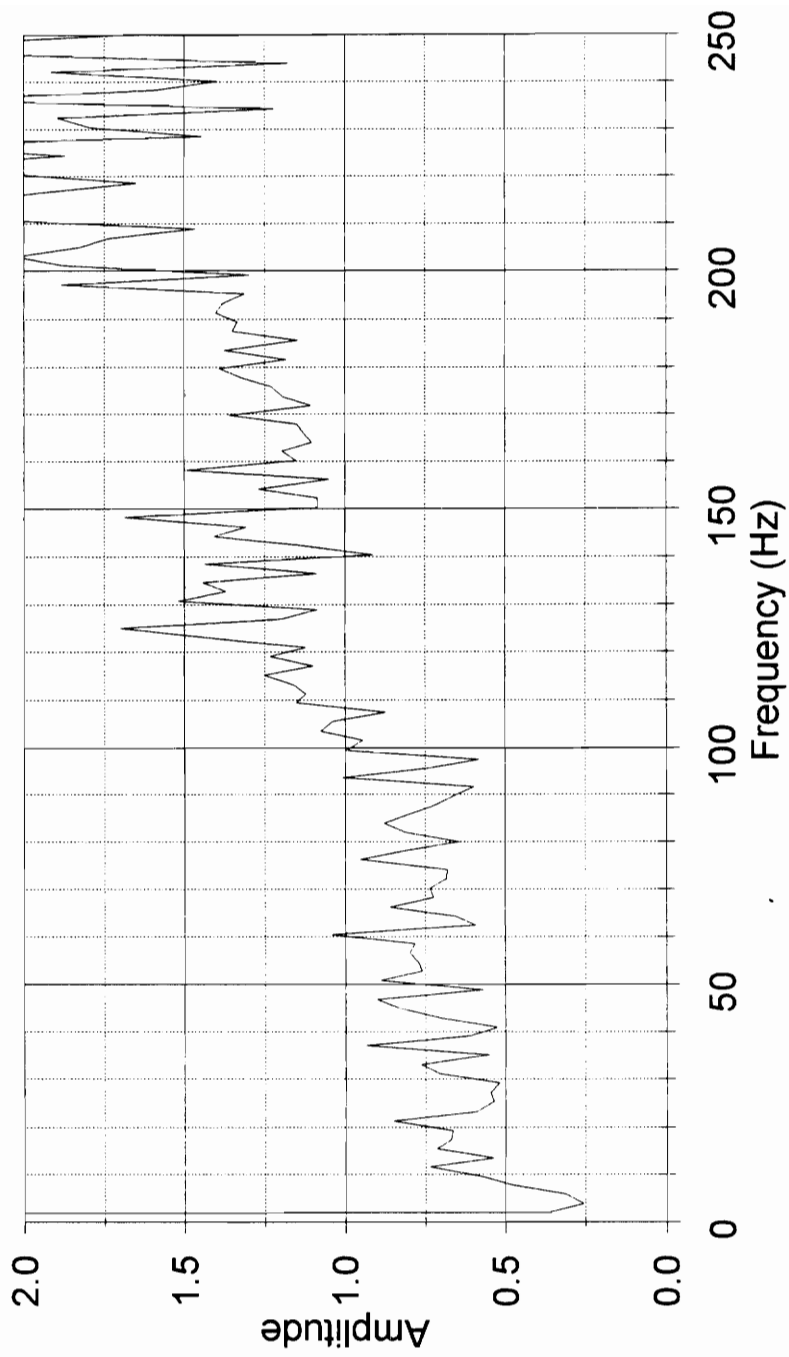
Microphone, Load D, Bearing 3



### Difference in New and Altered FFT's Microphone, Load C, Bearing 4

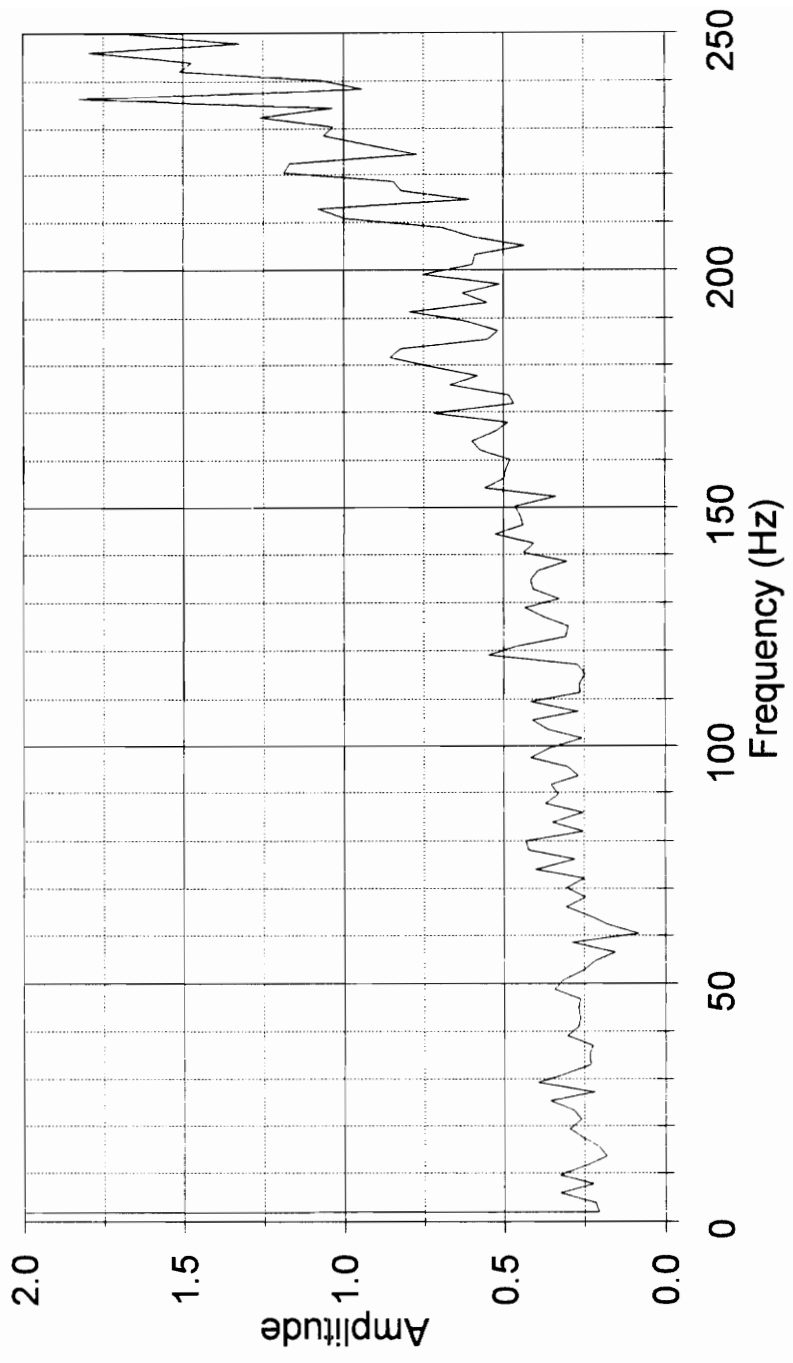


### Difference in New and Altered FFT's Microphone, Load D, Bearing 4

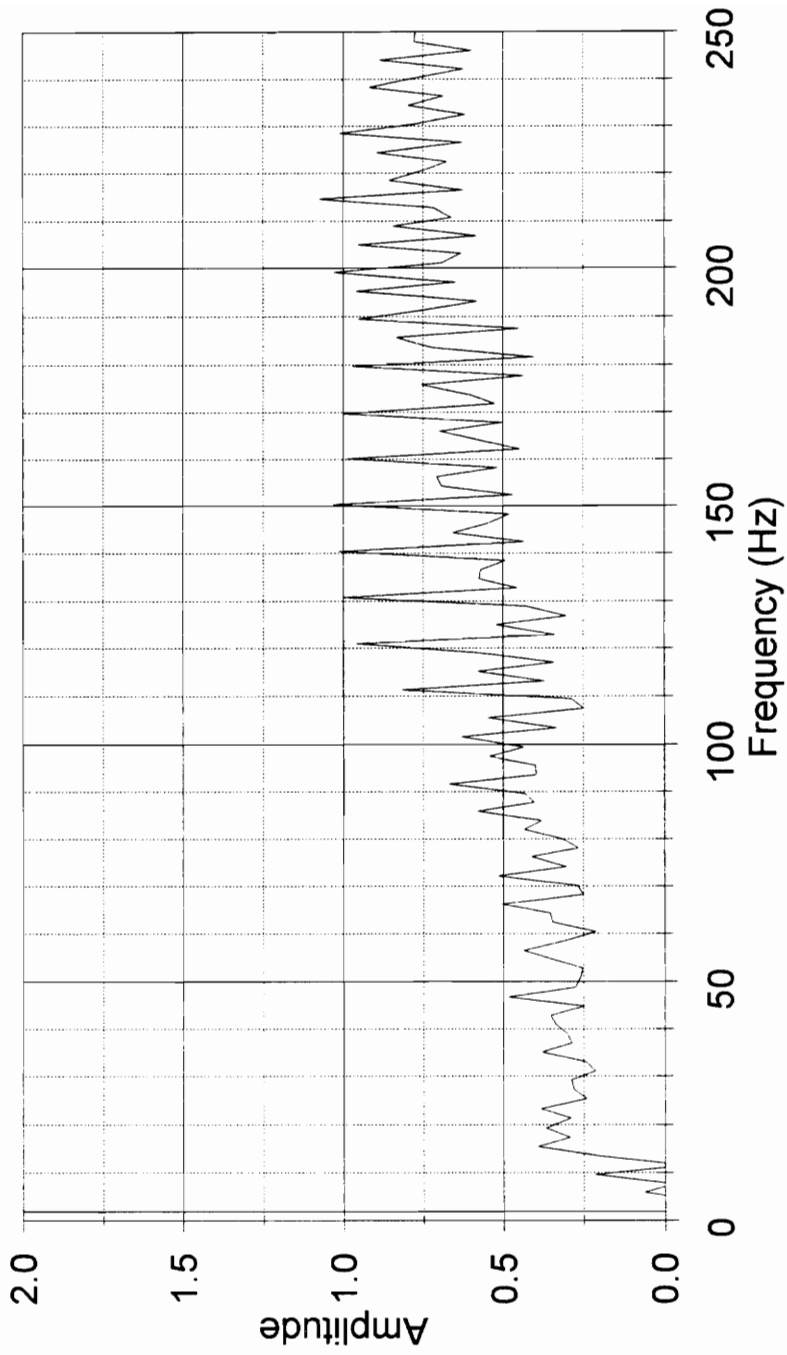


# Difference in New and Altered FFT's

Microphone, Load C, Bearing 5

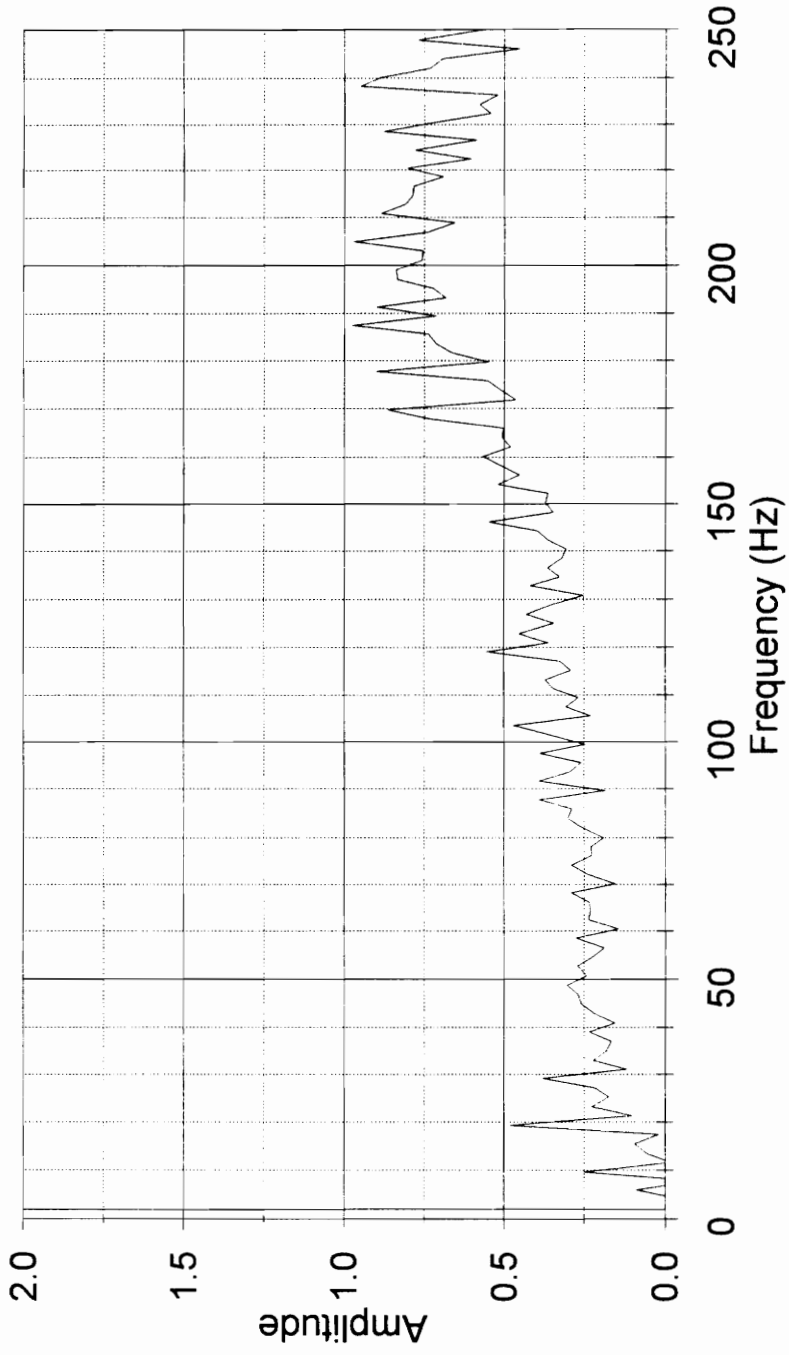


### Difference in New and Altered FFT's Microphone, Load D, Bearing 5



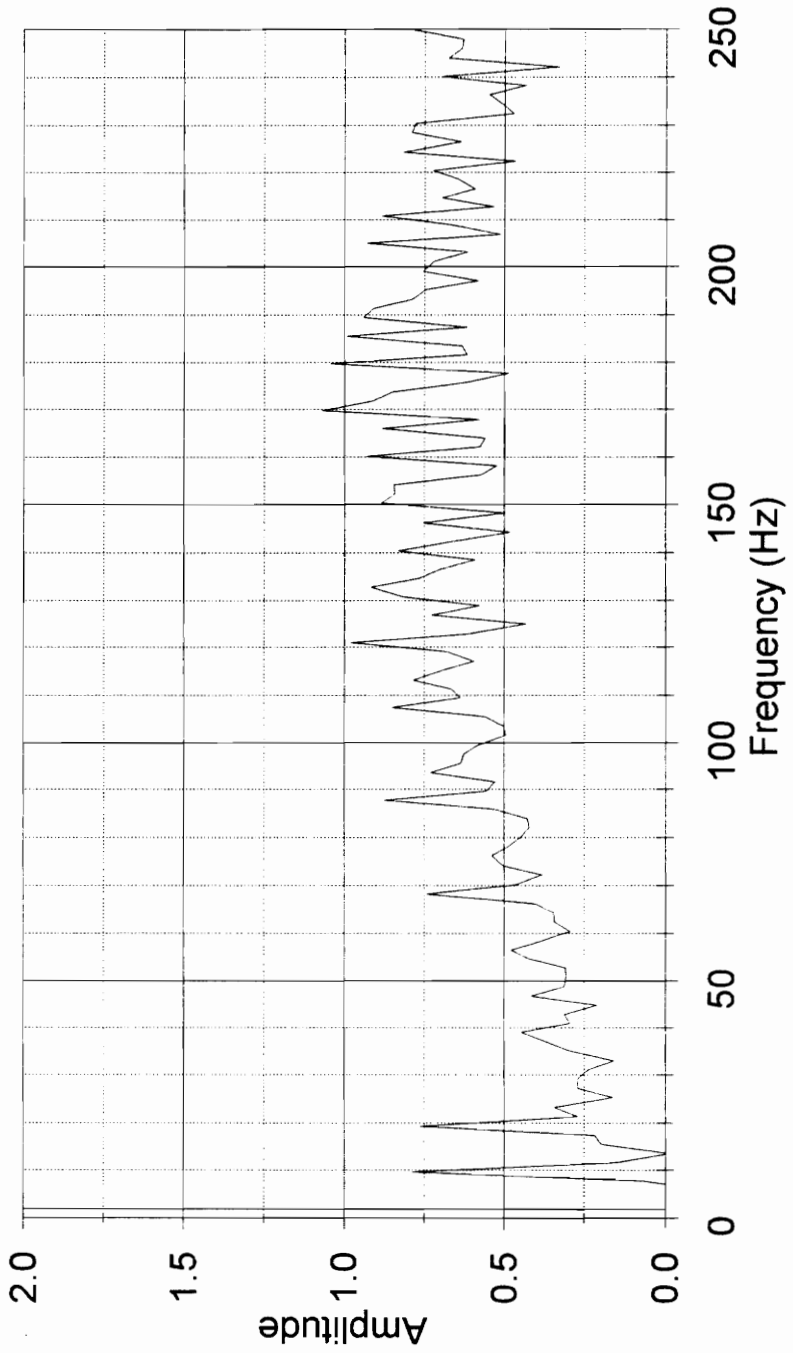
# Difference in New and Altered FFT's

Microphone, Load C, Bearing 6



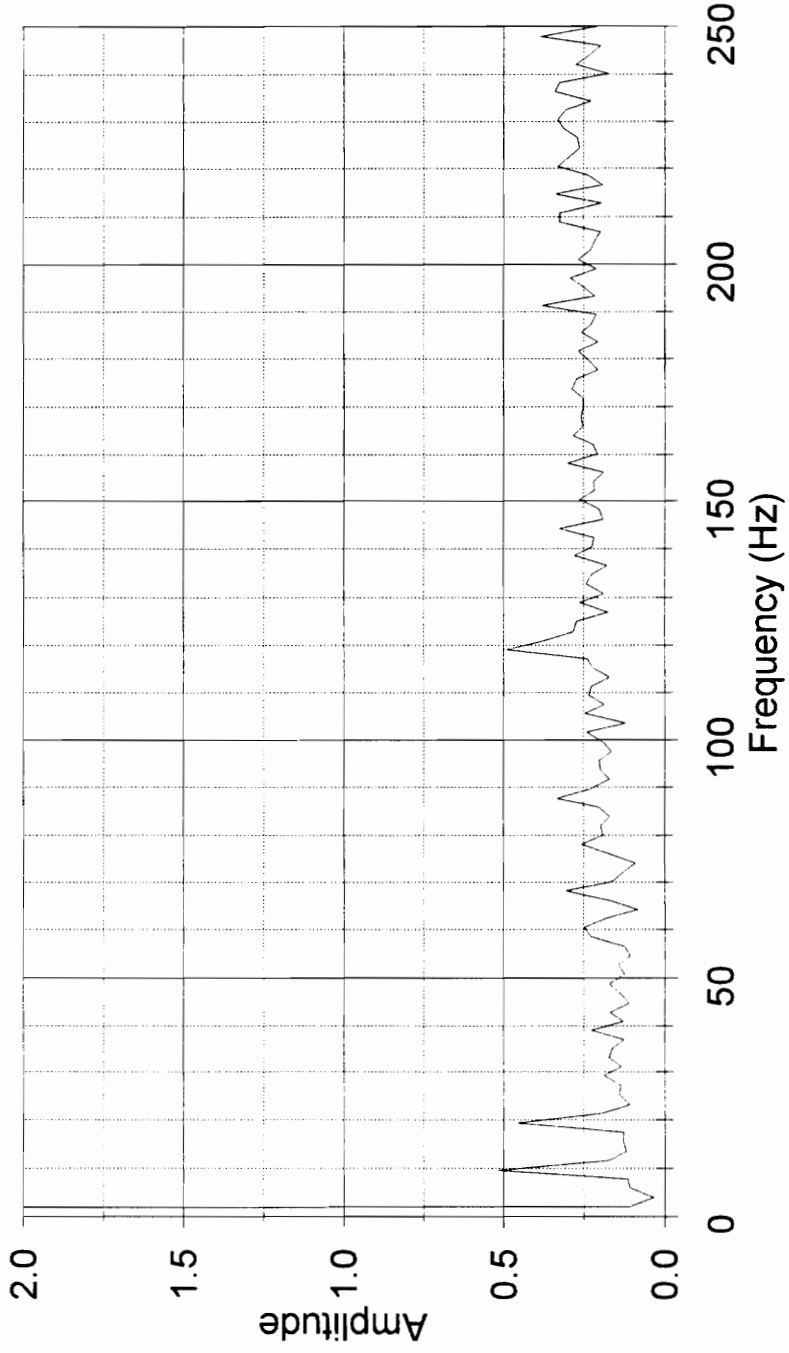
# Difference in New and Altered FFT's

Microphone, Load D, Bearing 6



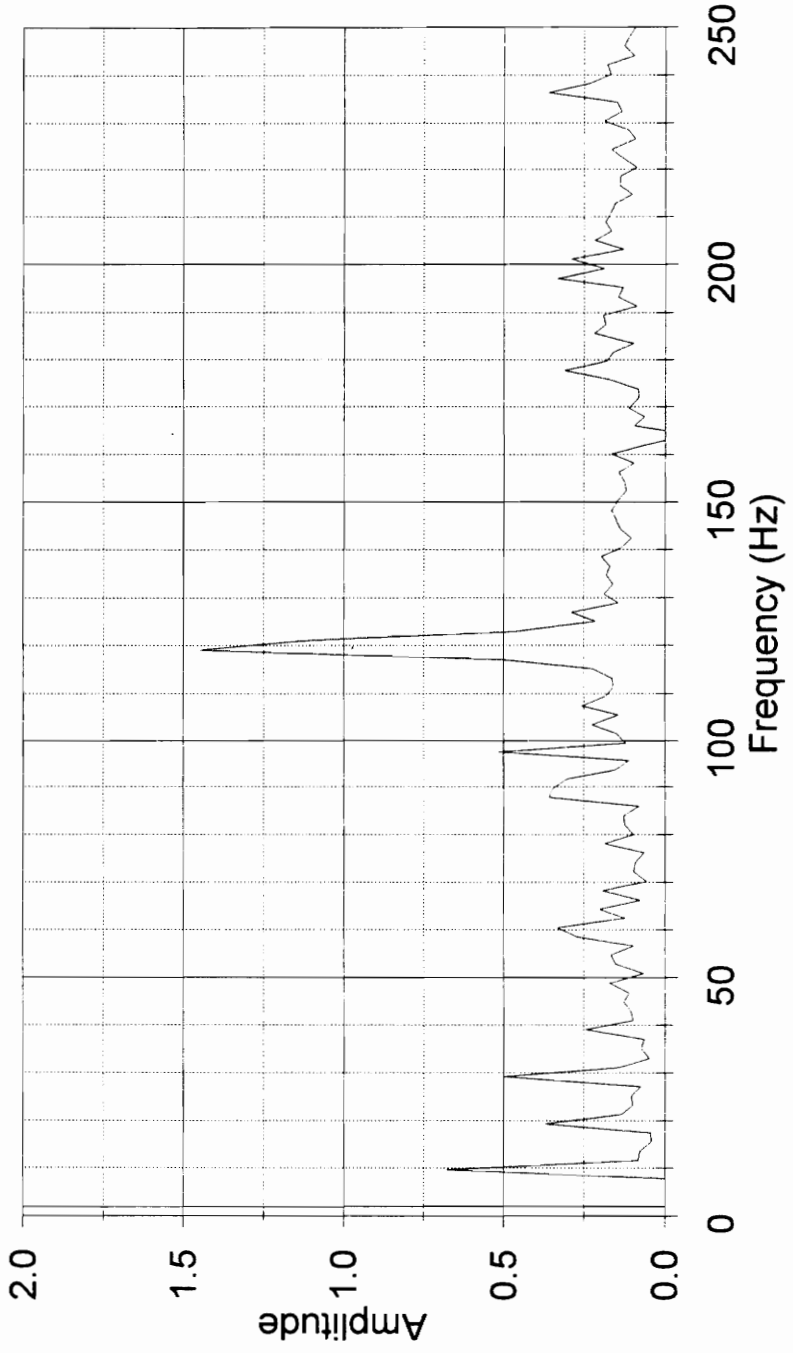
# Difference in New and Altered FFT's

## Microphone, Load C, Bearing 7



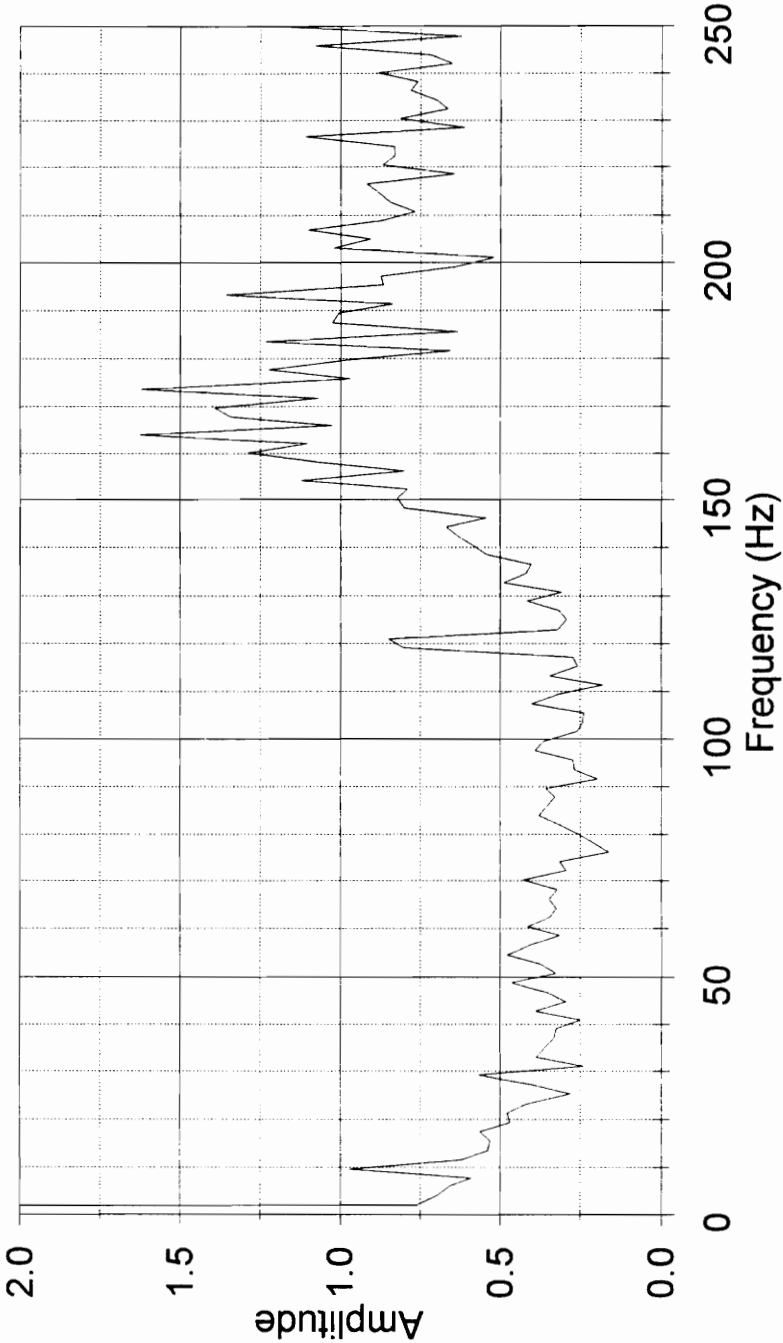
# Difference in New and Altered FFT's

## Microphone, Load D, Bearing 7

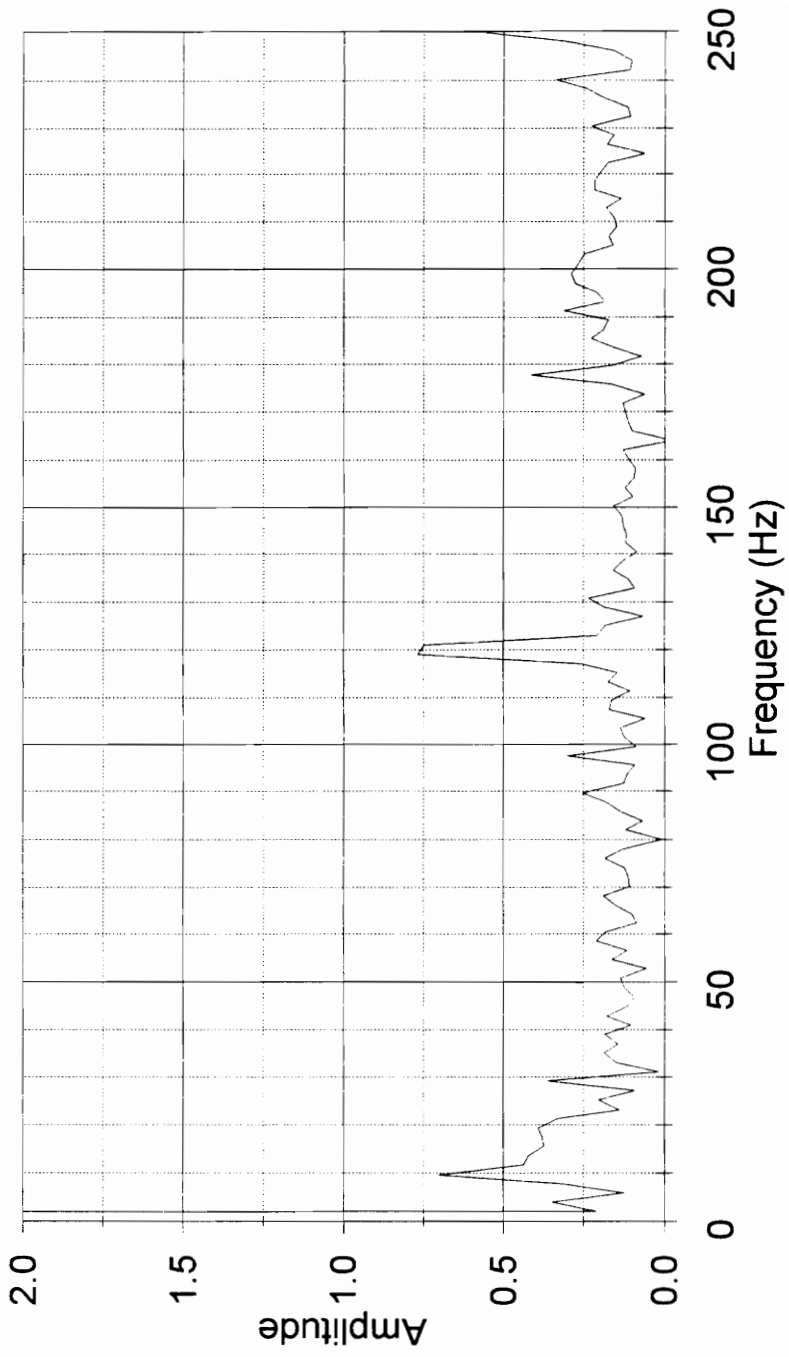


# Difference in New and Altered FFT's

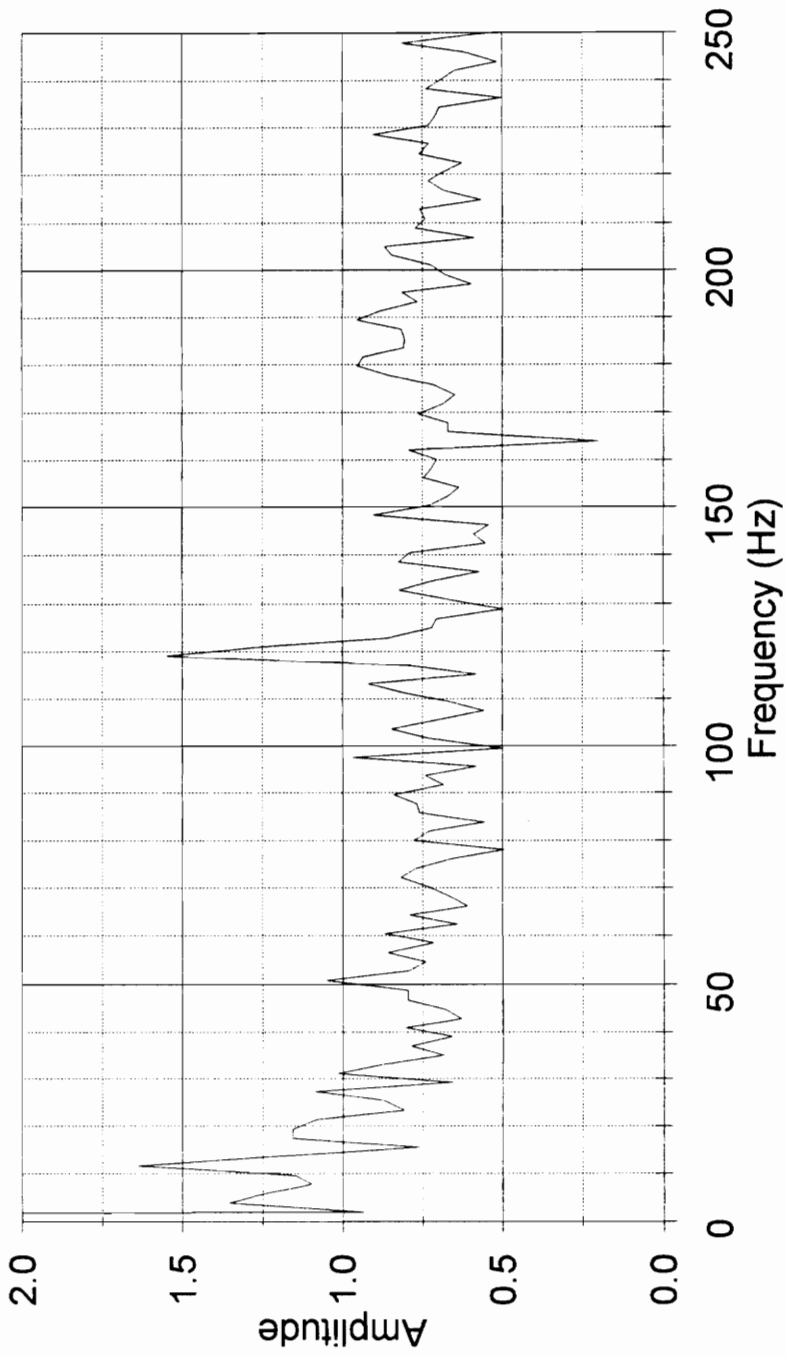
Microphone, Load C, Bearing 8



### Difference in New and Altered FFT's Microphone, Load D, Bearing 8

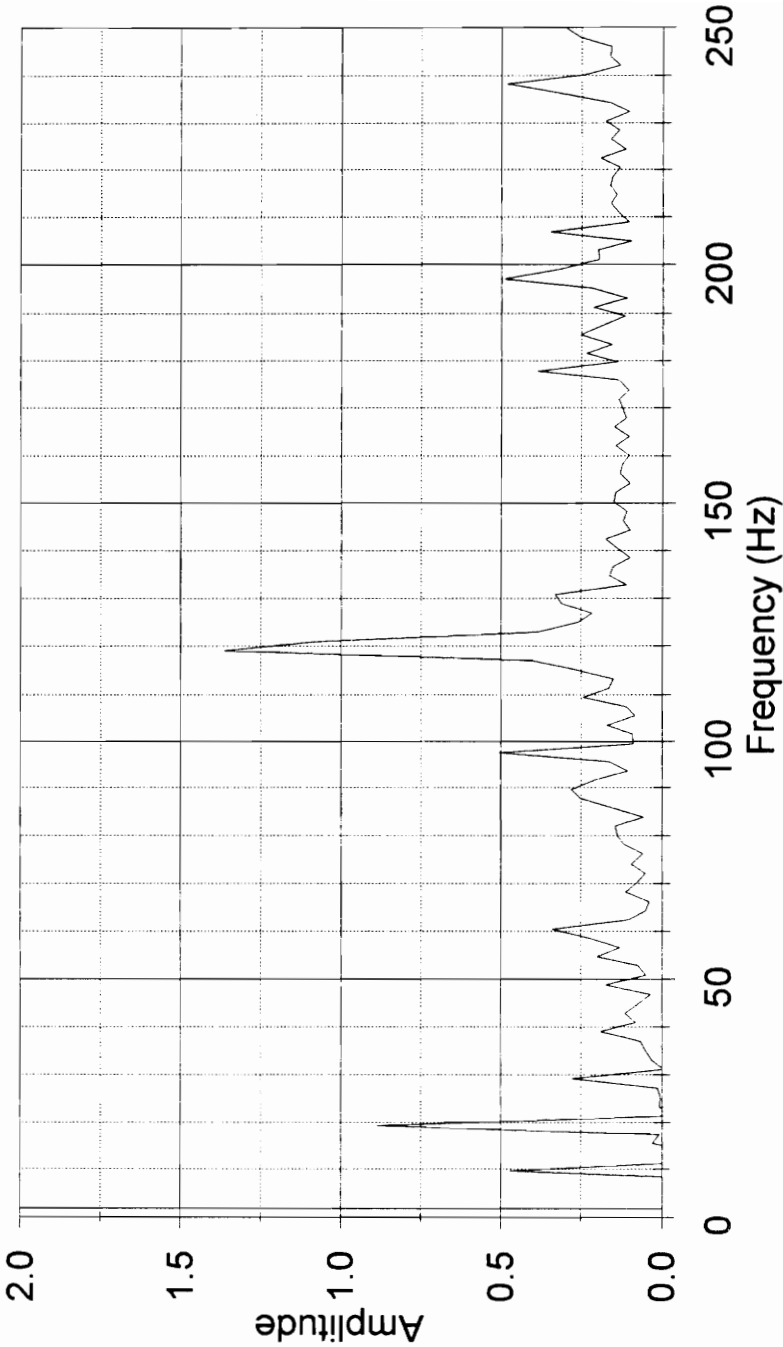


### Difference in New and Altered FFT's Microphone, Load C, Bearing 9



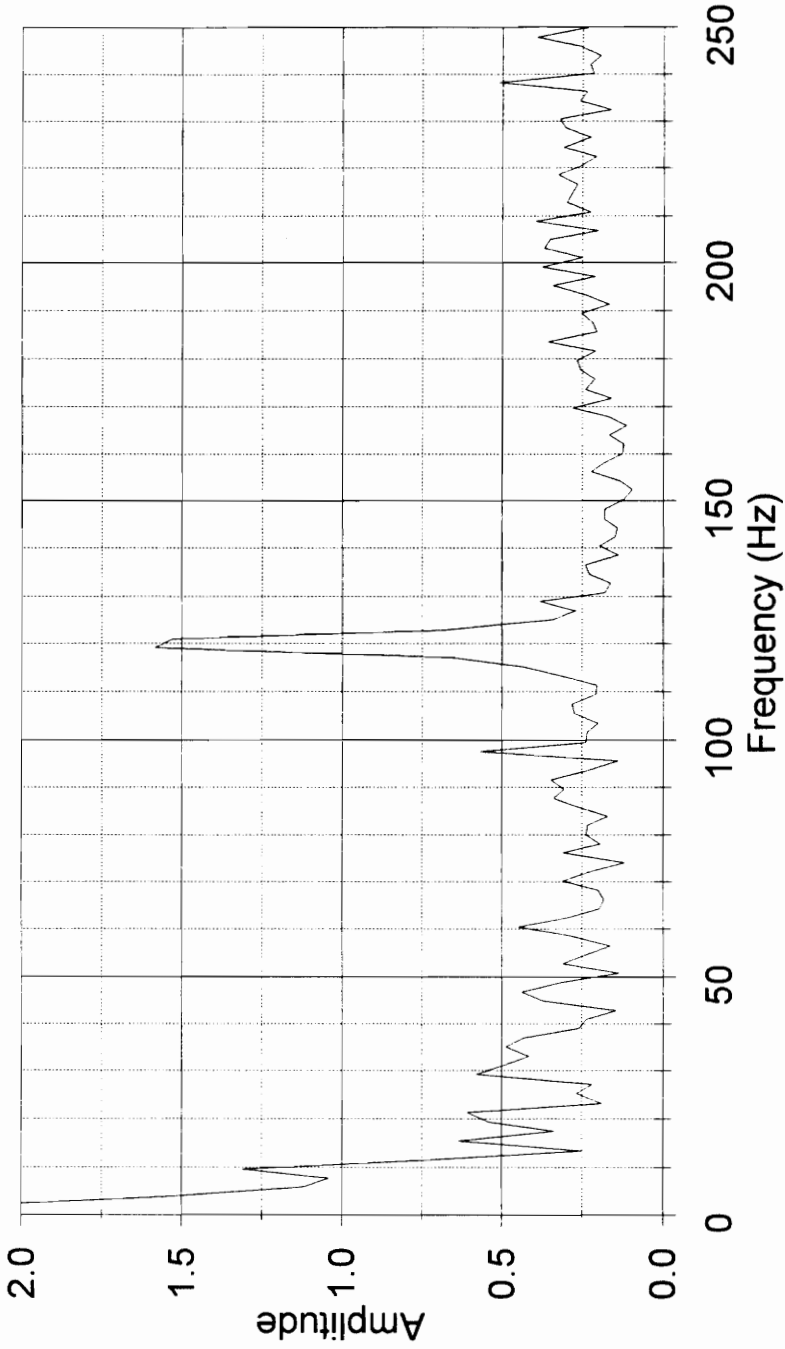
# Difference in New and Altered FFT's

Microphone, Load D, Bearing 9



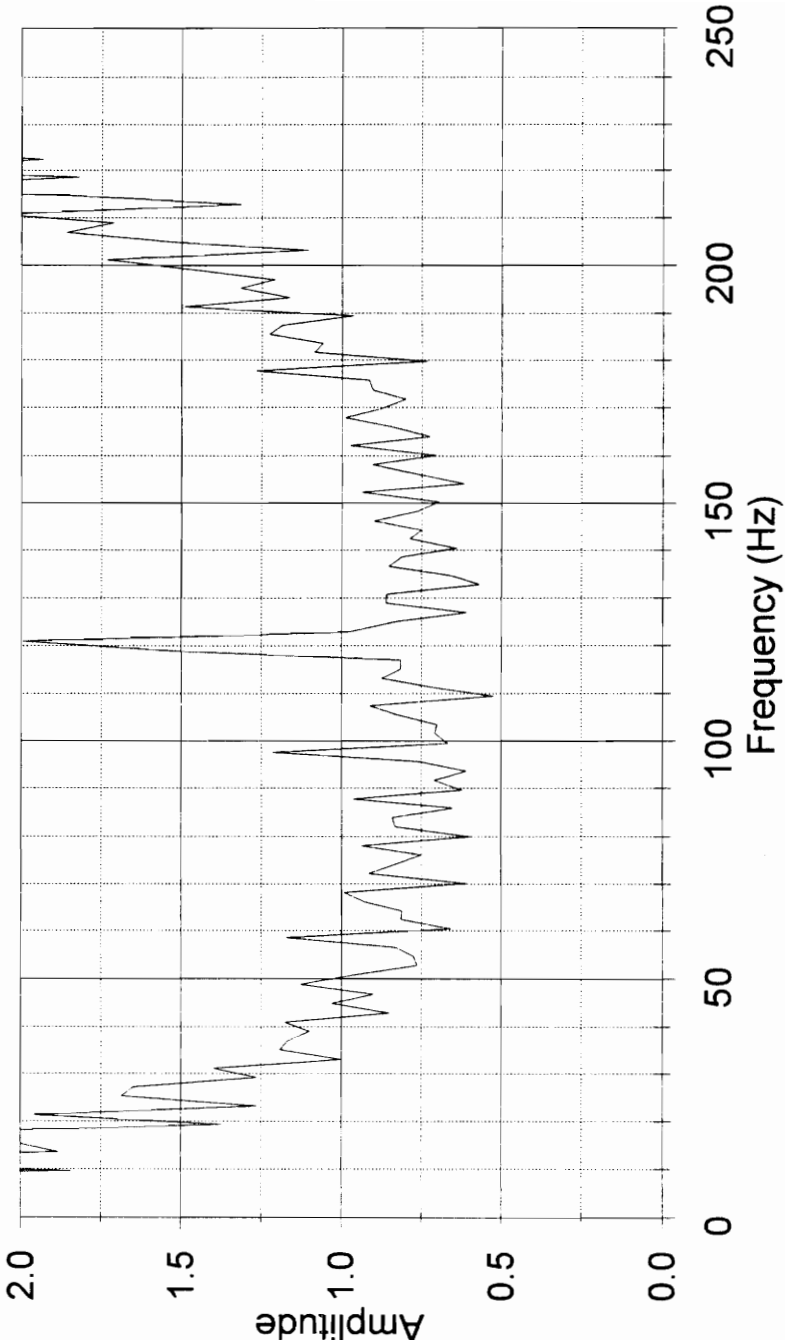
# Difference in New and Altered FFT's

Microphone, Load C, Bearing 10



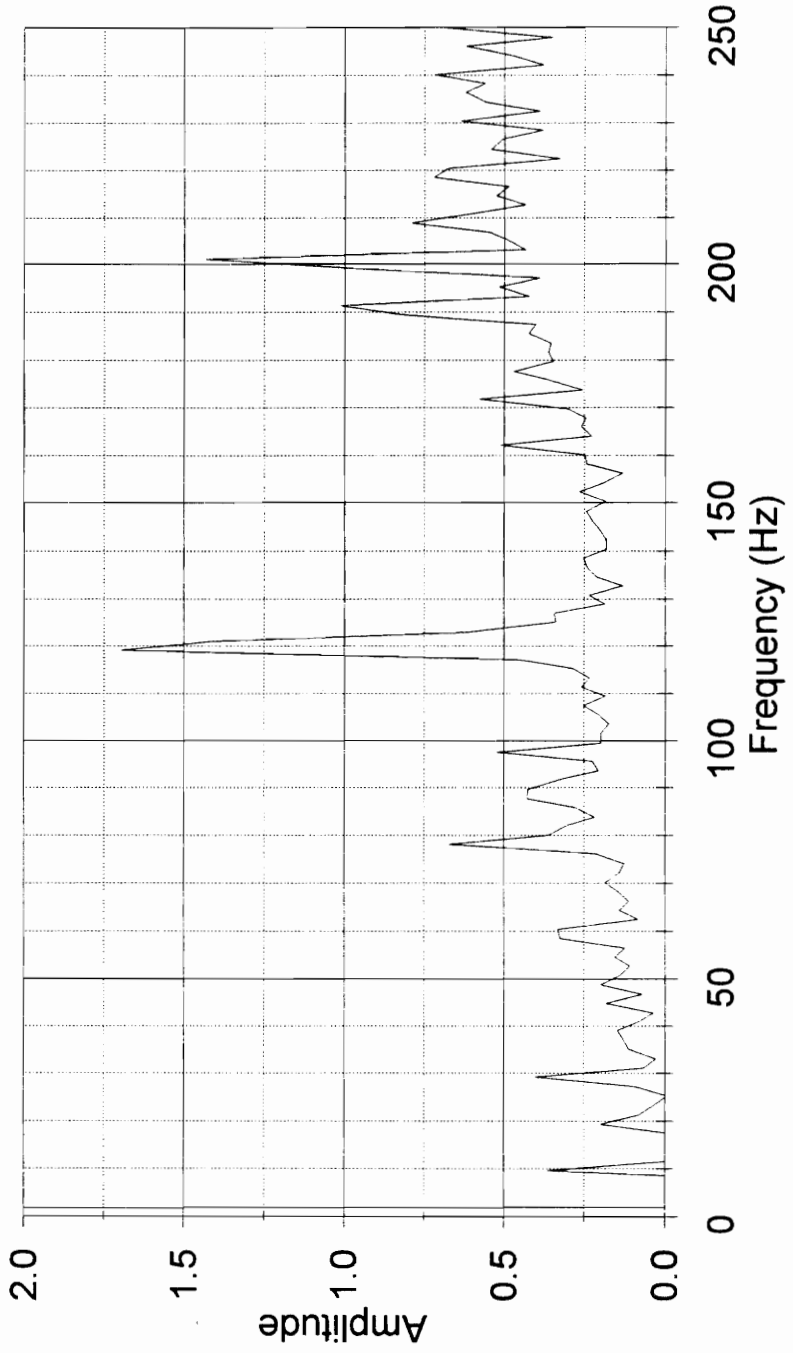
# Difference in New and Altered FFT's

Microphone, Load D, Bearing 10



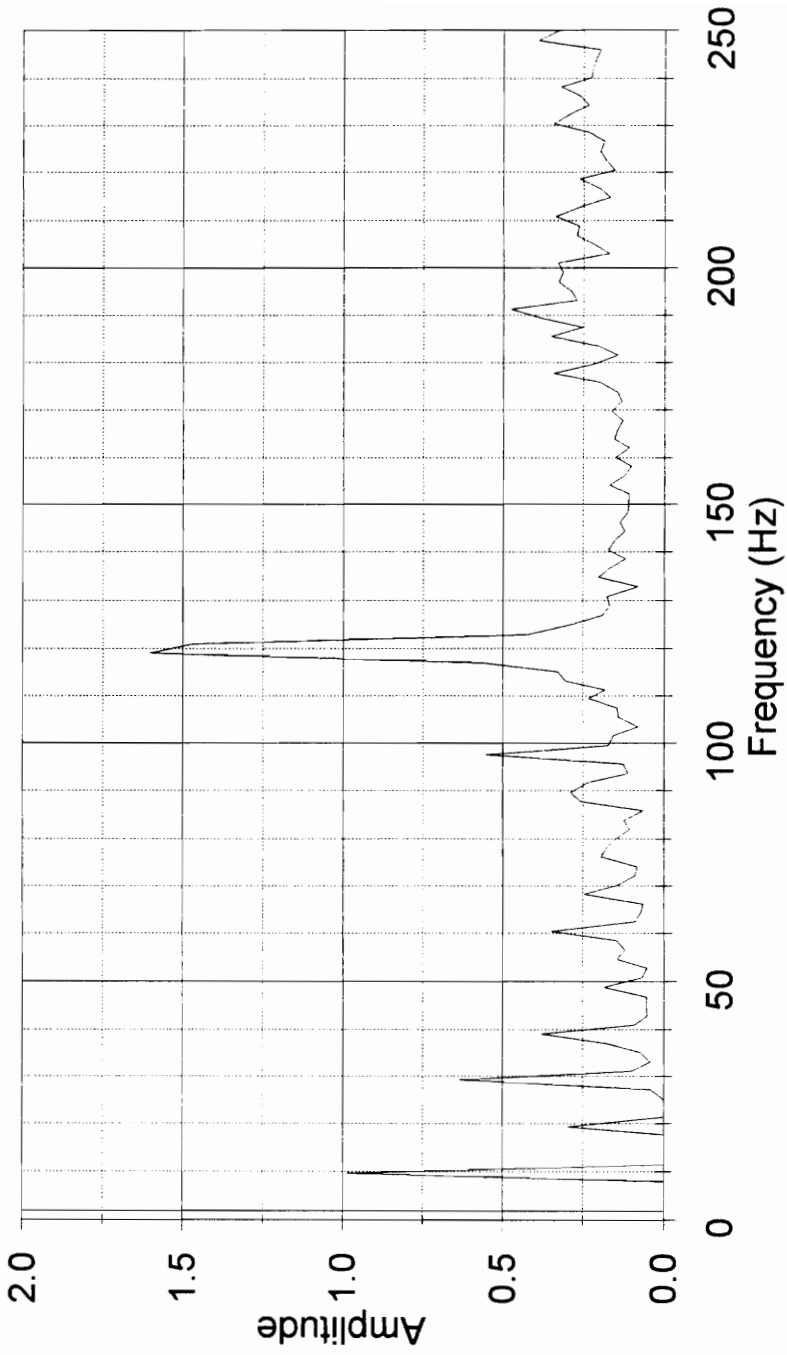
# Difference in New and Altered FFT's

Microphone, Load C, Bearing 11



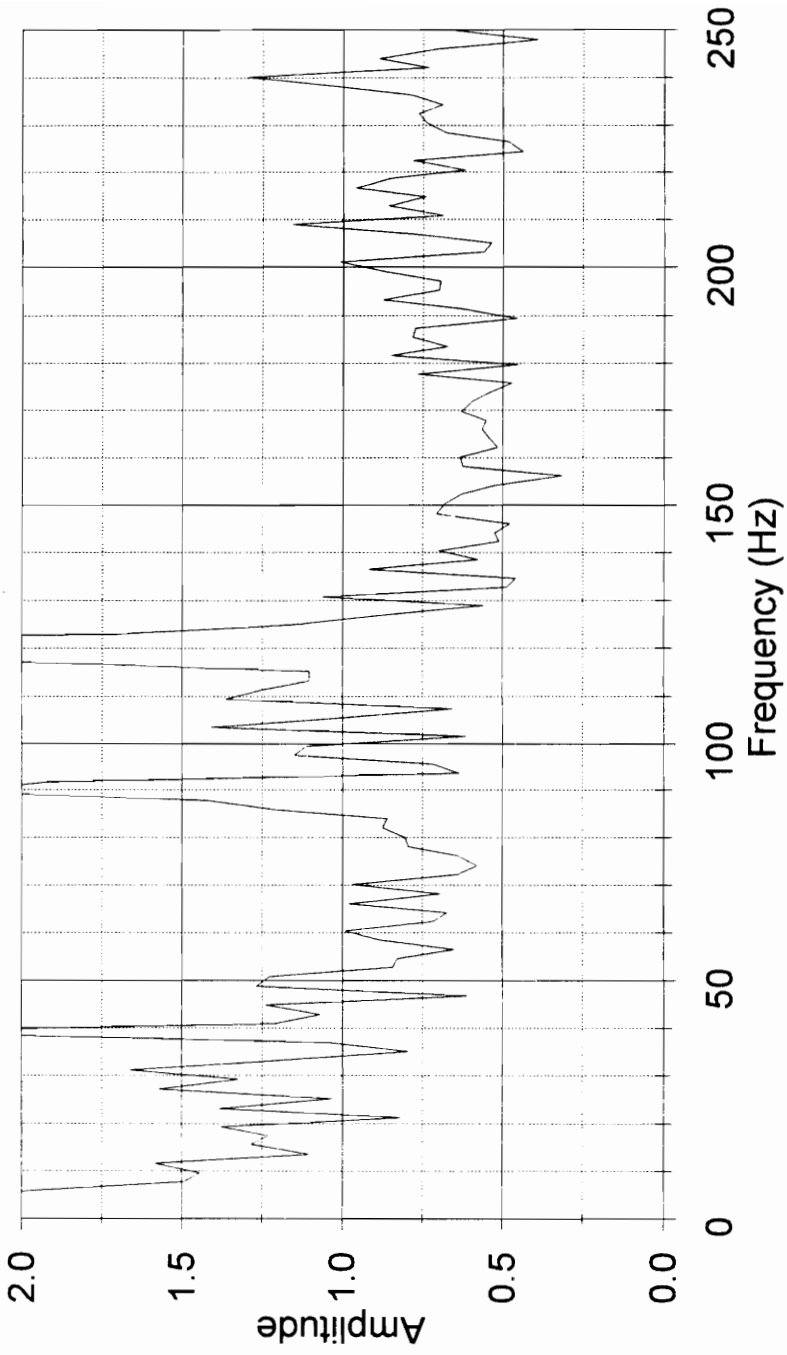
# Difference in New and Altered FFT's

Microphone, Load D, Bearing 11



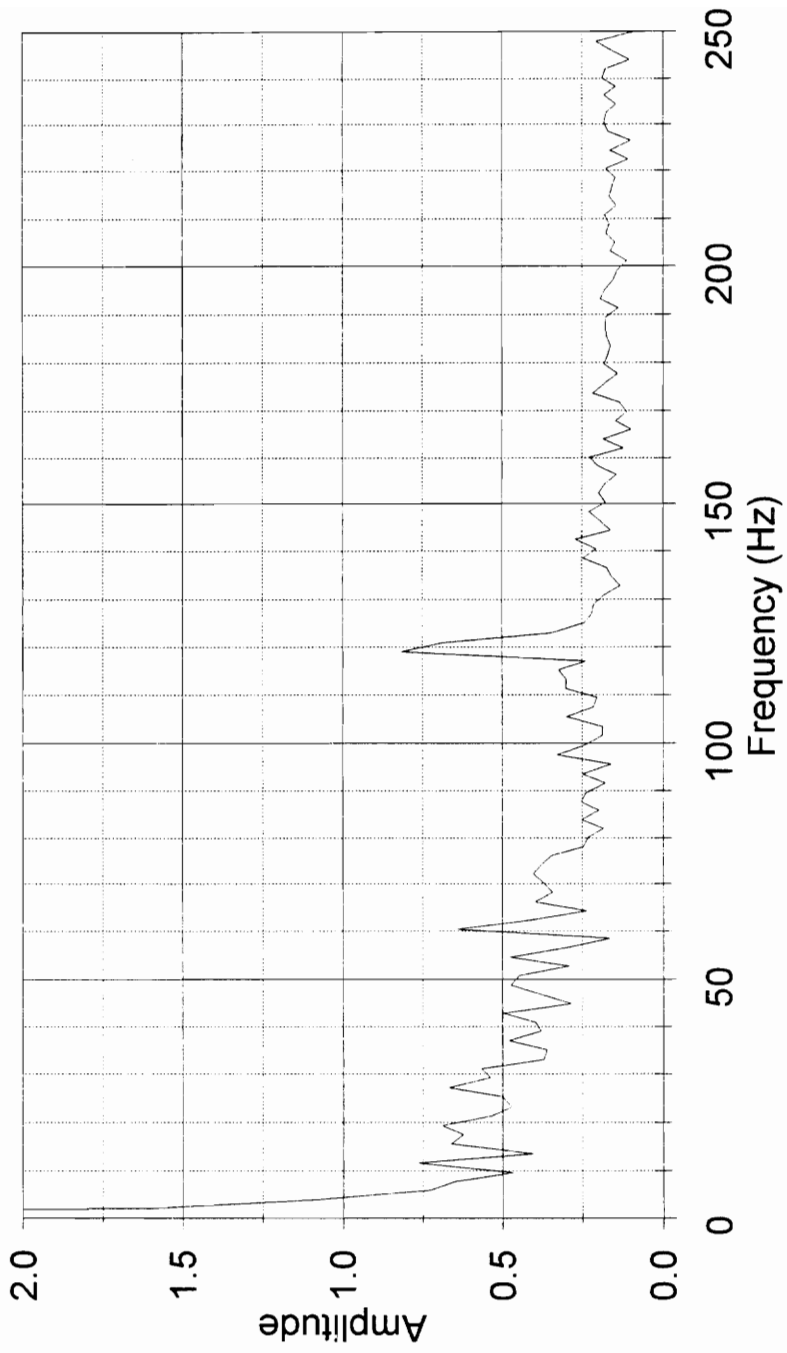
# Difference in New and Altered FFT's

Microphone, Load C, Bearing 12



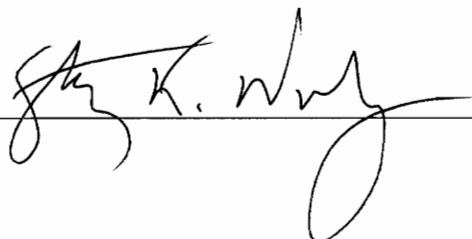
# Difference in New and Altered FFT's

Microphone, Load D, Bearing 12



## Vita

Stacy K. Worley was born on May 15, 1969, in Abingdon, Virginia. He was raised in the foothills of the Appalachian mountains on his family farm where burley tobacco and Polled Hereford cattle are produced. The positions he has held include laboratory technician for Morrison Moulded Fiber Glass and the Virginia Tech Agricultural Engineering Department. He has served for eight years as a Drill Sergeant in the United States Army Reserve. He received a B.S. in Agricultural Engineering from Virginia Polytechnic Institute and State University in 1992. After receiving his undergraduate degree, he began his graduate program in pursuit of a M.S. in Agricultural Engineering. Following the completion of his Master's degree, he will be pursuing a Ph.D. in Agricultural and Biological Engineering at The Pennsylvania State University at University Park.



A handwritten signature in black ink, reading "Stacy K. Worley", is written over a horizontal line. The signature is stylized and cursive.